

# Prague Medical REPORT

(Sborník lékařský)

Multidisciplinary Biomedical Journal  
of the First Faculty of Medicine,  
Charles University

Vol. 123 (2022) No. 4

## Reviews

ADHD – What Is the Meaning of Sex-dependent Incidence Differences? / Mourek J., Pokorný J. page 215

## Primary Scientific Studies

A Response of the Pineal Gland in Sexually Mature Rats under Long-term Exposure to Heavy Metal Salts / Hryntsova N., Hodorová I., Mikhaylik J., Romanyuk A. page 225

Malignancy Rates in Thyroid Nodules Classified as Bethesda III and IV; Correlating Fine Needle Aspiration Cytology with Histopathology / Pereira C. page 243

Clinical Course of COVID-19 and Cycle Threshold in Patients with Haematological Neoplasms / Santarelli I. M., Sierra M., Gallo Valet M. L., Rodríguez Fermepin M., Fernández S. I. page 250

Amyotrophic Lateral Sclerosis: An Analysis of the Electromyographic Fatigue of the Masticatory Muscles / Gonçalves L. M. N., Siéssere S., Cecilio F. A., Hallak J. E. C., de Vasconcelos P. B., Marques Júnior W., Regalo I. H., Palinkas M., Regalo S. C. H. page 258

## Case Reports

Pervitin Intoxication with Two-peak Massive Myoglobinemia, Acute Kidney Injury and Marked Procalcitonin Increase Not Associated with Sepsis / Svobodová E., Drábek T., Brodská H. page 266

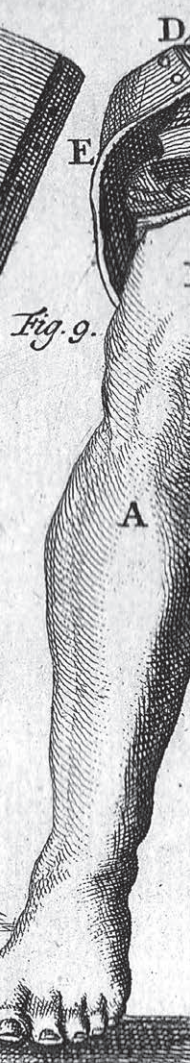
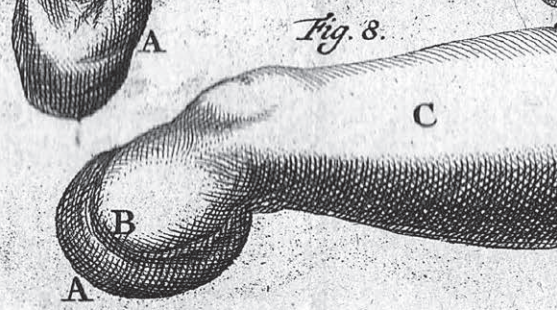
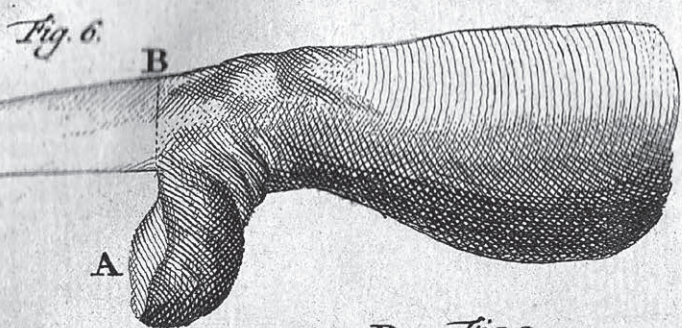
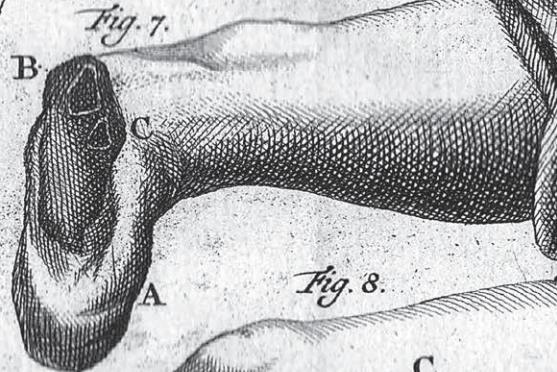
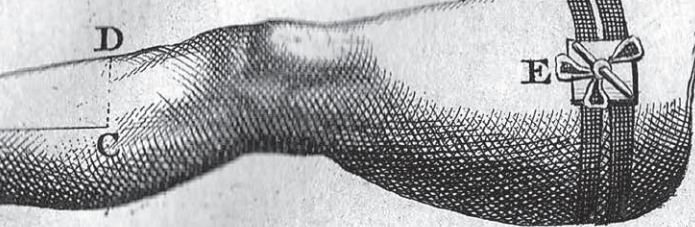
Delayed Spontaneous Pneumothorax in a Previously Healthy Nonventilated COVID-19 Patient / Zahornacký O., Porubčín Š., Rovňáková A., Jarčuška P. page 279

**Instructions to Authors** page 287

**Annual Contents** page 291

**Annual Nominal Index** page 294

**Annual Referee Index** page 296



**Prague Medical Report (Prague Med Rep) is indexed and abstracted by Index-medicus, MEDLINE, PubMed, EuroPub, CNKI, DOAJ, EBSCO, and Scopus.**

**Abstracts and full-texts of published papers can be retrieved from the World Wide Web (<https://pmr.lf1.cuni.cz>).**

# ADHD – What Is the Meaning of Sex-dependent Incidence Differences?

**Jindřich Mourek, Jaroslav Pokorný**

Institute of Physiology, First Faculty of Medicine, Charles University, Prague, Czech Republic

Received June 23, 2022; Accepted October 18, 2022.

**Key words:** ADHD – Inhibitory mechanisms – Catecholamines – Ascorbic acid – Biological axiom

**Abstract:** There is a clear experience in clinical practice: boys with a diagnosis of ADHD are clearly in greater numbers than girls. It is noteworthy that even in the “older” review articles, the cause of sex-dependent incidence is not mentioned. If we accept the neurodevelopmental hypothesis of such disorder, then the possible genetic predisposition breaks down into two separate groups. On the genome of an individual with ADHD and on the genome of the parents. However, it cannot be overlooked that the incidence of ADHD (3–7%) corresponds to the incidence and sex differences of the number of newborns born at a certain risk (premature birth, immaturity, hypotrophy, hypoxic-ischemic syndrome, low birth weight, etc.). This association of possible genetic predisposition with “external” risks in the genesis of ADHD raises the question of whether a higher incidence of ADHD, as well as higher morbidity and mortality in males, are a) the norm and the female is privileged, or b) the female is the norm and the male is handicapped. The picture of ADHD includes various cognitive dysfunctions with one possible cause in norepinephrine and dopamine insufficiency. Experimental work shows that in response to stress females release more catecholamines in the CNS than males. Since catecholamines stimulate membrane  $\text{Na}^+ \text{K}^+$  ATPase activity, this means both the value of the membrane potential and the threshold for activation is increased. Females are more successful in responding to and adapting to a stressful situation due to their higher production of noradrenaline in the CNS.

**Mailing Address:** Prof. Jaroslav Pokorný, MD., DSc., Institute of Physiology, First Faculty of Medicine, Charles University, Albertov 5, 128 00 Prague 2, Czech Republic; Mobile Phone: +420 603 964 772; e-mail: pokorny@lf1.cuni.cz

<https://doi.org/10.14712/23362936.2022.20>

© 2022 The Authors. This is an open-access article distributed under the terms of the Creative Commons Attribution License (<http://creativecommons.org/licenses/by/4.0>).

## Introduction

Despite great research efforts in ADHD treatment options, there are still many issues that have not been fully clarified yet. Here we try to extend our previous discussions on this topics (Mourek and Pokorný, 2021). If we look only at research conclusions that are not too old, a clear clinical experience prevails: boys with a diagnosis of ADHD are evidently more common in outpatient clinics than girls. At the same time, the authors do not hesitate to state the mutual incidence ratio of ADHD, which at that time was 10:1 (Bouček and Pidrman, 2005). With the onset of work that began to emphasize the genetic link (cause) of ADHD, the index (ratio) of sex-dependent ADHD began to change gradually, either in the sense that differences were not mentioned (e.g. Du Rietz et al., 2018), or only in the notes without specifying (Rubia, 2018). It is noteworthy that even in the “older” comprehensive studies on ADHD, the possible mechanism behind the differences in sex-dependent incidence of this disease is not mentioned at all (Tarver et al., 2014), or only touched (Konrad and Eickhoff, 2010). If genetic analysis was done, the sex difference was omitted and only male patients were studied (Swanson et al., 2000), though the work concerned newborns (Lou et al., 2004) or the young generation (Paclt et al., 2010). Contemporary papers admit the sex ratio ranging from 2:1 to 10:1 (Ramtekkar et al., 2010; Willcutt, 2012; Mowlem et al., 2019). Gender differences were not found in impulsivity, academic performance, social functioning, fine motor skills, parental education, or parental depression. However, compared with ADHD girls, ADHD boys displayed lower intellectual impairment, higher levels of hyperactivity, and higher rates of other externalizing behaviors (Gaub and Carlson, 1997).

## Genetic predisposition

With the advancing therapeutic experience, the authors became interested in the real causes of the difference in the incidence of ADHD in males and females. The genetic predisposition breaks down into two separate groups. One is the genome of an individual with ADHD and the other is the genome of the parents. Studies on the genetic factors in the genesis of ADHD brought about several fundamental facts.

A) ADHD occurs in 3–7% (elsewhere 3–5%) children (according to anamnesis).

B) At the same time, there is a long-standing and “unshakable” fact that the same – or similar percentage – corresponds to the high-risk newborns (premature birth, immaturity, hypotrophy, hypoxic-ischemic syndrome, low birth weight, etc.). This connection of both “external” risks on the genesis of ADHD syndrome with a possible genetic predisposition is currently respected (Momany et al., 2017; Saez et al., 2018; Shaw et al., 2020).

At the same time, there is a long-established fact that the male gender has – compared to the female – a lifelong handicap: males have a higher mortality rate practically throughout their life, i.e. from the neonatal period to death. Since birth, there is also a higher morbidity, a higher incidence of prematurity and respiratory

distress syndrome (Steen et al., 2014; Pongou, 2015). Also more males are born with a birth defect (Zdravotnická ročenka České republiky, 2015).

We can therefore ask whether these facts constitute a “physiological” norm, i.e. the female gender is the norm or it is privileged by nature. This is not a pun, but a serious question of deeper biological significance, including the developmental aspects of the facts described above. The idea of the role of X and Y chromosomes in the sex-dependent differences in morbidity and mortality of males and females (i.e. not only in newborns) is related to the number of genes (Y chromosome contains only 50, while X approximately 3,000!). However, other pressing issues arise.

To date, the idea of ADHD as a neurodevelopmental disease is generally accepted, namely with a reflection on noradrenaline and dopaminergic signalling. This hypothesis reflects results of the therapy that has been using drugs blocking their reuptake. However, it is still difficult to link this fact to possible recessive elements on the Y chromosome. In this regard, a targeted genetic search (Šerý et al., 2015) is in place. Parallel findings of a lower volume of some areas of the CNS (central nervous system) (basal ganglia, corpus callosum, etc.) (Rubia, 2018; Tang et al., 2019) raise more and more questions. The smaller volume can be explained by lower number of neurons, their smaller volume, less numerous glial elements, reduced dendrification and reduced interneuronal connections or a smaller intercellular spaces. These structural changes may be related to the individual handicap from the beginning of life (low birth weight, immaturity, etc.) and can bring various defects in cognitive functions. Manifestation of ADHD symptoms can therefore be either a specific or completely general reaction.

### **Metabolic disorders**

It is necessary to mention also the research findings that links and interprets ADHD to metabolic disorders. Changes in functional relationship between the glial and neuronal compartments has been mentioned (Russell et al., 2006) as well as the imbalance (mostly in terms of increase) of oxygen radical production (Kul et al., 2015; Sezen et al., 2016). The defective activity of mitochondria (without gender discrimination) and the resulting possible insufficiency in ATP production may be highly significant (Verma et al., 2016), suggesting an impairment of all mitochondrial functions, including their scavenger capacity.

### **Catecholamines**

The catecholamine network in the CNS is very extensive, surprisingly, despite of the relatively small number of catecholaminergic neurons (locus coeruleus, substantia nigra and VTA – area tegmentalis ventralis) (Smeets and Gonzales, 2000; Mravec and Kiss, 2004). Axons of these neurons can form up to several thousand (!) synapses. Very specific property is also their ability (limited) of self-regeneration – probably with justified significance (Bjorklund and Stenevi, 1979). Catecholamines are – from a developmental point of view – a very strong conservative element.

The acknowledged fact about the combined effects of genetic predisposition + multifactorial epigenetic effects (during pregnancy, childbirth and early postnatal period) on the ADHD manifestation was finalized in the therapeutic area with treating ADHD as a noradrenaline and dopamine insufficiency.

The major problem of experimental analysis of the ADHD syndrome is the absence of a relevant animal model. Our research was therefore aimed at the already suggested hypothesis of the role of catecholamines in ADHD. The study is entirely based on laboratory rats (Wistar type). Animal studies are always argued whether the results apply to humans. However, we know – and this is a general experience – that animal experiments are a good steppingstone for further research.

Dopamine beta-hydroxylase (DBH) (E.C. 1.14.17.1) is an enzyme that converts dopamine to norepinephrine. This enzyme has been identified in synaptic vesicles of sympathetic nerve terminals, blood plasma, adrenal medulla, etc. Although it can hydrolyse various substrates, its activity in noradrenaline synthesis can be considered by far the most common and biologically most important. The fact that norepinephrine and dopamine – to a lesser extent adrenaline – are critical and essential molecules for functioning and behavior was first stated in 1965 (Kaufman and Friedman, 1965). The results of our first measurement are presented in Figure 1.

Throughout postnatal life, female Wistar rats showed a significantly higher concentration of dopamine beta-hydroxylase in plasma than males. This applies to the early postnatal period, to the period of the so-called “weaning” (around the

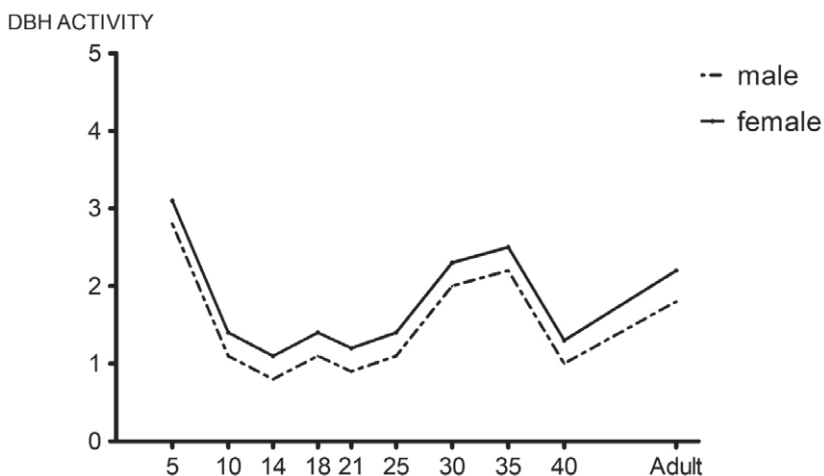


Figure 1 – Changes in dopamine beta hydroxylase in the plasma of female and male rats (Wistar). The measurements took place at intervals from the 5<sup>th</sup> day of postnatal life to adulthood (age 2 months). Enzyme activity is expressed in nmol/min/ml. Results in females are connected with a solid line, dashed in males.

## DBH ACTIVITY

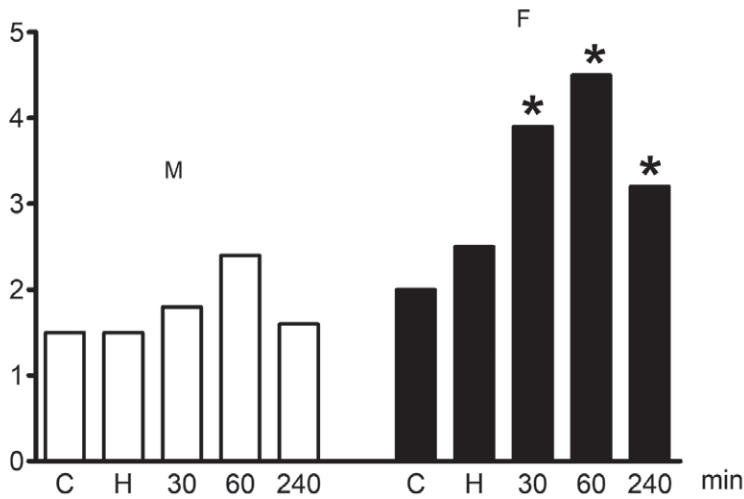


Figure 2 – The effect of stress, i.e. the effect of aerogenic altitude hypoxia on dopamine beta hydroxylase activity in the plasma of adult males (M) and females (F). The hypoxia corresponded to 7,000 m and lasted 20 minutes under euthermic conditions. C – control value, H – measurement immediately after the end of hypoxia, subsequent measurement after the end of hypoxia in time periods given in minutes. Activity expressed in nmol/min/ml. The asterisk indicates the statistical significant difference to control values ( $P < 0.05$ ).

21<sup>st</sup> day of postnatal life) and to the period of completed puberty (the 35<sup>th</sup> day of postnatal life). We exposed adult animals to 20 minutes of experimental stress, i.e. to so-called short-term altitude hypoxia, corresponding to 7,000 m, ( $pO_2 = 8.6$  kPa) in a euthermic environment (Koudelová and Mourek, 1990). The results are presented in Figure 2.

We found highly statistically significant differences (much higher values of DBH) in females 30, 60 and 240 minutes after the stress. This higher response in females means a lot: it is accompanied with demonstrable benefits for the body = norepinephrine effects of on metabolism, cardiovascular system, etc. This can finally bring a more successful managing the previous stressful situation.

**Table 1 – Ascorbic acid (ascorbate) content in cortex, mesencephalon and cerebellum in adult females and male rats (Wistar)**

	Cortex	Mesencephalon	Cerebellum
Females	4.06 ± 0.09	2.50 ± 0.91	4.28 ± 0.32
Males	2.59 ± 0.04	1.57 ± 0.04	1.64 ± 0.05

Values are given in mmol/kg w.w. tissues (w.w. – wet tissues, immediately after dissection); averages ± SD (standard deviation)

### Ascorbic acid

The synthesis of norepinephrine has one *sine qua non* condition for the effectiveness of DBH – this condition (or cofactor) is the presence of ascorbic acid as a reducing agent. Therefore, if DBH has consistently higher levels in females, and if these higher levels are to be able to increase activities at the same time, then a higher quantum of ascorbic acid must be available in the female. Therefore, we performed experiments to monitor the content of ascorbic acid in individual regions of the CNS (Koudelová and Mourek, 1991), including an experiment with stress. Results (on adult females and males [Wistar]) – in a simplified form presents Table 1.

Both in the cortex (grey matter) and in the subcortical areas of the mesencephalon or in the cerebellum, the ascorbic acid content was significantly higher in females than in males. It can be explained that DBH activity in females has a significantly higher capacity than in males. In another experiment, we measured ascorbic acid in the CNS (cortex and brain stem) after the exposure to a stressful situation (hypoxia corresponding to 9,000 m and lasting 20 minutes under euthermic conditions,  $pO_2 = 6.4$  kPa). The results are given in Figure 3.

In both the cortex and medulla oblongata, stress-induced increase of ascorbate levels was always significantly higher in females – compared to males. These results correspond to our results with DBH. In reality, this means a greater capacity for the production of noradrenaline in the CNS, with larger (more adequate) functional

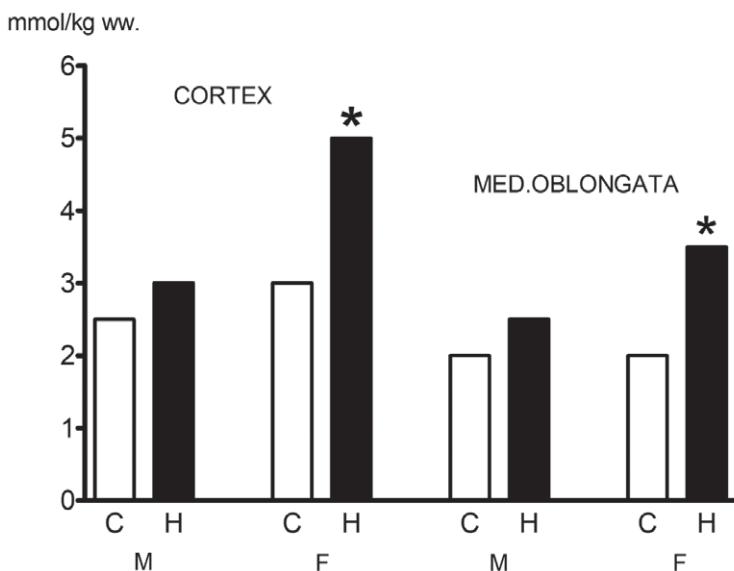


Figure 3 – The content of ascorbic acid (ascorbate) in the cerebral cortex and in the medulla oblongata of 21-day-old laboratory rats. C – control value, H – value after altitude hypoxia (9,000 m for 20 minutes). F – females, M – males. The asterisk indicates the statistical significance to control values ( $P < 0.01$ ). The ascorbate content is expressed in mmol/kg w.w.

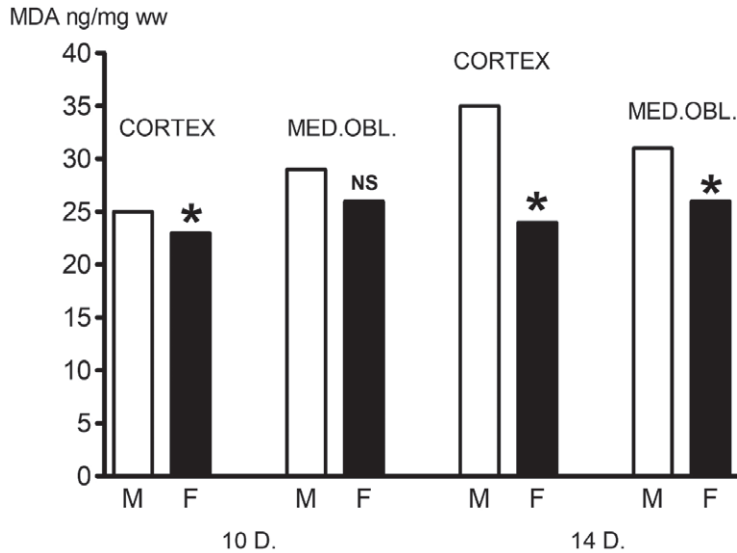


Figure 4 – Influence of altitude hypoxia (7,000 m, 20 minutes) on lipoperoxidation processes (production of malonyldialdehyde [MDA] in the cerebral cortex and spinal cord of 10- and 14-day-old laboratory rats [Wistar]). F – females, M – males. The asterisk indicates the statistical significant difference between males and females ( $P < 0.01$ ). MDA production in ng/mg w.w.

capacity. Indeed, catecholamines significantly increase membrane Na-K ATPase activity (E.C.6.1.3.) both *in vivo* and *in vitro* experiments (Mourek, 1979, 1985, 1987). This enzyme is an important factor contributing to the level of the resting membrane potential. An increased value of the resting membrane potential means a lower level of the neuronal excitability (the threshold for the activation is increased). Thus, in terms of today's ADHD therapy, females are significantly better provided than males.

In the introduction, we cited the authors (Kul et al., 2015; Sezen et al., 2016) who consistently report increased production of oxygen radicals (ROS) in individuals with ADHD. ROS attack various molecular structures of the mammalian cells, but they still have a certain “preference”. These may be unsaturated fatty acids (especially localized in cell membranes) that in the oxidative milieu may undergo a disintegration process. Already in 2005 (Mourek et al., 2005) we carried out an experiment using laboratory rats at the age of 10 and 14 days of postnatal life. Both male and female animals were repeatedly exposed to the stressor, represented by a 20-minute stay in simulated conditions of altitude hypoxia (corresponding to 7,000 m,  $pO_2 = 8.6$  kPa). Subsequently, production of malonylaldehyde was measured in the cortex and in the spinal cord. The results are documented in Figure 4.

In all 4 groups, female rats showed lower malonylaldehyde production than males. Three of those differences were significant.

As already mentioned, since the very beginning of their existence, individuals with XY chromosomal combination have higher morbidity and mortality. Perinatal morbidity and/or exposition to risk conditions in boys represent a putative error factor for the developmental cascades, especially for such a sensitive and at the same time energy and substrate demanding development process as is the formation of CNS microstructure.

## Conclusion

The presented results of experiments on laboratory rats represent a *de facto* hypothesis that can be applied to humans. Considering all its critical issues, we presume a certain validity of our findings to the possible therapeutic procedures. We consider the question whether the sufficient (= physiological) release of noradrenaline (and dopamine, to a lesser extent also adrenaline) in the CNS catecholaminergic neuronal circuits represents the basic regulatory element for the level of neuronal membrane Na-K ATPase activity in the regulation of neuronal excitability. The state, value and variability of the resting membrane potential of neurons is directly linked to their functional activity in the sense of a binary response (+ or –). We are fully aware that beside our hypothesis, there can be (and probably are) other “players” in the game.

We have demonstrated in three series of experiments that females carrying XX chromosomes are biologically favoured. This leads us to the final idea that the disparity between boys and girls in the incidence of ADHD symptoms is an expression of the basic biological axiom about the advantage (protection) of XX carriers. They are more important for the survival of the species.

## References

- Bjorklund, A. N., Stenevi, U. (1979) Regeneration of monoaminergic and cholinergic neurons in the mammalian central nervous system. *Physiol. Rev.* **59(1)**, 62–100.
- Bouček, J., Pidrman, V. (2005) *Psychofarmaka v Medicíně*. Grada, Praha.
- Du Rietz, E., Coleman, J., Glanville, K., Choi, S. W., O'Reilly, P. F., Kuntsi, J. (2018) Association of polygenic risk for attention-deficit/hyperactivity disorder with co-occurring traits and disorders. *Biol. Psychiatry Cogn. Neurosci. Neuroimaging* **3(7)**, 635–643.
- Gaub, M., Carlson, C. L. (1997) Gender differences in ADHD: A meta-analysis and critical review. *J. Am. Acad. Child Adolesc. Psychiatry* **36(8)**, 1036–1045.
- Kaufman, S., Friedman, S. (1965) Dopamine-β-hydroxylase. *Pharmacol. Rev.* **17(2)**, 71–100.
- Konrad, K., Eickhoff, S. B. (2010) Is the ADHD brain wired differently? A review on structural and functional connectivity in attention deficit hyperactivity disorder. *Hum. Brain Mapp.* **31(6)**, 904–916.
- Koudelová, J., Mourek, J. (1990) Influence of sex and hypoxia on plasma dopamine-beta-hydroxylase activity in the rat. *Physiol. Bohemoslov.* **39**, 409–416.
- Koudelová, J., Mourek, J. (1991) Lipid peroxidation and changes of ascorbic acid level in hypoxic brain of 21-day-old rats. *Wiss. Z. Humboldt Univ., R. Medizin* **40**, 47–51.
- Kul, M., Unal, F., Kandemir, H., Sarkarati, B., Kilinc, K., Kandemir, S. B. (2015) Evaluation of oxidative metabolism in child and adolescent patients with attention deficit hyperactivity disorder. *Psychiatry Investig.* **12(3)**, 361.

- Lou, H. C., Rosa, P., Pryds, O., Karrebæk, H., Lunding, J., Cumming, P., Gjedde, A. (2004) ADHD: Increased dopamine receptor availability linked to attention deficit and low neonatal cerebral blood flow. *Dev. Med. Child Neurol.* **46(3)**, 179–183.
- Momany, A. M., Kamradt, J. M., Ullsperger, J. M., Elmore, A. L., Nigg, J. T., Nikolas, M. A., (2017) Sex moderates the impact of birth weight on child externalizing psychopathology. *J. Abnorm. Psychol.* **126(2)**, 244.
- Mourek, J. (1979) Effect of adrenaline on ATPase activities in different parts of developing brain. *Physiol. Bohemoslov.* **28**, 573–576.
- Mourek, J. (1985) Vliv *in vitro* izoprenalinu na aktivitu Na-K a Mg dependentní ATPasy v mozku různě starých kryš. *Sb. Lek.* **87**, 209–215.
- Mourek, J. (1987) Beta receptory mozkové kůry a jejich význam pro aktivitu Na-K ATPázy u různě starých kryš. *Sb. Lek.* **89**, 335–339.
- Mourek, J., Pokorný, J. (2021) Příspěvek k interpretačním možnostem syndromu ADHD. *Ceska Slov. Psychiatr.* **117(3)**, 138–143.
- Mourek, J., Šmídová, L., Dohnalová, A. (2005) Lipoperoxidative activities in the cerebral cortex and medulla oblongata, related to age, sex, oxygen deficiency and short-term fasting. *Prague Med. Rep.* **106(3)**, 253–260.
- Mowlem, F. D., Rosenqvist, M. A., Martin, J., Lichtenstein, P., Asherson, P., Larsson, H. (2019) Sex differences in predicting ADHD clinical diagnosis and pharmacological treatment. *Eur. Child Adolesc. Psychiatry* **28(4)**, 481–489.
- Mravec, B., Kiss, A. (2004) The brain catecholamines. Brief anatomy and participation in the stress reaction and regulation of cardiovascular function. *Cesk. Fysiol.* **53**, 102–116. (in Slovak)
- Pact, I., Drtílková, I., Kopečková, M., Theiner, P., Šerý, O., Čermáková, N. (2010) The association between TaqI A polymorphism of ANKK1 (DRD2) gene and ADHD in the Czech boys aged between 6 and 13 years. *Neuro Endocrinol. Lett.* **31(1)**, 131–136.
- Pongou, R. (2015) Why is mortality higher in boys than in girls? A new hypothesis based on preconception environment and evidence from large sample of twins. *Demography* **50**, 421–444.
- Ramtekkar, U., Reiersen, A., Todorov, A., Todd, R. (2010) Sex and age differences in attention-deficit/hyperactivity disorder symptoms and diagnoses: Implications for DSM-V and ICD-11. *J. Am. Acad. Child Adolesc. Psychiatry* **49**, 217–228.
- Rubia, K. (2018) Cognitive neuroscience of attention deficit hyperactivity disorder (ADHD) and its clinical translation. *Front. Hum. Neurosci.* **12**, 1–23.
- Russell, V. A., Oades, R. D., Tannock, R., Killeen, P. R., Auerbach, J. G., Johansen, E. B., Sagvolden, T. (2006) Response variability in attention-deficit/hyperactivity disorder: A neuronal and glial energetics hypothesis. *Behav. Brain Funct.* **2(1)**, 1–25.
- Saez, M., Barceló, M. A., Farrerons, M., López-Casasnovas, G. (2018) The association between exposure to environmental factors and the occurrence of attention-deficit/hyperactivity disorder (ADHD). A population-based retrospective cohort study. *Environ. Res.* **166**, 205–214.
- Šerý, O., Pact, I., Drtílková, I., Theiner, P., Kopečková, M., Zvolský, P., Balcar, V. J. (2015) A 40-bp UZISVNTN polymorphism in the 3'-untranslated region of DAT1/SLC6A3 is associated with ADHD but not with alcoholism. *Behav. Brain Funct.* **11(1)**, 1–8.
- Sezen, H., Kandemir, H., Savik, E., Basmacı Kandemir, S., Kilicaslan, F., Bilinc, H., Aksoy, N. (2016) Increased oxidative stress in children with attention deficit hyperactivity disorder. *Redox Rep.* **21(6)**, 248–253.
- Shaw, J. C., Crombie, G. K., Zakar, T., Palliser, H. K., Hirst, J. J. (2020) Perinatal compromise contributes to programming of GABAergic and glutamatergic systems leading to long-term effects on offspring behaviour. *J. Neuroendocrinol.* **32(1)**, e12814.

- Smeets, W., Gonzales, A. (2000) Catecholamine system in brain of vertebrate: New perspectives through a comparative approach. *Brain Res.* **35**, 308–379.
- Steen, E. E., Källén, K., Maršál, K., Norman, M., Hellström-Westas, L. (2014) Impact of sex on perinatal mortality and morbidity in twins. *J. Perinat. Med.* **42(2)**, 225–231.
- Swanson, J. M., Flodman, P., Kennedy, J., Spence, M. A., Moyzis, R., Schuck, S., Murias, M., Moriarity, J., Barr, C., Smith, M., Posner, M. (2000) Dopamine genes and ADHD. *Neurosci. Biobehav. Rev.* **24(1)**, 21–25.
- Tang, X., Seymour, K. E., Crocetti, D., Miller, M. I., Mostofsky, S. H., Rosch, K. S. (2019) Response control correlates of anomalous basal ganglia morphology in boys, but not girls, with attention-deficit/hyperactivity disorder. *Behav. Brain Res.* **23(367)**, 117–127.
- Tarver, J., Daley, D., Sayal, K. (2014) Attention-deficit hyperactivity disorder (ADHD): An updated review of the essential facts. *Child Care Health Dev.* **40(6)**, 762–774.
- Verma, P., Singh, A., Nthenge-Ngumbau, D. N., Rajamma, U., Sinha, S., Mukhopadhyay, K., Mohanakumar, K. P. (2016) Attention deficit-hyperactivity disorder suffers from mitochondrial dysfunction. *BBA Clin.* **6**, 153–158.
- Willcutt, E. G. (2012) The prevalence of DSM-IV attention-deficit/hyperactivity disorder: A meta-analytic review. *Neurotherapeutics* **9**, 490–499.
- Zdravotnická ročenka České republiky (2015) Vývoj novorozenecké, kojenecké a perinatální úmrtnosti. ÚZIS ČR, Praha.

# A Response of the Pineal Gland in Sexually Mature Rats under Long-term Exposure to Heavy Metal Salts

**Nataliia Hryntsova<sup>1</sup>, Ingrid Hodorová<sup>2</sup>, Josef Mikhaylik<sup>2</sup>, Anatoly Romanyuk<sup>3</sup>**

<sup>1</sup>Department of Morphology, Medical Institute, Sumy State University, Sumy, Ukraine;

<sup>2</sup>Department of Anatomy, Faculty of Medicine, Pavol Jozef Šafárik University in Košice, Košice, Slovak Republic;

<sup>3</sup>Department of Pathological Anatomy, Medical Institute, Sumy State University, Sumy, Ukraine

Received December 11, 2020; Accepted November 2, 2022.

**Key words:** Pineal gland – GPX-1 – Heavy metals – Reactive astrogliosis – Oxidative stress

**Abstract:** Pollution with heavy metal salts is an important environmental problem today, having an adverse effect on public health. The endocrine system maintains homeostasis in the body. The antioxidant protection (GPX-1) of the pineal gland in mature rats was studied. Animals of the experimental group represented a model of microelementosis, achieved by adding a mixture of heavy metal salts for 90 days to drinking water: zinc ( $\text{ZnSO}_4 \times 7\text{H}_2\text{O}$ ) – 5 mg/l, copper ( $\text{CuSO}_4 \times 5\text{H}_2\text{O}$ ) – 1 mg/l, iron ( $\text{FeSO}_4$ ) – 10 mg/l, manganese ( $\text{MnSO}_4 \times 5\text{H}_2\text{O}$ ) – 0.1 mg/l, lead ( $\text{Pb}(\text{NO}_3)_2$ ) – 0.1 mg/l, and chromium ( $\text{K}_2\text{Cr}_2\text{O}_7$ ) – 0.1 mg/l. Morphological, statistical and immunohistochemical (GPX-1) research methods were used. Long-term (90-days) intake of heavy metal salts mixture in the body of experimental animals brought about development of the general adaptation syndrome, the stage of chronic stress “subcompensation” in the pineal gland. Morphological rearrangements were of nonspecific polymorphic nature as severe hemodynamics disorder in the

*This study was supported by VEGA 1/0173/19, Scholarship of the Government of the Slovak Republic (2020), the research project “Modern views on the morphogenesis of general pathological processes”, state registration No. 0119U100887 (02.2019-02.2024).*

**Mailing Address:** Assoc. Prof. Nataliia Hryntsova, PhD., Department of Morphology, Medical Institute, Sumy State University, Sanatorium 33, 40000 Sumy, Ukraine; Phone: +38(095)39 28 837; e-mail: natalia.gryntsova@gmail.com

organ, impairment of vascular wall morphology, development of tissue hypoxia and oxidative stress, accompanied by processes of accelerated apoptosis in part of pinealocytes, by a significant decrease in glutathione peroxidase level in the organ and reactive astrogliosis as a response to the damaging agent's action. Along with the negative changes in the pineal gland, a compensatory-adaptive processes with signs of functional stress also occurred. A sufficiently high degree of glutathione peroxidase activity in 39% of pinealocytes located perivascularly, active adaptive glial reaction and activation of synthetic processes in some pinealocytes were also observed.

---

## Introduction

Pollution with heavy metal salts is an important environmental problem today, having an adverse effect on public health. Such a negative effect determines development and course of oncological pathology, disorders of the body homeostasis and morphological transformations in various tissues (Romanjuk et al., 2018a, 2019), as each trace element with excessive exposure can be potentially toxic (Bharti et al., 2014). It is believed that the formation of free radicals, lipid peroxidation and changes in the antioxidant defence system play an important role in the toxic effects of heavy metals. Thus, heavy metals are able to penetrate freely into any cell due to their good fat solubility, to cause various modifications in the structure of DNA and RNA with changes in the function of many transcription factors, to raise lipid peroxidation of membrane formations, bind sulfhydryl groups of enzymes and proteins, and to change the electrolyte balance with accumulation of intracellular calcium ions. Under the influence of metals, the functional balance between oxidative and antioxidant mechanisms generally shifts in favour of the former with a decrease in the activity of superoxide dismutase, catalase, glutathione peroxidase and a decrease in the level of natural antioxidants such as glutathione. The set of serious lesions also includes damage to mitochondria and the microsomal apparatus of cells (Hemdan et al., 2005; Valko et al., 2005). Various human diseases and toxicity are often associated with oxidative stress. This pathophysiological stress has multiple effects, but is particularly characterized by decreased enzymatic activity, including catalase (CAT), superoxide dismutase (SOD), glutathione peroxidase (GPX-1) and glutathione reductase (GR) (Rzeuski et al., 1998; Bharti et al., 2014).

### *The human pineal gland and oxidative stress*

At present, the human pineal gland is the least studied endocrine gland, which occupies one of the central places in the endocrine regulation of all organs and systems' vital activity, carries out adaptive reactions of the body to changing environmental conditions. It is known that the melatonin hormone (indole metabolite of the tryptophan amino acid, which is mainly produced by the pineal gland) is the strongest natural inhibitor of free radical processes in the body (Russel, 2000; Bharti et al., 2014). In experiments *in vitro* melatonin reduces the formation

of hydroxyl radical by 5 to 14 times more efficiently than other known inhibitors such as glutathione (Arushanyan, 2004). In both *in vitro* and *in vivo* experiments, it has been shown that epiphyseal indoles, and in particular melatonin, are able to neutralize the manifestations of oxidative stress that occurs when intoxicated by various metal compounds. It is known that melatonin protects endocrine tissue from peroxidation initiated by ferrous sulphate (Karbownik and Lewinski, 2003), copper (Daniels et al., 1998), chromium (Susa et al., 1997), lead acetate (El-Missiry, 2000; El-Sokkary et al., 2003). At the same time melatonin acted as a “trap” for free radicals and simultaneously improved the functional state of the natural antioxidant system by activating the enzymes that were part of it: superoxide dismutase, catalase, glutathione peroxidase (Arushanyan and Elbekyan, 2006). In this case, according to the literature, the origin of melatonin antitoxic effect may be due to the direct chemical interaction of the hormone and individual metals. Thus, using electrochemical methods it has been shown that various metals (aluminium, copper, iron, zinc) can form complexes with melatonin, which acts as their chelator (Limson et al., 1998; Arushanyan and Elbekyan, 2006).

Heavy metal salts, particularly lead, have a multiple toxic effect on the blood and the cardiovascular systems. Thus, lead inhibits enzymes involved in the synthesis of haem and globin and as a result reduces the amount of hemoglobin, which affects the formation of erythrocytes. Impairment of porphyrin synthesis and due to iron and aminolevulinic acid accumulation may be one of the causes for activation of oxidative stress and lipid peroxidation (Trachtenberg et al., 2015). The hemocoagulation system is also sensitive to the action of lead in low doses. Increased hemostasis activity, development of hypercoagulation syndrome and disseminated intravascular blood coagulation, inhibition of fibrinolytic activity, which indicates the activation of thrombosis, have been experimentally established (Trachtenberg et al., 2010, 2015).

As a result of the hemotoxic effect of lead, hemic and circulatory hypoxia occurs, which results in the development of tissue hypoxia in the body, activation of free radical oxidation and oxidative stress, which causes implementation of lead's vasotoxic effect (Apikhtina et al., 2012; Trachtenberg et al., 2015). A characteristic feature of oxidative stress is that when the damage increases above a certain critical level, the cell's self-elimination program – apoptosis – is activated (Trachtenberg et al., 2001).

The activity of oxidative stress reactions depends on the absolute or relative content of endogenous antioxidants in the tissues (tocopherols, ascorbic acid, thio- and selenium-containing compounds). Their increased or decreased concentration may affect the intensity of oxidative stress (Belenichev, 2014).

#### *Family of glutathione peroxidases (GPX)*

Among selenoproteins, highly reported on, there is the family of glutathione peroxidases (GPX), which are involved in the regulation of the redox state and in

protection against oxidative damage. The glutathione peroxidase activity in the pineal gland is higher compared to other brain structures (Razygraev, 2004). Relatively high concentrations of selenium were found in the pineal gland, which is due to its antioxidant properties, in particular to its ability to neutralize reactive oxygen intermediates formed during the synthesis of melatonin (Reiter, 1996; Kravtsiv and Yanovich, 2008). The GPX-1 enzyme is a homotetramer and contains selenocysteine. This means that GPX-1 expression is affected by the level of selenium in the studied tissue or organ.

#### *Astroglia of the pineal gland*

In the pineal gland, the degree of oxidative stress and pinealocytes apoptosis development can be impliedly judged by the quantitative indices of pinealocytes and glial elements present in the gland, as well as by the morphological features of the pinealocytes' nuclear apparatus (Gubina-Vakulik, 2006). After all, according to modern views on the functions and morphology of astroglia, astrocytes are able to synthesize gas transmitters, including carbon monoxide (CO), which is involved in the mechanisms of inflammation and apoptosis. In addition, the increase in the number of glial elements in the pineal gland certainly has a compensatory-adaptive value, particularly in the processes of RNA, amino acids, growth factors transfer to pinealocytes and by controlling water-ion homeostasis in the gland (Goryainov et al., 2013). It is impossible to overestimate the contribution of astrocytes in the protection of the gland's parenchyma from oxidative stress through the synthesis of hydrogen sulphide (H<sub>2</sub>S). This gas gliotransmitter has synaptic modulator and neuroprotective properties, protecting against oxidative stress (Goryainov et al., 2013). Therefore, activity assessment of antioxidant enzymes and markers of free radical damage in the pineal gland is important for assessing the toxicity of heavy metal salts mixture for the antioxidant system of the pineal gland. According to the authors, the effect of heavy metal salts mixture on the antioxidant system of the pineal gland is an urgent problem and requires a detailed study.

The purpose of the work is to study the system of the pineal gland's antioxidant protection in sexually matured male rats under the conditions of long-term exposure to a mixture of heavy metal salts.

### **Material and Methods**

#### *Animals*

The experiment was performed on 24 white sexually mature male rats weighing 200–250 g, aged 7–8 months, which were divided into 2 groups (the control and the experimental ones). Animals of both groups were kept in the normal vivarium conditions, where equal keeping conditions, nutrition, proper care and natural light (day/night) were maintained, with a constant ambient temperature (20–22 °C). The animals had free access to drinking water. The study was carried out in the autumn-winter period.

### *Experimental microelementosis model*

The experimental group included rats, which for 90 days received drinking water with a mixture of heavy metal salts: zinc ( $\text{ZnSO}_4 \times 7\text{H}_2\text{O}$ ) – 5 mg/l, copper ( $\text{CuSO}_4 \times 5\text{H}_2\text{O}$ ) – 1 mg/l, iron ( $\text{FeSO}_4$ ) – 10 mg/l, manganese ( $\text{MnSO}_4 \times 5\text{H}_2\text{O}$ ) – 0.1 mg/l, lead ( $\text{Pb}(\text{NO}_3)_2$ ) – 0.1 mg/l, and chromium ( $\text{K}_2\text{Cr}_2\text{O}_7$ ) – 0.1 mg/l. The selected concentration of salts in the mixture was due to the presence of such concentrations of these salts in the soil and drinking water of some regions in Ukraine according to literature sources (Romanjuk et al., 2018a, b, 2019).

### *Termination of microelementosis induction*

After the 90<sup>th</sup> day of the experimental procedure, animals of both groups were anesthetised by thiopental injection (at the dose of 30–40 mg/10 g body weight) before the subsequent surgical and histological procedures. All the animal studies were conducted in accordance with the provisions of the European Convention for the Protection of Vertebrate Animals for Experimental and Scientific Purposes (Strasbourg, 1986) and the “General Ethical Rules for Animal Experiments” approved by the First National Congress of Bioethics (Kyiv, 2001, Ukraine), Protocol No. 4 of 06/03/2020 Commission of Bioethics of Sumy State University. The subject of the study is the pineal gland of experimental and control animals.

### *Pineal gland extraction technique and histological studies*

To study the morphological changes in the structural components of the pineal gland conventional procedures of microanatomical (histological) study method were used. In order to carry out morphological, morphometric and immunohistochemical studies of the pineal gland, the organ was extirpated and histological tissue specimens were made according to the original method developed by the authors (Hryntsova and Romanyuk, 2020; Hryntsova et al., 2020). In this case, for the purpose of atraumatic extirpation, the pineal gland was not completely dissected

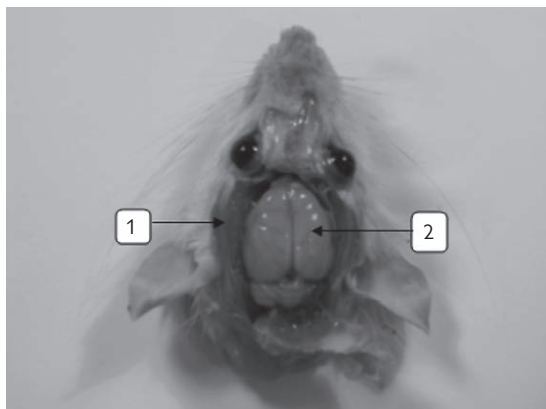


Figure 1 – Circumferential dissection of the skull on the parietotemporal bones (1), exposure of the brain (2) (digital photo).

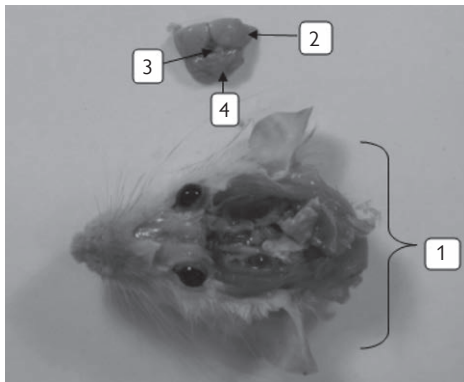


Figure 2 – Extirpation of the pineal gland with the organo-complex (together with fragments of the brain and cerebellum adjacent to the pineal gland) (digital photo).

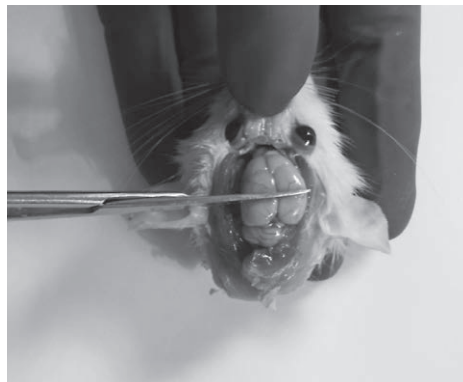


Figure 3 – Head of a decapitated rat with extirpated brain (1). Organo-complex: a fragment of the brain (2), the pineal gland (3), a fragment of the cerebellum (4) before fixation (digital photo).

from the epithalamus of diencephalon, instead, it was extirpated together with fragments of the brain and cerebellum adjacent to it (Figures 1–3).

The pineal gland, together with the adjacent tissues, was immersed in the fixing fluid (5% formalin solution) for the period of 12–24 hours (Figure 3).

The dehydration process was carried out in a number of ethyl alcohol portions with ascending concentrations of 70°, 80°, 90°, 96°, after which the objects were embedded in paraffin. Sections from 4 to 5  $\mu\text{m}$  thick were made of histological blocks with a rotary microtome, followed by making permanent histological preparations and staining with hematoxylin-eosin according to standard procedure. The developed method permitted to rationally prepare the pineal gland, which prevented its injury and permitted to prepare high-quality histological specimens for light-optical, morphometric and immunohistochemical study methods.

Assessment of the pineal gland's morphological state was performed by a number of microscopic indices: state of stromal and parenchymal components, state of the vascular bed, changes in blood rheology, state of pinealocytes and astrocytic glia, including determination of neurocytoglial index and GPX-1 immunohistochemical marker, which is one of the most important antioxidative enzymes in mammals. To determine the gliocyto-neuronal index the ratio of the neuroglia location density to the density of pinealocytes location was found. To determine the density of pinealocytes and neuroglia in the pineal gland their absolute number was counted in the microscope field of view (ob. 40, oc. 10), studying at least 30 fields of view (Salkov et al., 2015). In this case viable pinealocytes only were taken into account.

General morphological and morphometric analysis was performed using the “Leica DM 500” light-optical microscope, with  $\times 4$ ,  $\times 10$ ,  $\times 40$  lenses, binoculars 7, 10. Photo documentation of the results obtained was performed with a digital video camera

“Leica DM IC C50 HD Camera”. “Leica Application Suite LAS EZ version 20.0 (Build: 292) Copyright @ 2010” software was used.

#### *Marker expression research GPX-1 method*

To study the changes of glutathione peroxidase activity in the cytoplasm of pinealocytes the immunohistochemical method was used.

Pineal glands were embedded in paraffin blocks using standard procedures.

1) Sections of 5 µm were cut, deparaffinised (dehydration in xylene and rehydration in alcohols in decreasing concentrations) and rinsed in EnVision Flex Wash Buffer (#K800721-2, Agilent Dako, Santa Clara, CA, USA, later in the text referred to as wash buffer). Endogenous peroxidase activity was blocked by incubation of slides in a mixture of methanol and hydrogen peroxide. After another rinsing in wash buffer, antigens were revitalized in the microwave.

2) Blocking

To block staining of non-specific structures slides were rinsed in wash buffer, and 2% milk blocking solution in Tris buffer was added.

3) Antigen-antibody reaction

Rabbit polyclonal GPX-1 antibodies produced by Bioss Antibodies Inc. (USA) were used in the reaction in a dilution of 1:250, serial number bs-3882R, reactivity: human, mouse and rat, isotype: IgG. Immunohistochemical reactions were performed in accordance with the Bioss Antibodies Inc. protocol (USA). The primary anti-GPX-1 rabbit polyclonal antibody was applied overnight at 4 °C, followed by rinsing in wash buffer. Subsequently, Biotinylated Link (#K0675, Agilent Dako, Santa Clara, CA, USA) was used, then slides were rinsed with wash buffer, and Streptavidin-HRP (#K0675, Agilent Dako, Santa Clara, CA, USA) was applied.

4) Final rendering

The tissue sections were again washed in wash buffer, and 3,3-diaminobenzidine (DAB) (#K5207, Agilent Dako, Santa Clara, CA, USA) was applied. The slides were rinsed in tap water, counterstained by hematoxylin, and embedded into Pertex® Mounting Medium 00811-EX (manufactured by Histolab Products AB).

The negative controls were created by omitting the primary antibody. Two observers independently evaluated the results of the immunostaining under a light microscope.

The level of GPX-1 marker of antioxidant activity expression was revealed immunohistochemically in the cytoplasm of pinealocytes. The expression of the GPX-1 marker was assessed by the number of the gland's cells whose cytoplasm had the colour characteristic for GPX-1.

#### *Statistical analysis*

Assessment of GPX-1 expression was performed semi-quantitatively by counting the number of stained cells per 100 cells in three fields of view, the result was expressed

as a percentage and assessed on the accepted scale: 1) no expression of GPX-1 (–), 2) 0–20% – low expression of GPX-1 (+), 3) 21–50% – moderate expression of GPX-1 (++) , 4) 51–100% – significant expression of GPX-1 (+++) (Lutsik and Yashchenko, 2018). Processing of digital results was performed by applied statistical methods using the Microsoft Word Excel 2010 text editor with AtteStat 12.0.5 application. Reliability of the difference between the experimental and control data of morphometric and immunohistochemical parameters was assessed using the Student's *t*-test, the probability of error less than 5% ( $p \leq 0.05$ ) was considered sufficient.

## Results

After 90 days of the experiment, the pineal gland of the experimental animals had an oval shape, maintained its anatomical integrity and connection with the vascular plexus. Heavy metal salts caused noticeable negative changes in all structural components of the gland: stromal, vascular and parenchyma. The capsule of the gland was slightly thickened, the intertrabecular spaces were expanded, in some areas – significantly. Quite pronounced morphological changes were observed in the vascular bed of dystonic nature compared to the control animals. In some areas, the lumen of the vessels was expanded, and in others, the vessels were spasmodic. Large vessels of the subcapsular zone and deep areas of parenchyma were full-blooded, with signs of impaired blood rheological properties. Erythrocytes completely filled the lumen of blood vessels, in some places they were very close to each other, their contours were not clearly delineated, blood stasis was formed, erythrocyte aggregation, sludge phenomenon were observed. The vascular wall

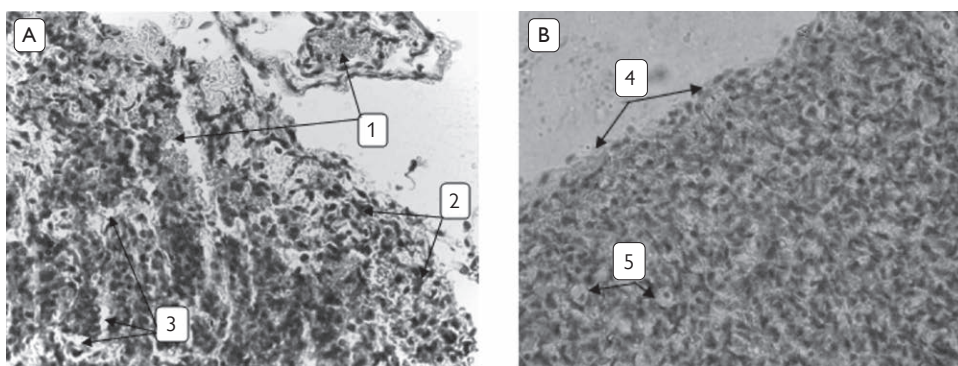


Figure 4 – Morphological rearrangements of the structural components in the pineal gland of experimental (A) and control (B) animals under the conditions of 90-day exposure to of heavy metal salts. A: 1 – plethora of the subcapsular zone vessels with signs of the blood rheological properties impairment; 2 – reactive astrogliosis; 3 – expansion of intertrabecular spaces; B: 4 – connective tissue capsule; 5 – light pinealocyte (hematoxylin-eosin staining,  $\times 400$ ).

was also affected, especially in the large afferent vessels of the epiphysis in the subcapsular zone. There was the vascular wall's thickening and its permeability increase, which was manifested in the release of erythrocytes into the extravascular space with the formation of diapedetic hemorrhages of different areas, expansion of the perivascular space. Around the vessels of the subcapsular zone, especially with impaired permeability of the vascular wall, and hemorrhages, a clearly pronounced active glial reaction was observed in the form of reactive astrogliosis. In addition to local, there was also a general diffuse glial reaction observed (Figure 4).

The results of light optical studies were confirmed by the previous immunohistochemical studies of Ki-67 proliferation marker (Romanjuk et al., 2018b), according to which the assessment of the Ki-67 protein's expression level revealed its moderate proliferative activity in peripheral astrocytes (35–40%). The intensity of cell nuclei staining was assessed as moderate (++).

Vascular plethora of the gland was accompanied by edema. Intertrabecular capillaries in some areas were spasmodic and were not visualized, possibly due to edema and disintegration of the fibrous component in the connective tissue trabeculae. In other fields of view, the lumen of the capillaries was significantly expanded with erythrocytes in their lumen, forming "rouleau" (Figure 5).

The pineal gland's parenchyma of experimental animals was distinct in some sponginess and accumulation of edematous fluid in the intertrabecular spaces. Discomplexation of cellular trabeculae and some disorders of cytoarchitecture were observed. In some fields of view around the pinealocytes pericellular edema was formed. The structure of the pineal gland's parenchyma was characterized by a mosaic nature of morphological changes. The tissue specimens were dominated by

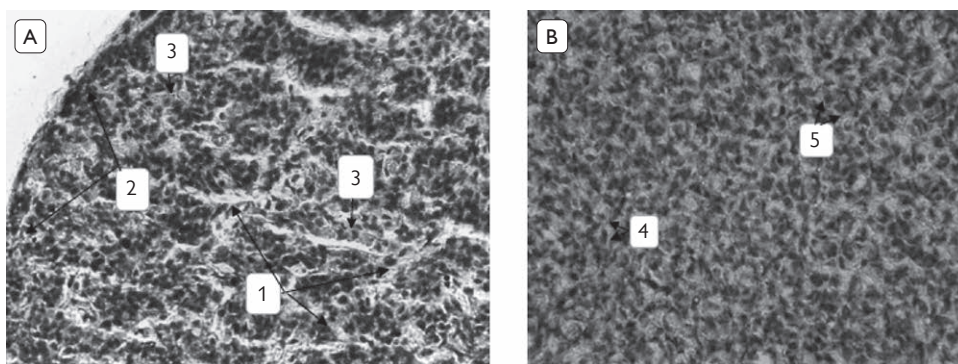


Figure 5 – Morphological rearrangements of the structural components in the pineal gland of experimental (A) and control (B) animals under the conditions of 90-day exposure to heavy metal salts. A: 1 – edema and disintegration of the fibrous component in the connective tissue trabeculae of the gland; 2 – reactive astrogliosis; 3 – “rouleau” in the lumen of the capillaries; B: 4 – light pinealocyte; 5 – dark pinealocyte (hematoxylin-eosin staining,  $\times 400$ ).

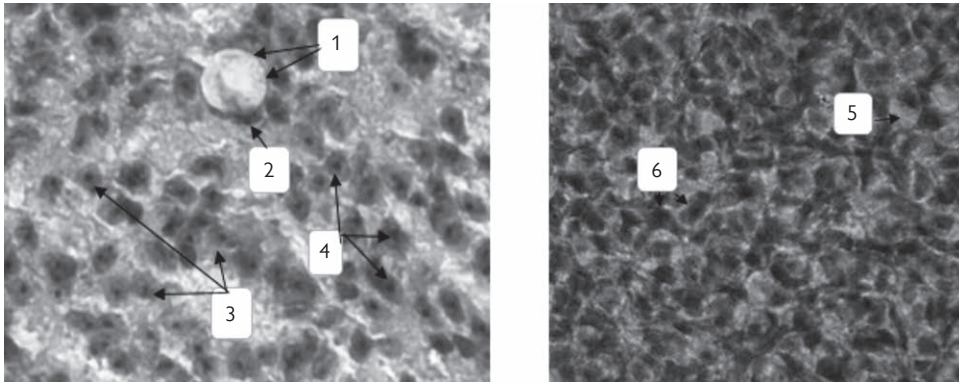


Figure 6 – Morphological rearrangements of the structural components in the pineal gland of experimental (A) and control (B) animals under the conditions of 90-day exposure to heavy metal salts. A: 1 – light pinealocyte with vacuolated cytoplasm; 2 – the nucleus with an eccentrically position; 3 – hypertrophied pinealocyte nuclei; 4 – hyperchromic, hypertrophied nucleolus; B: 5 – light pinealocyte; 6 – dark pinealocyte (hematoxylin-eosin staining,  $\times 800$ ).

light pinealocytes with cleared, often vacuolated cytoplasm and nuclei, both of oval and slightly deformed, angular shape. In vacuolated cells, the nuclei were shifted to the periphery, located eccentrically. On the periphery there were dark pinealocytes, frequently surrounded by astrocytic glia. In some cells, the size of the nuclei was increased compared to that of the control, their chromatin network was cleared, with a hyperchromic, hypertrophied nucleolus located in the center of the nucleus. Such pinealocytes were frequently found near the hemocapillary wall. In some nuclei, the nucleoli were slightly shifted to the karyomembrane. A relatively small

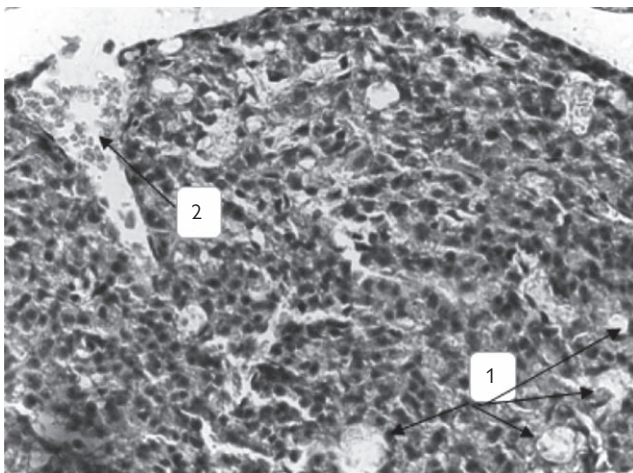


Figure 7 – Morphological rearrangements of structural components in the pineal gland of experimental animals under the conditions of 90-day exposure to heavy metal salts. 1 – multiple polymorphic cysts in the gland's parenchyma; 2 – blood rheological properties (hematoxylin-eosin staining,  $\times 400$ ).

proportion of cells had deformed, hyperchromic nuclei, frequently with signs of pyknotic rearrangements. Their chromatin network was homogeneous; nucleoli were not visualized (Figure 6).

Small oxyphilic secretory granules were visualized in the cytoplasm of a moderate part of pinealocytes, as well as in the lumen of blood vessels. The gland's parenchyma had a moderate number of small, medium, and in some areas of single large sized cysts, stained by oxyphilic method (Figure 7).

In some nuclei chromatin margination and an increase in the number of nuclei with nucleoli were observed. The presence of pinealocytes with angular nuclei and highly vacuolated cytoplasm in the parenchyma of the gland, according to a number of authors indicates the synthesis and accumulation of indolamines in these cells (Bondarenko et al., 2013). However, most of the pinealocytes showed signs of polypeptide synthesis in them.

In order to study one of the links of the antioxidant system of the pineal gland protection, a comparative immunohistochemical study of the pineal gland tissue micropreparations obtained from experimental and control animals on the level of GPX-1 expression was performed. In the control animals' specimens, a significant number of pinealocytes was found with the presence of the GPX-1 marker in their cytoplasm, which correlates with the literature data (Razygraev, 2004). When assessing the results of the reaction, the presence of the studied marker in the cytoplasm of almost all pinealocytes (88% of GPX-1 – positive cells with diffuse location in the cytoplasm of the GPX-1 marker was determined (Figure 8).

However, the degree of expression had some signs of mosaicism. Thus, a particularly significant number of such glandulocytes was found in the peripheral areas of the pineal gland, taking into account the greater synthetic activity of pinealocytes in these areas of the body. Here, cells with a significant level of GPX-1

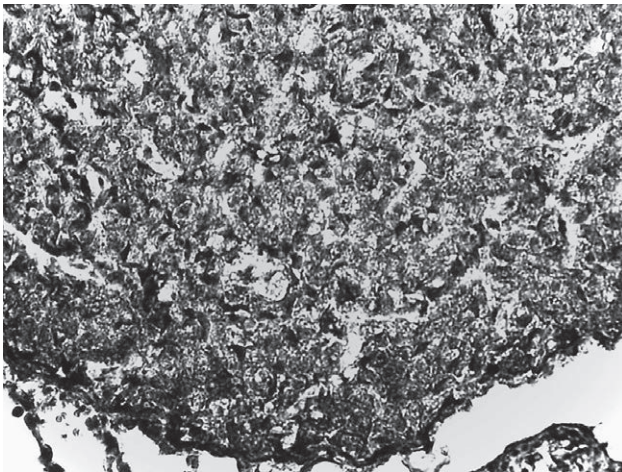


Figure 8 – Immunohistochemical study of GPX-1 expression in the cytoplasm of pinealocytes in the control animals (magnification  $\times 400$ ).

**Table 1 – Expression level of GPX-1 in pinealocytes of the pineal gland in experimental and control animals, n=12**

GPX-1 expression	Control group total number 12 animals	Experimental group total number 12 animals
Low positive 1	17.22 ± 0.84	–
Moderately positive 2	31.55 ± 0.27	13.88 ± 1.14
Strong positive 3	39.23 ± 0.15	25.12 ± 1.09

(+++)  
expression in the cytoplasm were identified, while in the parenchyma and its central regions, the expression level was defined as + and ++ (Table 1).

In the pineal parenchyma of the experimental animals, the expression of GPX-1 was lower in the experimental group than in the control group, as evident from Table 1.

Against the background of the general negative reaction of pinealocytes (–), 39% of GPX-1-positive secretory-active cells with a diffuse location of the GPX-1 marker in the cytoplasm with a moderate (++) and high (+++) level of GPX-1 expression were visualized, especially in the peripheral areas of the gland (Table 1). A correlation was found between the presence of the GPX-1 marker in the pinealocytes cytoplasm and the presence of secretory granules in their cytoplasm, as well as the location of such secretory-active cells in the perivascular spaces (Figure 9).

In order to quantify cellular structures of the pineal gland, the density of pinealocytes and neuroglia, as well as the neurocytoglial index of control and experimental animals were determined by comparing the results of the study. In this

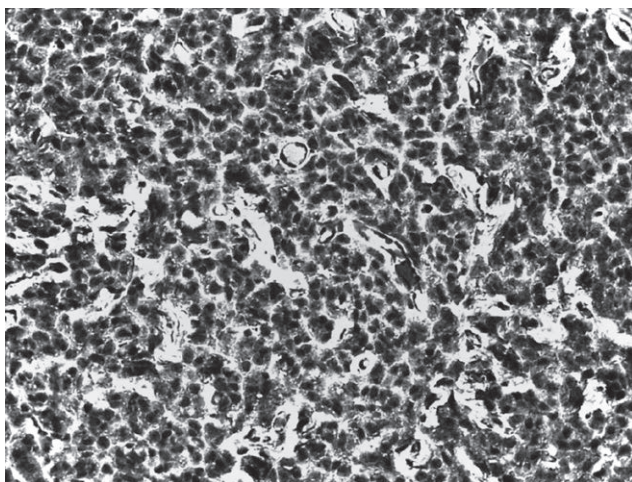


Figure 9 – Immunohistochemical study of GPX-1 expression in the cytoplasm of experimental animals pinealocytes after 90 days of consuming heavy metal salts (magnification ×400).

**Table 2 – Morphometric parameters of pinealocytes and astrocytic glia of the pineal gland in experimental and control animals, n=12**

Index	Study groups of animals	
	control animals	experimental animals
Absolute number of pinealocytes	115.25 ± 11.8418	85.00 ± 6.0139*
Absolute number of astrocytic glia cells	38.75 ± 5.2341	84.75 ± 10.9725**
Glyocyto-neuronal index	0.336 ± 0.4420	0.997 ± 1.8245

Reliable in comparison with the control: \* $p \leq 0.05$ ; \*\* $p \leq 0.01$

case, the morphometric indices of the density of pinealocytes in the experimental animals were significantly reduced by 26% ( $p \leq 0.05$ ,  $t = 2.277626$ ) compared to the control animals. At the same time, the density of glial elements in the pineal gland of experimental animals was significantly increased in comparison with the control by 2.2 times ( $p \leq 0.01$ ,  $t = 3.783842$ ). Glyocyto-neuronal index in the pineal gland of experimental animals increased by 2.96 times ( $p \geq 0.05$ ) compared to that of the control animals (Table 2).

## Discussion

Thus, the obtained data of the immunohistochemical study indicate a high level of antioxidant protection of GPX-1 in the pineal gland of control animals. Prolonged exposure of experimental animals to the mixture of heavy metal salts (including lead salts) caused negative changes in all structural components of the gland: stromal, vascular, parenchymal. These changes have signs of a homeostasis shift in the form of impaired rheological properties of blood, morphology of the vascular wall, its increased permeability, full blood vessels, which leads according to (Shafran et al., 2004) to the development of oxidative stress (Hryntsova et al., 2022) and to manifestations of tissue hypoxia in the gland's parenchyma.

Ischemic damage to the pineal gland certainly had negative consequences for the secretory activity of pinealocytes and mechanisms of hormone diffusion into the blood as a result of disorders of the plasmalemma membrane in pinealocytes and morphological changes in the vascular wall. This is evidenced by the increased number of pinealocytes with vacuolated cytoplasm and the presence of cristae with different sizes and shapes in the pineal gland's parenchyma of the experimental animals. Such morphological properties of the gland's cells and parenchyma, in our opinion, may indicate a delay in the evacuation of hormones into the vascular bed and impairment of the antioxidant defence system of the body as a whole. However, considering the pathogenesis of dystrophic changes in the parenchyma of the pineal gland, including pinealocytes, it is impossible not to mention the possibility of direct toxic effects of heavy metals directly on pinealocytes, given the anatomical absence of blood-brain barrier in this organ. The study of morphological

and morphometric features of pinealocytes and astrocytic glia in the pineal gland of experimental animals permits to indirectly assess the degree of oxidative stress and apoptosis processes in cells (Gubina-Vakulik, 2006). In some nuclei a chromatin margination and an increase in the number of nuclei with nucleoli were observed, which according to the authors is a sign of some activation in synthetic cell activity (Shkorbatov, 2005), but other authors still consider chromatin margination as one of the manifestations of pinealocytes' accelerated apoptosis (Gubina-Vakulik, 2006).

The authors suggest that the cause of the death of some pinealocytes by apoptosis may be long-term exposure of heavy metals on the pineal gland, including such well-known mechanisms of action of heavy metals on the living organism as activation of free radical oxidation, initiation of peroxidation of proteins, lipids and development of oxidative stress (Shahid et al., 2014).

These processes are indicated by a significant decrease in the density of pinealocytes of experimental animals compared to that of control animals, and at the same time a significant increase in the density of glial elements (as confirmed by immunohistochemical studies of the Ki-67 marker – Romanjuk et al., 2018b) and gliocyto-neuronal index.

The formed perivascular astroglial proliferates represent an adaptive response of glia to the action of the damaging agent (Drozdova et al., 2017) and may indirectly indicate more intensive processes of pineal cell apoptosis in these animals (Gubina-Vakulik, 2006). In addition, the increased number of glial elements in the pineal gland certainly has a definite compensatory-adaptive value, especially in the processes transferring RNA, amino acids and growth factors (Goryainov et al., 2013).

All these signs indicate, directly or indirectly, activation of apoptotic processes in the pineal gland in response to the damaging agent. However, it is impossible to neglect other properties of astrocytic neuroglia in glial proliferates, which, in our opinion, are aimed at achieving water-ion homeostasis in the gland by improving the trophism of pinealocytes, barrier function, preventing the penetration of heavy metals into the parenchyma of the gland.

The study of GPX-1 enzymatic activity in the cytoplasm of experimental animals' pinealocytes after 90 days of heavy metal salts consuming led to a decrease in the number of pinealocytes positive for this immunohistochemical marker in comparison with the indicators of control animals. In pineal preparations of experimental animals, a relationship between the presence of GPX-1 expression in the cytoplasm of pinealocytes and the presence of secretory granules in their cytoplasm was revealed. This location of secretory-active pinealocytes with moderate (++) and high (+++) levels of GPX-1 expression in the cytoplasm may be explained by their better supply of oxygen and nutrients compared to cells in deeper areas. The obtained results indicate the development of complex compensatory and adaptive processes in the pineal gland, which are parallel to the indicated negative changes.

It seems likely that long-term exposure to heavy metal salts caused increased oxidative stress in most cells of the pineal gland.

With regard to pathogenic mechanisms of imbalance development in the antioxidant system of the pineal gland, it is possible to assume that such a decrease in glutathione peroxidase activity of pinealocytes also developed due to antagonism between heavy metals and selenium. After all, it is well known that selenium plays an important role in endocrine functions. GPX-1 contains selenocysteine, selenium-dependent glutathione peroxidase. Relatively high concentrations of selenium were found in the pineal gland, which was associated with its antioxidant properties, in particular with its ability to neutralize reactive oxygen intermediates formed during the synthesis of melatonin (Reiter, 1996). This means that the expression of GPX-1 was affected by the level of selenium in the pineal gland, as the action of melatonin was modulated depending on the content of selenium in the gland. The most informative index of selenium supply of the body is the concentration of SePP (selenoprotein P) in the blood and the activity of glutathione peroxidase (Köhrle et al., 2005; Kravtsiv and Yanovich, 2008).

According to the literature, metals are able to form strong sulphide bonds, which lead to blocking of functional SH-groups (sulfhydryl groups) in a number of antioxidant enzymes (Trachtenberg et al., 2010, 2015), including glutathione peroxidase, which contains selenocysteine. The mechanism of GPX-1 inhibition is based on the binding of heavy metals to reduced glutathione (GSH) in the active site of these enzymes (Rusetskaya and Borodulin, 2015).

The high degree of GPX-1-positive pinealocytes' cytoplasm colour intensity and the presence of secretory granules in their cytoplasm may indicate, in our opinion, the maximum stress degree of adaptive secretory processes in these pinealocytes.

In addition, in our opinion, there is a very interesting correlation between the presence of the GPX-1 marker in the cytoplasm of pinealocytes and the presence of secretory granules in their cytoplasm, as well as the location of such secretory active cells in the perivascular spaces. In our opinion, this can be explained by their better supply of oxygen and nutrients due to active glial proliferates, which increased number was found in the peripheral areas of the gland compared to deeper areas. Adaptive processes in the gland included an increase in the number of cells with nuclei in which the nucleoli were visualized, which is also a sign of increased synthetic activity of cells.

## **Conclusion**

Thus, the long-term (90-days) intake of heavy metal salts mixture leads in the experimental animals to the development of the general adaptation syndrome, that represents a stage of chronic stress “subcompensation” in the pineal gland.

Morphological rearrangements are of nonspecific polymorphic nature as severe hemodynamics disorder in the organ, impairment of vascular wall morphology, development of tissue hypoxia and oxidative stress, processes of accelerated apoptosis in part of pinealocytes, a significant decrease in glutathione peroxidase level in the organ and reactive astrogliosis as a response to the damaging agent's action.

Along with the negative changes in the pineal gland, there also occur compensatory-adaptive processes with signs of functional stress. A sufficiently high degree of glutathione peroxidase activity in 39% of pinealocytes located perivascularly, active adaptive glial reaction and activation of synthetic processes in some pinealocytes were observed.

*Acknowledgements: The authors thank to Mgr. Lucia Nehodova and Mgr. Marcela Vyrostkova (Department of Anatomy, Faculty of Medicine, Pavol Jozef Šafárik University in Košice, Slovak Republic) for their valuable advice and assistance in carrying out immunohistochemical studies.*

## References

- Apikhtina, O. L., Dmitrukha, N. M., Kotsyuruba, A. I. (2012) The mechanism of hemotoxic action of lead. *J. National Acad. Med. Sci. Ukr.* **18(1)**, 100–109. (in Ukraine)
- Arushanyan, E. B. (2004) *Antistress Potential of Epiphyseal Melatonin. Melatonin in Health and Disease*. Nauka, Moscow. (in Russian)
- Arushanyan, E. B., Elbekyan, K. S. (2006) Immunotoxicity of metal salts and the protective role of epiphyseal factors. *Biomed. Chem.* **52(6)**, 547–555. (in Russian)
- Belenichev, I. F. (2014) *Neuroprotection and Neuroplasticity*. Polygraph plus, Kiev. (in Ukraine)
- Bharti, V. K., Srivastava, R. S., Kumar, H., Bag, S., Majumdar, A. C., Singh, G., Pandi-Perumal, S. R., Brown, G. M. (2014) Effects of melatonin and epiphyseal proteins on fluoride-induced adverse changes in antioxidant status of heart, liver, and kidney of rats. *Adv. Pharmacol. Sci.* **2014**, 532969.
- Bondarenko, A. A., Gubina-Vakulik, G. I., Gevorgyan, A. R. (2013) Pineal gland and hypothalamic-pituitary-thyroid system: Age and chronobiological aspects. Institute Endocrinol. Pathol., Kharkiv. (in Ukraine)
- Daniels, W. M., van Rensburg, S. J., van Zyl, J. M., Taljaard, J. J. (1998) Melatonin prevents beta-amyloid-induced lipid peroxidation. *J. Pineal Res.* **24**, 78–82.
- Drozдова, G. A., Samigullina, A. F., Nurgaleeva, E. A. (2017) Posthypoxic reaction of astroglial cells of the visual cortex in the experiment. *Kazan Med. Zh.* **98(6)**, 984–988. (in Russian)
- El-Missiry, M. A. (2000) Prophylactic effect of melatonin on lead-induced inhibition of heme biosynthesis and deterioration of antioxidant systems in male rats. *J. Biochem. Mol. Toxicol.* **14**, 57–62.
- El-Sokkary, G. H., Kamel, E. S., Reiter, R. J. (2003) Prophylactic effect of melatonin in reducing lead-induced neurotoxicity in the rat. *Cell. Mol. Biol. Lett.* **8**, 461–470.
- Goryainov, S. A., Protskiy, S. V., Okhotin, V. E. (2013) On the role of astroglia in the brain in health and disease. *Annals Clin. Experiment. Neurol.* **7(1)**, 45–51.
- Gubina-Vakulik, G. I. (2006) An attempt to generalize the results of a histopathological examination of the epiphysis of the brain. *Bukov. Med. Visnik.* **10(4)**, 34–36.
- Hemdan, N. Y., Emmrich, F., Adham, K., Wichmann, G., Lehmann, I., El-Massry, A., Ghoneim, H., Lehmann, J., Sack, U. (2005) Dose-dependent modulation of the *in vitro* cytokine production of human immune competent cells by lead salts. *Toxicol. Sci.* **86**, 75–83.
- Hryntsova, N. B., Romanyuk, A. M. (2020) Method of identification and atraumatic extraction of pineal gland in rats. Utility model patent No. 142276/25.05.20 of the State Register of utility model patents of Ukraine.
- Hryntsova, N. B., Romanyuk, A. M., Lindin, M. S., Lindina, Y. M. (2020) Modified method of preparation of histological preparations of the pineal gland of rats. Patent for utility model No. 142314/25.05.20 of the State Register of Patents of Ukraine for utility models.

- Hryntsova, N. B., Romanyuk, A. M., Zaitseva, S. S., Gordienko, O. V., Khomenko, I. V., Kiptenko, L. I. (2022) Effect of L-tocopherol on morphological reformations of rat pineal gland under the impact of heavy metal salts. *World Med. Biol.* **1(79)**, 184–188.
- Karbownik, M., Lewinski, A. (2003) Melatonin reduces Fenton reaction-induced lipid peroxidation in porcine thyroid tissue. *J. Cell. Biochem.* **90(4)**, 806–811.
- Köhrle, J., Jakob, F., Contempré, B., Dumont, J. E. (2005) Selenium, the thyroid, and the endocrine system. *Endocr. Rev.* **26**, 944–984.
- Kravtsiv, R. Y., Yanovich, D. O. (2008) The role of selenium in the functioning of the endocrine system, organs and tissues of animals. *Biol. Anim.* **10(1–2)**, 33–48. (in Ukraine)
- Limson, J., Nyokong, T., Daya, S. (1998) The interaction of melatonin and its precursors with aluminium, cadmium, copper, iron, lead, and zinc: An adsorptive voltammetric study. *J. Pineal Res.* **24**, 15–21.
- Lutsik, S. O., Yashchenko, A. M. (2018) Immunohistochemical study of the adrenal glands of the offspring of rats that developed under the conditions of experimental hypo- and hyperthyroidism of the maternal organism. *World Med. Biol.* **4(66)**, 175–180.
- Razygraev, A. V. (2004) Activity of glutathione peroxidase in the tissue of the pineal gland of rats and its change during aging. *Adv. Gerontol.* **4**, 19–22.
- Reiter, R. J. (1996) Functional aspects of the pineal hormone melatonin in combating cell and tissue damage induced by free radicals. *Eur. J. Endocrinol.* **134**, 412–420.
- Romanjuk, A., Lyndin, M., Lyndina, Y., Sikora, V., Hrintsova, N., Timakova, O., Gudymenko, O., Gladchenko, O. (2018a) Changes in the hematopoietic system and blood under the influence of heavy metal salts can be reduced with vitamin E. *Turk Patoloji Derg.* **34**, 73–81.
- Romanjuk, A., Hryntsova, N., Romanjuk, O., Lyndin, M., Karpenko, L. (2018b) Morphological and immune histochemical alterations of astrocyte neuroglia of epiphysis under conditions of long-term influence of heavy metals salts on the organism. 30<sup>th</sup> European Congress of Pathology, 8–12 September 2018, Bilbao, Spain. *Virchows Archiv (Eur. J. Pathol.)* **473**, 27 (Suppl. 1).
- Romanjuk, A., Hryntsova, N., Karpenko, L. (2019) The long-term effect of the complex of heavy metal salts on the morphofunctional changes in the structural components of the intermediate lobe of the mature rat's pituitary gland – The female. *Problems Endocrinol. Pathol.* **2**, 98–103.
- Rusetskaya, N. Y., Borodulin, V. B. (2015) Biological activity of selenorganic compounds at heavy metal salts intoxication. *Biomed. Khim.* **61(4)**, 449–461. (in Russian)
- Russel, J. (2000) Melatonin: Lowering the high price of free radicals. *News Physiol. Sci.* **15**, 246–250.
- Rzeuski, R., Chlubek, D., Machoy, Z. (1998) Interactions between fluoride and biological free radical reactions. *Fluoride* **31(1)**, 43–45.
- Salkov, V. N., Khudoerkov, R. M., Voronkov, D. N., Noss, N. S. (2015) Morphological parameters of the heterogeneity of the substantia nigra in elderly men and women. *Arkh. Patol.* **77(4)**, 51–54. (in Russian)
- Shafran, L. M., Bolshoi, D. V., Pykhteeva, E. G., Tretyakova, E. M. (2004) The role of lysosomes in the mechanism of protection and cell damage under the action of heavy metals. *Modern Problems Toxicol.* **3**, 52–56.
- Shahid, M., Pourrut, B., Dumat, C., Nadeem, M., Aslam, M., Pinelli, E. (2014) Heavy-metal-induced reactive oxygen species: Phytotoxicity and physicochemical changes in plants. *Rev. Environ. Contam. Toxicol.* **232**, 1–44.
- Shkrobatov, Y. G. (2005) Structural and electrochemical power of the nuclei of the civil society of people with the sound of physical and chemical factors and the great functionality of the body. MDS Thesis, Kiev State University.
- Susa, N., Ueno, S., Furukawa, Y., Ueda, M., Sugiyama, M. (1997) Potent protective effect of melatonin on chromium(VI)-induced DNA single-strand breaks, cytotoxicity, and lipid peroxidation in primary cultures of rat hepatocytes. *Toxicol. Appl. Pharmacol.*, **144**, 377–384.

- Trachtenberg, I. M., Korolenko, T. K., Utko, N. A., Muradyan, H. K. (2001) Lead and oxidative stress. *Probl. Modern Toxicol.* **4**, 28–36.
- Trachtenberg, I. M., Lubyanova, I. P., Apykhtina, E. L. (2010) The role of lead and iron as man-made chemical pollutants in the pathogenesis of cardiovascular diseases. *Ukr. Med. Bull.* **7–8**, 36–39.
- Trachtenberg, I. M., Dmitrukha, N. M., Lugovsky, S. P. (2015) Lead is a dangerous pollutant. The problem is old and new. *Modern Probl. Toxicol. Food Chemical Safety* **3**, 14–24.
- Valko, M., Morris, H., Cronin, M. T. (2005) Metals, toxicity and oxidative stress. *Curr. Med. Chem.* **12**, 1161–1208.

# Malignancy Rates in Thyroid Nodules Classified as Bethesda III and IV; Correlating Fine Needle Aspiration Cytology with Histopathology

**Chirag Pereira**

Department of General Surgery, Royal Lancaster Infirmary, Lancaster, United Kingdom

Received June 29, 2022; Accepted October 18, 2022.

**Key words:** FNAC – Thyroid cancer – Bethesda system – Thyroidectomy

**Abstract:** Fine needle aspiration cytology (FNAC) is an integral part in the diagnostic work up of thyroid nodules. FNAC reports are based on Bethesda system for thyroid cytopathology which is one of the most commonly used systems worldwide. The main objective of the present study was to evaluate the malignancy rates in Bethesda category III and IV thyroid nodules over a six-year period. 642 thyroid FNAC were performed over a six-year period. The medical records of all these patients were reviewed using electronic patient records. Cases reported to have Bethesda category III and IV were included in the study. Data for these patients were reviewed to determine the relationship between these categories and thyroid cancer. There were 41 cases of category III of which 19 underwent surgery and the malignancy rates were found to be 26.3%. Category IV consisted of 50 cases of which 45 underwent surgery and the malignancy rates were 26.6%. The results from our study are similar to findings in larger multicentric studies which found that malignancy rates for Bethesda category III and IV were 10–30% and 25–40%, respectively.

**Mailing Address:** Chirag Pereira, MBBS, MS, MRCS, Department of General Surgery, Royal Lancaster Infirmary, Ashton Road, Lancaster – LA14RP, United Kingdom; e-mail: chirag.pereira@mbht.nhs.uk

<https://doi.org/10.14712/23362936.2022.22>

© 2022 The Author. This is an open-access article distributed under the terms of the Creative Commons Attribution License (<http://creativecommons.org/licenses/by/4.0>).

## Introduction

Distinguishing a benign from a malignant thyroid nodule can be challenging at times. Fine needle aspiration cytology (FNAC) plays a crucial role in the diagnosis of thyroid nodules. Although an imperative investigation, reports at times can be ambiguous and hence perceived differently by surgeons and endocrinologist (Redman et al., 2006). Due to these shortcomings a standardized reporting system such as Bethesda system for reporting thyroid cytopathology plays an important role. Based on this system, thyroid FNAC are classified into six categories which are, category I – non diagnostic, category II – benign, category III – atypia of undetermined significance (AUS) or follicular lesion of undetermined significance (FLUS), category IV – follicular neoplasm, category V – suspicious for malignancy and category VI – malignant. Introduction of this system of reporting has not only improved the overall quality of reporting FNAC but also reduced the number of unwanted thyroidectomies (Crowe et al., 2011).

Thyroid nodules classified as Bethesda category III are difficult to distinguish as benign or malignant and are reported as atypia of undetermined significance or follicular lesion of undetermined significance. According to the 2017 Bethesda consensus (Cibas and Ali, 2017), risk of malignancy from these nodules is 6–18% when non-invasive follicular thyroid neoplasm (NIFTP) is not considered as cancer versus 10–30% when NIFTP is considered as cancer and can be managed initially with a repeat FNAC.

A few recently published papers have suggested higher malignancy rates associated with Bethesda category III. Bethesda category IV includes follicular neoplasm or suspicious of follicular neoplasm. At a cytological level both follicular cancer and benign follicular neoplasm look identical making it difficult for pathologist to distinguish the two. Identification of either capsular or vascular invasion on FNAC can confirm malignant diagnosis (Ohuri et al., 2010).

The aim of this study is to evaluate the risk of thyroid cancer for Bethesda category III and category IV nodules over a six-year period.

## Material and Methods

This is a retrospective observational study of all thyroid nodules with a Bethesda category III and IV results investigated by department of general surgery, surgical oncology and otorhinolaryngology between January 2015 and December 2020. All reports were obtained using the hospitals electronic patient record system. Since no intervention was carried out on patients and this is a retrospective review, ethical committee waiver of consent was approved.

In the case of larger nodules FNAC was performed directly into palpable nodule while in the case of smaller nodules it was done under ultrasound guidance. All FNAC were reported according to Bethesda classification. All category III cases were classified as either AUS or FLUS. All smears were fixed with alcohol and stained with Papanicolaou stain. Following the initial FNAC patients were given the

option of undergoing surgery versus a repeat FNAC in 1–3 months in Bethesda category III.

Inclusion criteria included all patients with Bethesda category III and IV nodules and had operative details and histology available. Patients whose electronic records did not have the above information were excluded from the study. There were 106 patients in total included in this study of which 47 were category III and 59 were category IV. The histopathological reports were compared with FNAC reports in order to determine rate of malignancy.

## Results

A total of 642 thyroid FNAC were performed from January 2015 to December 2020. The total number of males was 112 and females 530. Age ranged from 16 to 78 years. Based on Bethesda system there were 18 in category I, 442 in category II, 47 in category III, 59 in category IV, 35 in category V and 41 in category VI (Table 1).

Category 3 was further divided into AUS and FLUS which included 32 and 15, respectively. Out of the 47 cases in category 3, 6 patients were lost to follow-up. Among the remaining 41 cases, 6 (14.7%) had immediate surgery of which 5 (83.3%) were found to be benign and 1 (16.6%) malignant. The remaining 35 (85.3%) underwent repeat FNAC of which 3 (8.5%) were reported as category I, 19 (54.2%) as category II and 13 (37.1%) as category III. Patients with repeat FNAC reported as category III underwent surgery and 9 (69.2%) were benign and 4 (30.7%) were malignant (Figure 1).

There were 59 patients in category IV of which 9 were lost to follow-up. The remaining 50 cases underwent surgery of which 38 were benign and 12 were malignant (Figure 2).

Malignancy was diagnosed in 5 (26.3%) out of 19 cases diagnosed as category III and 12 (26.6%) out of 50 cases diagnosed as category 4 that had undergone surgery (Table 2).

Based on histopathology, benign cases included follicular adenoma, Hashimoto's thyroiditis and nodular colloid goitre while malignant diagnosis included papillary

**Table 1 – Patient categorization based of Bethesda System for Reporting Thyroid Cytopathology**

Bethesda category	No. of cases (%)
Category I	18 (2.8%)
Category II	442 (68.8%)
Category III	47 (7.3%)
Category IV	59 (9.1%)
Category V	35 (5.4%)
Category VI	41 (6.3%)

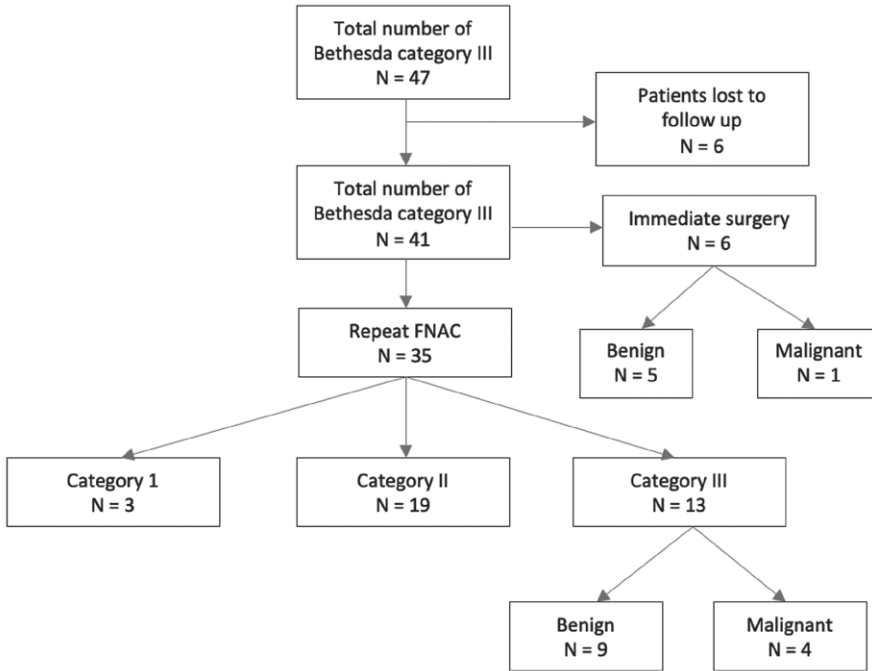


Figure 1 – Flow chart of category III thyroid nodules on fine needle aspiration cytology.

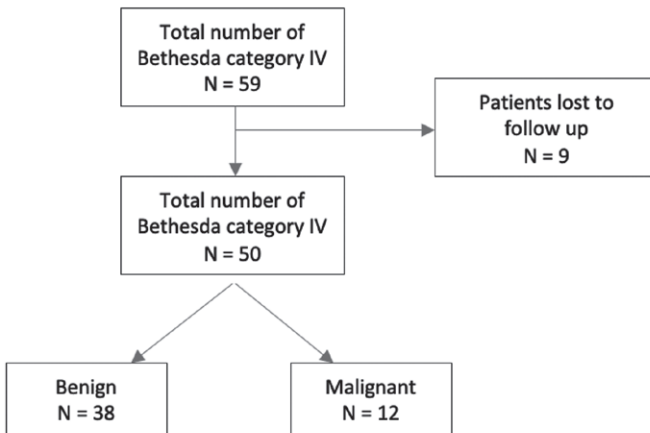


Figure 2 – Flow chart of category IV thyroid nodules on fine needle aspiration cytology.

carcinoma thyroid (PTC), follicular carcinoma thyroid and Hurtle cell carcinoma. The most common type of cancer in category IV was PTC (66.6%) followed by follicular cancer thyroid (25%). The only malignant tumour in category III was papillary cancer thyroid (Figure 3). Among the 5 cases of PTC in category III, 1 case was

**Table 2 – Malignancy ratios of thyroid nodules following surgery**

	Benign (%)	Malignant (%)	Total
Bethesda III	14 (73.6%)	5 (26.3%)	19
AUS	10 (71.4%)	4 (28.5%)	14
FLUS	4 (80.0%)	1 (20.0%)	5
Bethesda IV	38 (76.0%)	12 (24.0%)	50

AUS – atypia of undetermined significance; FLUS – follicular lesion of undetermined significance

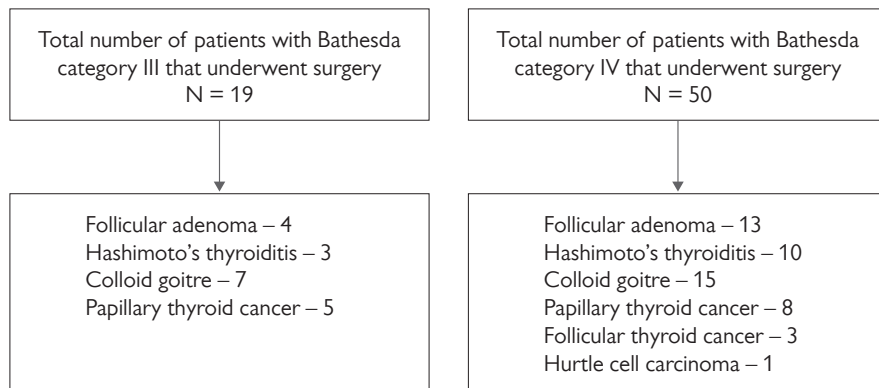


Figure 3 – Flow chart of Bethesda category III and IV and histopathology results following surgery.

NIFTP, 3 were conventional and 1 was tall cell variant. Among the 8 cases of PTC in category IV, there were 2 cases of follicular variant of PTC while the remaining 6 were conventional PTC.

## Discussion

Bethesda System for Reporting Thyroid Cytology has played an important role in standardizing reports for thyroid FNAC. The main aim of this system was to have a clear understanding about the potential malignancy rates among various sub categories. The main limitation of this system are category III and category IV where the risk of malignancy remains unclear (Somma et al., 2010). Some researchers have a shared opinion that either by reducing or eliminating certain Bethesda categories, it would help in easy decision-making in patient management. However, studies have shown that eliminating category III or IV increases the rates of false positivity, false negativity and lowers the sensitivity of FNAC (Shi et al., 2009).

In the present study, the mean age was 47 years and there were a greater number of females as compared to males. This was comparable to other published

studies (Ho et al., 2014; Yaprak Bayrak and Erucar, 2020). The present study evaluated FNAC reports of 642 patients with thyroid nodules. Among these patients 7.3% were category III and 9.1% were category IV based on initial FNAC. Some case series reported a much higher incidence i.e., 22.6% were category III and 14% were category IV (Yaprak Bayrak and Erucar, 2020). A case series by Ho et al. (2014) showed similar incidence of category III as the present study.

Malignancy rates in respect to Bethesda category III and category IV will vary from institute to institute with higher rates seen more commonly in multicentric studies. Studies that evaluated a larger population with thyroid nodules showed that malignancy rates in Bethesda category III range from 10–30% while category IV ranges from 25–40% (Ho et al., 2014; Cibas and Ali, 2017). Studies with smaller cohorts showed that malignancy rates can be as high as 40% in category III (Alexander et al., 2012; Canberk et al., 2016). In the present study, malignancy rates were 26.3% and 26.6% for category III and category IV respectively which are similar to studies with a larger cohort. Undoubtedly, these rates play an important role when surgeons need to decide whether patients need surgery or regular observation and follow-up. Mathur et al. (2014) evaluated 4,827 FNAC of which 255 patients with Bethesda category III underwent surgery and malignancy rates were 39%, which is much higher as compared to our study. In another large cohort by Jo et al. (2010) the malignancy rates for category III was 17% and category IV was 25%, which is comparable to our study. Difference in malignancy rates seems to depend on the interpretation of FNAC by various cytopathologist.

In the present study, the malignancy rates of patients that underwent immediate surgery was 16.6% and 28.8% for category III and category IV, respectively. The malignancy rates in thyroid nodules following a repeat FNAC were 30.7% and 26.3% in category III and category IV, respectively. Similar findings were also seen in a study by Yaprak Bayrak and Erucar (2020) where malignancy rates were higher following patients that had a repeat FNAC for category III thyroid nodules. Chirayath et al. (2019) carried out a prospective study to determine malignancy rates in Bethesda category III and IV. They recommended that patents with category III should undergo repeat FNAC while those with category IV can proceed directly to surgery. Papillary thyroid cancer was the most common cancer type in both category III and IV. This was similar to study done Cavalheiro et al. (2018).

## Conclusion

This study provides a more accurate analysis of cancer rates in patients with thyroid nodules classified as Bethesda category III and IV, as these patients underwent surgical excision. The study concludes that malignancy rates associated with Bethesda category III and IV are similar to already published data which relates to 10–30% and 25–40%, respectively.

## References

- Alexander, E. K., Kennedy, G. C., Baloch, Z. W., Cibas, E. S., Chudova, D., Diggans, J., Friedman, L., Kloos, R. T., LiVolsi, V. A., Mandel, S. J., Raab, S. S., Rosai, J., Steward, D. L., Walsh, P. S., Wilde, J. I., Zeiger, M. A., Lanman, R. B., Haugen, B. R. (2012) Preoperative diagnosis of benign thyroid nodules with indeterminate cytology. *N. Engl. J. Med.* **367(8)**, 705–715.
- Canberk, S., Gunes, P., Onenerk, M., Erkan, M., Kilinc, E., Gursan, N. K., Kilicoglu, G. Z. (2016) New concept of the encapsulated follicular variant of papillary thyroid carcinoma and its impact on the Bethesda system for reporting thyroid cytopathology: A single-institute experience. *Acta Cytol.* **60(3)**, 198–204.
- Cavalheiro, B. G., Leite, A. K. N., de Matos, L. L., Miazaki, A. P., Ientile, J. M., Kulcsar, M. A. V., Cernea, C. R. (2018) Malignancy rates in thyroid nodules classified as Bethesda categories III and IV: Retrospective data from a tertiary center. *Int. J. Endocrinol. Metab.* **16(1)**, e12871.
- Chirayath, S. R., Pavithran, P. V., Abraham, N., Nair, V., Bhavani, N., Kumar, H., Menon, U. V., Menon, A. S. (2019) Prospective study of Bethesda categories III and IV thyroid nodules: Outcomes and predictive value of BRAF<sup>V600E</sup> mutation. *Indian J. Endocrinol. Metab.* **23(3)**, 278–281.
- Cibas, E. S., Ali, S. Z. (2017) The 2017 Bethesda System for Reporting Thyroid Cytopathology. *Thyroid* **27(11)**, 1341–1346.
- Crowe, A., Linder, A., Hameed, O., Salih, C., Roberson, J., Gidley, J., Eltoum, I. A. (2011) The impact of implementation of the Bethesda System for Reporting Thyroid Cytopathology on the quality of reporting, “risk” of malignancy, surgical rate, and rate of frozen sections requested for thyroid lesions. *Cancer Cytopathol.* **119(5)**, 315–321.
- Ho, A. S., Sarti, E. E., Jain, K. S., Wang, H., Nixon, I. J., Shaha, A. R., Shah, J. P., Kraus, D. H., Ghossein, R., Fish, S. A., Wong, R. J., Lin, O., Morris, L. G. (2014) Malignancy rate in thyroid nodules classified as Bethesda category III (AUS/FLUS). *Thyroid* **24(5)**, 832–839.
- Jo, V. Y., Stelow, E. B., Dustin, S. M., Hanley, K. Z. (2010) Malignancy risk for fine-needle aspiration of thyroid lesions according to the Bethesda System for Reporting Thyroid Cytopathology. *Am. J. Clin. Pathol.* **134(3)**, 450–456.
- Mathur, A., Najafian, A., Schneider, E. B., Zeiger, M. A., Olson, M. T. (2014) Malignancy risk and reproducibility associated with atypia of undetermined significance on thyroid cytology. *Surgery* **156(6)**, 1471–1476.
- Ohuri, N. P., Nikiforova, M. N., Schoedel, K. E., LeBeau, S. O., Hodak, S. P., Seethala, R. R., Carty, S. E., Ogilvie, J. B., Yip, L., Nikiforov, Y. E. (2010) Contribution of molecular testing to thyroid fine-needle aspiration cytology of “follicular lesion of undetermined significance/atypia of undetermined significance”. *Cancer Cytopathol.* **118(1)**, 17–23.
- Redman, R., Yoder, B. J., Massoll, N. A. (2006) Perceptions of diagnostic terminology and cytopathologic reporting of fine-needle aspiration biopsies of thyroid nodules: A survey of clinicians and pathologists. *Thyroid* **16(10)**, 1003–1008.
- Shi, Y., Ding, X., Klein, M., Sugrue, C., Matano, S., Edelman, M., Wasserman, P. (2009) Thyroid fine-needle aspiration with atypia of undetermined significance: A necessary or optional category? *Cancer Cytopathol.* **117(5)**, 298–304.
- Somma, J., Schlecht, N. F., Fink, D., Khader, S. N., Smith, R. V., Cajigas, A. (2010) Thyroid fine needle aspiration cytology: Follicular lesions and the gray zone. *Acta Cytol.* **54(2)**, 123–131.
- Yaprak Bayrak, B., Eruyar, A. T. (2020) Malignancy rates for Bethesda III and IV thyroid nodules: A retrospective study of the correlation between fine-needle aspiration cytology and histopathology. *BMC Endocr. Disord.* **20(1)**, 1–9.

# Clinical Course of COVID-19 and Cycle Threshold in Patients with Haematological Neoplasms

**Ignacio Martín Santarelli<sup>1,2</sup>, Mariela Sierra<sup>2,3</sup>, María Lucía Gallo Vaulet<sup>4,5</sup>, Marcelo Rodríguez Fermepin<sup>4,5</sup>, Sofía Isabel Fernández<sup>1,2</sup>**

<sup>1</sup>Departamento de Medicina, Universidad de Buenos Aires, Hospital de Clínicas “José de San Martín”, Buenos Aires, Argentina;

<sup>2</sup>Facultad de Medicina, Universidad de Buenos Aires, Buenos Aires, Argentina;

<sup>3</sup>División de Infectología, Universidad de Buenos Aires, Hospital de Clínicas “José de San Martín”, Buenos Aires, Argentina;

<sup>4</sup>Universidad de Buenos Aires, Facultad de Farmacia y Bioquímica, Departamento de Bioquímica Clínica, Cátedra de Microbiología Clínica, Buenos Aires, Argentina;

<sup>5</sup>Universidad de Buenos Aires, Instituto de Fisiopatología y Bioquímica Clínica (INFIBIOC), Buenos Aires, Argentina

Received April 26, 2022; Accepted October 18, 2022.

**Key words:** Haematological neoplasms – Cycle threshold – COVID-19 – SARS-COV-2

**Abstract:** The SARS-CoV-2 viral load in a respiratory sample can be inversely quantified using the cycle threshold (Ct), defined as the number of amplification cycles required to detect the viral genome in a quantitative PCR assay using reverse transcriptase (RT-qPCR). It may be classified as high (Ct < 25), intermediate (25–30) and low (Ct > 30). We describe the clinical course of 3 patients with haematological neoplasms who contracted COVID-19. None of them had been vaccinated. Firstly, a 22-year-old male with a refractory acute lymphoblastic leukaemia experienced an oligosymptomatic COVID-19 and had a Ct of 23 with an ascending curve. Another male, aged 23, had recently begun treatment for a promyelocytic leukaemia. He had a subacute course with high oxygen requirements. His Ct dropped from 28, when he only experienced fever, to 14.8, during the most critical period and on the edge of ventilatory support. Viral clearance was documented 126 days after the beginning of the symptoms. Finally, a 60-year-old male had received rituximab as maintenance

**Mailing Address:** Ignacio Martín Santarelli, MD., Departamento de Medicina, Hospital de Clínicas “José de San Martín”, Av. Córdoba 2351, Piso 11, C1120, Ciudad de Buenos Aires, Argentina; Phone: +549 11 5764 0610; e-mail: isantarelli@fmed.uba.ar

therapy for a follicular lymphoma 3 months before contracting COVID-19. He had a fulminant course and required mechanical ventilation a few days later. We highlight the association between the course of CoViD-19 and the Ct. Viral shedding was longer than in immunocompetent hosts.

## Introduction

SARS-COV-2 viral load in a respiratory sample can be inversely quantified using the cycle threshold (Ct). In a quantitative reverse-transcription polymerase chain reaction test (RT-qPCR), the Ct is understood as the number of amplification samples required to detect the viral genome above a colorimetric threshold (fluorescence). Therefore, the lowest number of cycles correspond to the highest viral load, and vice versa. A standard RT-qPCR executes a maximum of 40 cycles (Engelmann et al., 2021).

Even though the evidence gathered so far is non-conclusive, the Ct values from nasal swabs seem to correlate with the risk of death from the disease caused by the novel coronavirus SARS-COV-2, COVID-19 (Faíco-Filho et al., 2020), its clinical evolution (Rabaan et al., 2021), and the viral infectivity (La Scola et al., 2020).

We hereby describe the clinical evolution of 3 patients with previous haematological neoplasms, in different stages, who contracted, COVID-19 and correlated it with Ct values of their nasal swabs.

## Case report

### Case 1

A 22-year-old male, carrier of a refractory high-risk acute lymphoblastic leukaemia after two different treatments, had been discharged until bridge therapy for haematopoietic stem cell transplantation became available. In December 2020, at home, he experienced fever and odynophagia. He was diagnosed with mild COVID-19 with a PCR in nasal swab in a different medical centre, which is why we were not able to establish the initial Ct. He did not experience any other symptoms and there were no radiologic findings compatible with pneumonia. His symptoms lasted about 5 days.

20 days later, he was re-admitted to receive blinatumomab, a T-cell bispecific engager monoclonal antibody (BiTE) that acts binding T-cells and leukemic cells that express CD19, promoting the destruction of the latter (Einsele et al., 2020). He was asymptomatic and in excellent general conditions. The chest X-ray was normal. The absolute neutrophil and lymphocyte counts were 1,700 and 1,510/ $\mu$ l respectively. The remainder of the laboratory exam was unremarkable. He did not receive any specific treatment for COVID-19. In accordance with the sanitary protocols valid at that time, we obtained a follow-up RT-qPCR which was detectable with a Ct of 23. He received the drug with no complications.

A RT-qPCR performed a week later reported a Ct of 33. 7 days afterwards, 34 after symptom onset, viral clearance was documented with a negative test.

## Case 2

A 23-year-old male with no past medical records was admitted for a new-onset, high-risk acute promyelocytic leukaemia in April 2021. This was his laboratory exam on admission: Haematocrit = 35%, haemoglobin = 12 g/dl, leukocytes = 43,870/ $\mu$ l (neutrophils = 21,935/ $\mu$ l, lymphocytes = 3,850/ $\mu$ l), platelets = 32,000/ $\mu$ l, prothrombin time = 56%, aPTT – activated partial thromboplastin time = 42 seconds, fibrinogen = 73 mg/dl. He started to receive the specific treatment with all-trans retinoic acid (ATRA), and, on the fifth day, the first infusion of idarubicin (AIDA protocol). 24 hours later he presented with fever. He had a positive RT-qPCR with an initial Ct of 28, and chest computed tomography (CCT) reported subtle sub-pleural ground-glass opacities compatible with viral infection (Figure 1). He had had no need for supplementary oxygen at first. Apart from transfusion support, he received convalescent plasma, in accordance with our institutional protocol at that time. He continued treatment for his leukaemia.

On day 19 from symptom onset, he began to require supplementary oxygen, first with a low-flow nasal cannula. He began to receive a 10-day course of dexamethasone 6 mg qd at this point. Ct on a follow-up nasal swab had dropped to 14.8. The most critical moment, from the respiratory point of view, was observed on the 30<sup>th</sup> day since symptom onset. He needed oxygen delivered through a high-flow non-rebreather mask. His hemogram reported a total leukocyte count of 1,080/ $\mu$ l, 820/ $\mu$ l neutrophils, and 100 lymphocytes/ $\mu$ l. The CCT demonstrated progression of the lung infiltrates (Figure 2), which coincided with the Ct nadir (13.8).

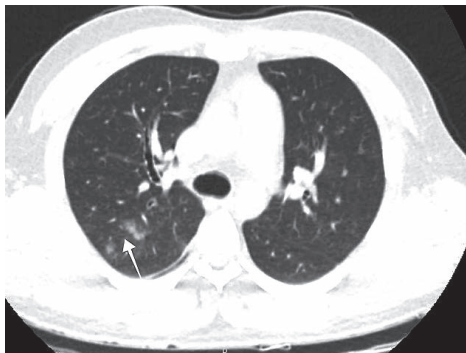


Figure 1 – Patient 2: Chest computed tomography on admission. Mild ground-glass opacities are observed (white arrow). The patient had no supplementary oxygen requirement. Ct (cycle threshold) was 28.

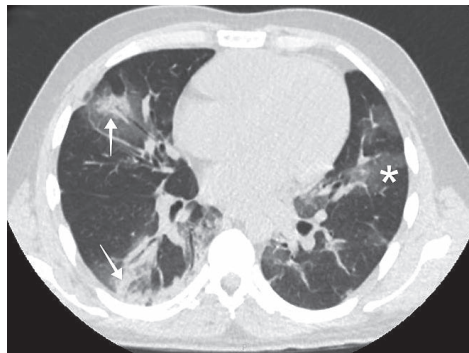


Figure 2 – Patient 2: Chest computed tomography on Ct (cycle threshold) nadir (13.8), on 30<sup>th</sup> day since symptom onset. Remarkable progression of lung ground-glass opacities (asterisk), with areas of parenchymatous consolidation (white arrows). The patient required oxygen through a non-rebreather mask.

He continued to need oxygen supplementation, regressively after 3 days with the maximum supply, for a total of 17 days. 71 days after symptom onset, RT-qPCR was still positive, but Ct was Ct. Viral clearance was confirmed on day 126 after symptom onset (approximately 4 months). He had no respiratory sequelae.

### Case 3

A 60-year-old male had been successfully treated for a grade-IV follicular lymphoma with 6 cycles of R-CHOP protocol (rituximab, cyclophosphamide, doxorubicin, vincristine and prednisone), and, after 6 months, he had a negative PET (positron emission tomography)/computed tomography. He had received the most recent maintenance treatment with rituximab 3 months before the hospital admission presented.

He consulted for a 7-day history of cough and myalgia, and fever on the day he attended to the hospital. He was febrile, hemodynamically stable and required oxygen administered by a low-flow nasal cannula. The most remarkable laboratory results were leukopenia (3,020/ $\mu$ l, with 2,310 neutrophils/ $\mu$ l and 870 lymphocytes/ $\mu$ l) and renal failure (creatinine clearance = 31 ml/min/1.72 m<sup>2</sup>). The CCT showed peripheral ground-glass opacities with predominance of both lung bases and superior lobes (Figure 3). The RT-qPCR for SARS-COV-2 genome was positive with an initial Ct of 10. Dexamethasone 6 mg qd was initiated. The patient progressively required greater oxygen supplementation. A follow-up CCT obtained a week later demonstrated radiologic progression of the bilateral ground-glass opacities with sub-pleural predominance. 20 days after symptom onset he required

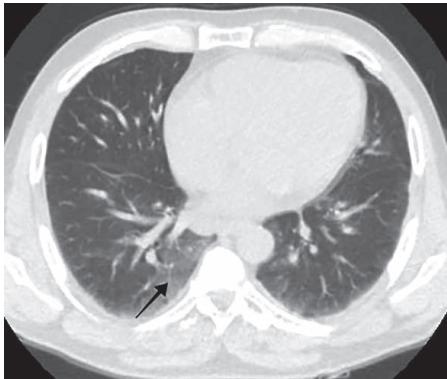


Figure 3 – Patient 3: Chest computed tomography on admission (day 7 since symptom onset), when he needed oxygen through low-flow nasal cannula. Ct (cycle threshold) was 10. Subpleural ground-glass opacities with basal predominance (black arrow).

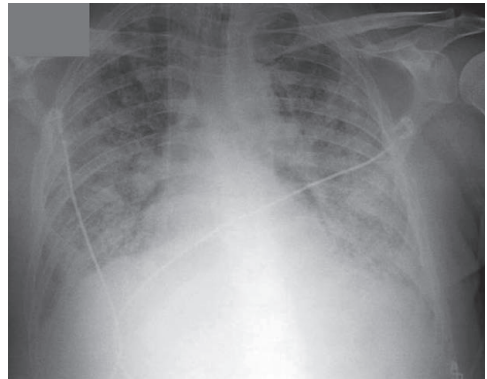


Figure 4 – Patient 3: Chest X-ray which shows near complete involvement of lung parenchyma by patchy infiltrates. This film was obtained the day before he died.

mechanical ventilation and died on the 40<sup>th</sup> day. Figure 4 shows multiple bilateral opacities on X-ray obtained the day before death.

It is important to highlight that none of these patients had been vaccinated for COVID-19.

## Discussion

Patients with leukaemias, lymphomas and myelomas are the most susceptible to severe forms of COVID-19, and have a higher mortality rate than the general population and even higher than other oncologic patients with solid tumours (Lee et al., 2020). The American Society of Hematology reported a 28% mortality rate in a registry of 250 patients with haematological neoplasms (Wood et al., 2020). Local data gathered in Argentina concluded a 20.8% mortality rate (Basquiera et al., 2021).

One multicentric and retrospective study developed in New York (Westblade et al., 2020) included patients with and without cancer and classified the SARS-COV-2 viral load, according to the Ct value, in high (Ct < 25), intermediate (25–30) and low (Ct > 30). Moreover, *in vitro*, it has not been possible to achieve viral transfection using respiratory samples with Ct > 34 inoculated to Vero E6 cells, suggesting that patients with this Ct value or higher are no longer contagious (La Scola et al., 2020). Viral shedding in immunocompromised patients tends to be longer than in the general population. It has been reported as long as 151 days after symptom onset (Choi et al., 2020).

In case 3, with a catastrophic end, it is of supreme importance to remember that rituximab, an anti-CD20 monoclonal antibody, causes a prolonged B-cell depletion, secondary hypogammaglobulinemia, and the consequent infectious complications. There has been a reasonable concern for patients who require this treatment during the COVID-19 pandemic. A small, retrospective study of 49 patients who had received this drug, for any medical reason, and contracted COVID-19, reported that 63.2% had to be admitted, 24.5% required intensive care, and 32.7% died (Levavi et al., 2021).

The interpretation of Ct has its limitations since several factors may influence the result (Rabaan et al., 2021). They have been classified as pre-analytic (collection technique, type of specimen, sampling time and viral kinetics), analytic (internal control, type of RT-qPCR, purity of reagents, pipetting defects) and post-analytical (interpretation of results).

Even though Ct has not been formally and universally validated for routine use (IDSA, 2021), it could be useful in individual cases when certain clinical decisions must be made. In the city of Buenos Aires, Argentina, the local Ministry of Health stated that, for immunocompromised patients with COVID-19, isolation may be safely ended when, after 21 days from symptom onset, Ct value is greater than 35, provided the test is positive (Buenos Aires Ciudad – Gobierno de la Ciudad Autónoma de Buenos Aires, 2021).

Last but not least, it is noteworthy that Ct and viral load are not the only laboratory determinations that can be used as clinical prediction tools in COVID-19. Two SARS-CoV-2 structural proteins elicit the generation of antibodies: nucleocapsid protein (N) and spike glycoprotein (S). The latter also functions as a viral attachment and fusion protein, enabling virus binding and entry via de angiotensin-converting enzyme 2 (ACE-2) (Murrell et al., 2021). Both of them can be quantitatively measured in serum and have shown to correlate with disease severity and intensive care unit admission, although correlation was higher for S (Ogata et al., 2020). On the other hand, sensitivity of antigen tests varies depending on the viral load, as was reported by Ford et al. (2021). A sensitivity greater than 90% was achieved only with samples with Ct values lower than 29 cycles (Ford et al., 2021). This singularity place quantitative antigen tests at a disadvantage for a comprehensive course predictive tool.

## Conclusion

We have presented 3 patients with haematologic neoplasms who contracted COVID-19 and had different clinical courses, ranging from a practically eventless disease to a fulminating pneumonia, whose Ct values accompanied the disease development.

We could not avoid mentioning that our study is a limited case series of the most representative patients we have encountered since the beginning of the COVID-19 pandemic, rather than original research from which definitive conclusions could be derived.

In accordance with other authors' experience, we believe that Ct is a potentially useful tool which could guide therapeutic decisions and monitor the course of COVID-19, especially in patients with haematologic neoplasms.

## References

- Basquiera, A. L., García, M. J., Rolón, J. M., Olmedo, J., Laviano, J., Burgos, R., Caeiro, G., Remaggi, G., Raña, P., Paoletti, M., González, C. M., Fernández, I., Pavlovsky, A., Perusini, M. A., Rodriguez, A., Guanchiale, L., Carvani, A., Mandrile, L., Figueroa, F., Vicente Reparaz, A., Fragapane Mathus, P. N., Garate, G., Fauque, M. E., Kantor, G., Cruset, S., Gonzalez Lorch, J. S., Szelagowski, M., Giarini, M. P., Oliveira, N., García, M. C., Ventriglia, M. V., Pereyra, P. H., Gutierrez, D. R., Kusminsky, G., Troccoli, J., Freitas, M. J., Cranco, S., Del V Sanchez, N., Rey, I., Funes, M. E., Jarchum, S., Freue, J., Miroli, A., Guerrero, O., López Ares, L., Campestri, R., Bove, V., Salinas, G. N., Cabrejo, M., Milone, J. H., Zabaljauregui, S., Gotta, D., Dupont, J. C., Stemmelin, G. (2021) Clinical characteristics and evolution of hematological patients and COVID-19 in Argentina: A report from the Argentine Society of Hematology. *Medicina (B. Aires)* **81(4)**, 536–645.
- Buenos Aires Ciudad – Gobierno de la Ciudad Autónoma de Buenos Aires (2021) Protocolo de Manejo de Casos SOSPECHOSOS y Confirmados de Coronavirus (COVID-19). Retrieved January 30, 2022, available at: [https://www.buenosaires.gob.ar/sites/gcaba/files/id\\_0\\_-\\_protocolo\\_de\\_manejo\\_frente\\_a\\_casos\\_sospechosos\\_y\\_confirmados\\_de\\_covid-19\\_130122\\_0.pdf](https://www.buenosaires.gob.ar/sites/gcaba/files/id_0_-_protocolo_de_manejo_frente_a_casos_sospechosos_y_confirmados_de_covid-19_130122_0.pdf)
- Choi, B., Choudhary, M. C., Regan, J., Sparks, J. A., Padera, R. F., Qiu, X., Solomon, I. H., Kuo, H.-H.,

- Boucau, J., Bowman, K., Adhikari, U. D., Winkler, M. L., Mueller, A. A., Hsu, T. Y.-T., Desjardins, M., Baden, L. R., Chan, B. T., Walker, B. D., Lichterfeld, M., Brigl, M., Kwon, D. S., Kanjilal, S., Richardson, E. T., Jonsson, A. H., Alter, G., Barczak, A. K., Hanage, W. P., Yu, X. G., Gaiha, G. D., Seaman, M. S., Cernadas, M., Li, J. Z. (2020) Persistence and evolution of SARS-CoV-2 in an immunocompromised host. *N. Engl. J. Med.* **383(23)**, 2291–2293.
- Einsele, H., Borghaei, H., Orlowski, R. Z., Subklewe, M., Roboz, G. J., Zugmaier, G., Kufer, P., Iskander, K., Kantarjian, H. M. (2020) The BiTE (bispecific T-cell engager) platform: Development and future potential of a targeted immuno-oncology therapy across tumor types. *Cancer* **126(14)**, 3192–3201.
- Engelmann, I., Alidjinou, E. K., Ogjez, J., Pagneux, Q., Miloudi, S., Benhalima, I., Ouafi, M., Sane, F., Hober, D., Roussel, A., Cambillau, C., Devos, D., Boukherroub, R., Szunerits, S. (2021) Preanalytical issues and cycle threshold values in SARS-CoV-2 real-time RT-PCR testing: Should test results include these? *ACS Omega* **6(10)**, 6528–6536.
- Faico-Filho, K. S., Passarelli, V. C., Bellei, N. (2020) Is higher viral load in SARS-CoV-2 associated with death? *Am. J. Trop. Med. Hyg.* **103(5)**, 2019–2021.
- Ford, L., Lee, C., Pray, I. W., Cole, D., Bigouette, J. P., Abedi, G. R., Bushman, D., Delahoy, M. J., Currie, D. W., Cherney, B., Kirby, M. K., Fajardo, G. C., Caudill, M., Langolf, K., Kahrs, J., Zochert, T., Kelly, P., Pitts, C., Lim, A., Aulik, N., Tamin, A., Harcourt, J. L., Queen, K., Zhang, J., Whitaker, B., Browne, H., Medrzycki, M., Shewmaker, P. L., Bonenfant, G., Zhou, B., Folster, J. M., Bankamp, B., Bowen, M. D., Thornburg, N. J., Goffard, K., Limbago, B., Bateman, A., Tate, J. E., Gieryn, D., Kirking, H. L., Westergaard, R. P., Killerby, M. E.; CDC COVID-19 Surge Laboratory Group (2021) Epidemiologic characteristics associated with severe acute respiratory syndrome coronavirus 2 (SARS-CoV-2) antigen-based test results, real-time reverse transcription polymerase chain reaction (rRT-PCR) cycle threshold values, subgenomic RNA, and viral culture results from university testing. *Clin. Infect. Dis.* **73(6)**, e1348–e1355.
- IDSA (2021) IDSA statement on the use of CT values final. (n.d.) Retrieved April 20, 2022, available at: <https://www.idsociety.org/globalassets/idsa/public-health/covid-19/idsa-amp-statement.pdf>
- La Scola, B., Le Bideau, M., Andreani, J., Hoang, V. T., Grimaldier, C., Colson, P., Gautret, P., Raoult, D. (2020) Viral RNA load as determined by cell culture as a management tool for discharge of SARS-CoV-2 patients from infectious disease wards. *Eur. J. Clin. Microbiol. Infect. Dis.* **39(6)**, 1059–1061.
- Lee, L. Y. W., Cazier, J.-B., Starkey, T., Briggs, S. E. W., Arnold, R., Bisht, V., Booth, S., Campton, N. A., Cheng, V. W. T., Collins, G., Curley, H. M., Earwaker, P., Fittall, M. W., Gennatas, S., Goel, A., Hartley, S., Hughes, D. J., Kerr, D., Lee, A. J. X., Lee, R. J., Lee, S. M., Mckenzie, H., Middleton, C. P., Murugaesu, N., Newsom-Davis, T., Olsson-Brown, A. C., Palles, C., Powles, T., Protheroe, E. A., Purshouse, K., Sharma-Oates, A., Sivakumar, S., Smith, A. J., Topping, O., Turnbull, C. D., Várnai, C., Briggs, A. D. M., Middleton, G., Kerr, R.; UK Coronavirus Cancer Monitoring Project Team (2020) COVID-19 prevalence and mortality in patients with cancer and the effect of primary tumour subtype and patient demographics: A prospective cohort study. *Lancet Oncol.* **21(10)**, 1309–1316.
- Levavi, H., Lancman, G., Gabrilove, J. (2021) Impact of rituximab on COVID-19 outcomes. *Ann. Hematol.* **100(11)**, 2805–2812.
- Murrell, I., Forde, D., Zelek, W., Tyson, L., Chichester, L., Palmer, N., Jones, R., Morgan, B. P., Moore, C. (2021) Temporal development and neutralising potential of antibodies against SARS-CoV-2 in hospitalised COVID-19 patients: An observational cohort study. *PLoS One* **16(1)**, e0245382.
- Ogata, A. F., Maley, A. M., Wu, C., Gilboa, T., Norman, M., Lazarovits, R., Mao, C.-P., Newton, G., Chang, M., Nguyen, K., Kamkaew, M., Zhu, Q., Gibson, T. E., Ryan, E. T., Charles, R. C., Marasco, W. A., Walt, D. R. (2020) Ultra-sensitive serial profiling of SARS-CoV-2 antigens and antibodies in plasma to understand disease progression in COVID-19 patients with severe disease. *Clin. Chem.* **66(12)**, 1562–1572.

- Rabaan, A. A., Tirupathi, R., Sule, A. A., Aldali, J., Mutair, A. A., Alhumaid, S., Muzaheed, Gupta, N., Koritala, T., Adhikari, R., Bilal, M., Dhawan, M., Tiwari, R., Mitra, S., Emran, T. B., Dhama, K. (2021) Viral dynamics and real-time RT-PCR Ct values correlation with disease severity in COVID-19. *Diagnostics (Basel)* **11(6)**, 1091.
- Westblade, L. F., Brar, G., Pinheiro, L. C., Paidoussis, D., Rajan, M., Martin, P., Goyal, P., Sepulveda, J. L., Zhang, L., George, G., Liu, D., Whittier, S., Plate, M., Small, C. B., Rand, J. H., Cushing, M. M., Walsh, T. J., Cooke, J., Safford, M. M., Loda, M., Satlin, M. J. (2020) SARS-CoV-2 viral load predicts mortality in patients with and without cancer who are hospitalized with COVID-19. *Cancer Cell* **38(5)**, 661–671.e2.
- Wood, W. A., Neuberg, D. S., Thompson, J. C., Tallman, M. S., Sekeres, M. A., Sehn, L. H., Anderson, K. C., Goldberg, A. D., Pennell, N. A., Niemeyer, C. M., Tucker, E., Hewitt, K., Plovnick, R. M., Hicks, L. K. (2020) Outcomes of patients with hematologic malignancies and COVID-19: A report from the ASH Research Collaborative Data Hub. *Blood Adv.* **4(23)**, 5966–5975.

# Amyotrophic Lateral Sclerosis: An Analysis of the Electromyographic Fatigue of the Masticatory Muscles

**Ligia Maria Napolitano Gonçalves<sup>1</sup>, Selma Siéssere<sup>1,2</sup>, Flávia Argentato Cecilio<sup>1</sup>, Jaime Eduardo Cecilio Hallak<sup>2</sup>, Paulo Batista de Vasconcelos<sup>1</sup>, Wilson Marques Júnior<sup>2</sup>, Isabela Hallak Regalo<sup>1</sup>, Marcelo Palinkas<sup>1,2</sup>, Simone Cecilio Hallak Regalo<sup>1,2</sup>**

<sup>1</sup>School of Dentistry of Ribeirão Preto, University of São Paulo, São Paulo, Brazil;

<sup>2</sup>National Institute and Technology – Translational Medicine (INCT.TM), São Paulo, Brazil

Received May 17, 2022; Accepted October 18, 2022.

**Key words:** Amyotrophic lateral sclerosis – Electromyographic fatigue – Median frequency – Masseter muscle – Temporal muscle

**Abstract:** Amyotrophic lateral sclerosis is a chronic degenerative disease that affects motor neurons, thereby promoting functional changes in the human body. The study evaluated the electromyographic fatigue threshold of the masseter and temporal muscles of subjects with amyotrophic lateral sclerosis. A total of eighteen subjects were divided into two groups: amyotrophic lateral sclerosis (n=9) and disease-free control (n=9). The groups were equally divided according to gender (7 males, 2 females). The fatigue threshold was analysed using median frequencies obtained during the 5-second window (initial [IP], mid [MP], and final [FP] periods) of electromyographic signalling of the masseter and temporal muscles bilaterally, with reduction in muscle force during maximal voluntary dental clenching. Significant difference ( $p<0.05$ ) in the left temporal muscle: IP ( $p=0.05$ ) and MP ( $p=0.05$ ) periods was demonstrated. The amyotrophic lateral sclerosis group showed a decrease in median frequency of the electromyographic signal of the masseter and temporal muscles compared to the control group. Amyotrophic lateral sclerosis promotes functional impairment of the stomatognathic system, especially at the electromyographic fatigue threshold of the masticatory muscles.

*This study was supported by FAPESP (Fundação de Amparo à Pesquisa do Estado de São Paulo), and National Institute and Technology – Translational Medicine (INCT.TM), São Paulo, Brazil.*

**Mailing Address:** Prof. Marcelo Palinkas, PhD., School of Dentistry of Ribeirão Preto, University of São Paulo, Avenida do Café s/n, Bairro Monte Alegre CEP 14040-904, Ribeirão Preto, São Paulo, Brazil; e-mail: palinkas@usp.br

## Introduction

Amyotrophic lateral sclerosis is an adult-onset neurodegenerative disease that affects the upper and lower neuromotor system at the bulbar, cervical, thoracic, and lumbar levels (van Es et al., 2017). It prevents correct functionality of the skeletal striated musculature, leading to progressive muscle atrophy and paralysis (Martin et al., 2020; Wobst et al., 2020; Peters et al., 2021; Goutman et al., 2022).

Subjects who develop amyotrophic lateral sclerosis have a clinical picture of fasciculation, progressive muscle weakness, and muscle deterioration. Changes start at the extremities, usually unilaterally. Difficulties in speaking and performing voluntary movements may also be observed (Gonçalves et al., 2018). However, sensory function and intellectual capacity remain unaffected (Gonçalves et al., 2018).

The incidence of amyotrophic lateral sclerosis is not fully established and reported rates vary, depending on the studied population (Zapata-Zapata et al., 2019). Annually, the worldwide incidence is approximately 1 to 2.6 cases per 100,000 subjects, and the prevalence is 6 cases per 100,000 (Talbot et al., 2016).

Voluntary muscle activities involve mechanisms controlling the cerebral cortex and the formation of cross-bridges of myosin with actin filaments, resulting in muscle fiber contractions (Kawai and Jin, 2021). When assessing muscle activities, voluntary muscle fatigue stands out (Berchicci et al., 2013) that is induced by sustained contractions. Contractions is a determinant function of muscle performance (Oliveira et al., 2017; Akagi et al., 2020) and observational studies have provided evidence demonstrating fatigue in subjects with Amyotrophic lateral sclerosis (Nazemi et al., 2016; de Carvalho et al., 2019).

Muscular imbalances resulting from chronic degenerative diseases can be evaluated by specific methods using surface electromyography, which analyses biomechanical effects from the muscular fatigue process (Wanshi Arnoni et al., 2019). However, the electromyographic fatigue threshold of masticatory muscles in subjects with amyotrophic lateral sclerosis has not been identified so far.

In this study, the electromyographic fatigue threshold of the masseter and temporal muscles of subjects with amyotrophic lateral sclerosis was investigated. The null hypothesis to be tested is that there will be no difference between the groups.

## Material and Methods

### *Study design*

The study was approved by the local ethics committee (process # 13071913.3.3001.5419). All subjects were given written and verbal information before participating and gave their written consent.

A post hoc sample size calculation was conducted with  $\alpha = 0.05$  and a power of 99%. For the main outcome: median values of the median frequency in the fatigue condition for the left temporal muscle (mean of initial periods, disease-free control group = 144.12 [24.58] and amyotrophic lateral sclerosis group = 183.10 [51.33]), an effect size of 0.96 was determined. The minimal sample size obtained

**Table 1 – Comparison of body mass index and age (years) between amyotrophic lateral sclerosis group (ALSG) and disease-free control group (CG) using Student's t-test (p<0.05)**

	Groups		P-value
	ALSG	CG	
Age	43.50 (4.50)	43.30 (4.90)	0.97
Body mass index	20.68 (1.53)	21.38 (1.46)	0.74

was 18 volunteers (9 in each group). Sample size calculation was performed with the G\* Power software (v.3.1.9.2, Franz Faul, Universität Kiel, Germany).

We evaluated subjects with ALS (amyotrophic lateral sclerosis) who attended the Department of Neurosciences and Behavioral Sciences, Ribeirão Preto, São Paulo, Brazil. From an initial cohort of thirty subjects with amyotrophic lateral sclerosis, nine subjects with the disease (mean age [SD – standard deviation] = 43.5 [4.5] years) were selected for the amyotrophic lateral sclerosis group on the basis of the eligibility screening criteria.

All subjects with amyotrophic lateral sclerosis were medicated with riluzole. The potential drug interactions with caffeine, anti-inflammatory, tranquillizer, vasodilator, and antidepressants were explained, to avoid the reduction of drug potentiation. The diagnosis of the disease was confirmed by an experienced neurologist.

The disease-free control group (mean age [SD] = 43.3 [4.9] years) comprised of subjects with normal occlusion (Angle's class I), without temporomandibular disorder, with all permanent teeth (except third molars) who were matched by age, gender, and body mass index with the subjects in the amyotrophic lateral sclerosis group (Table 1). The groups were equally divided into males and females (7 males, 2 females).

The exclusion criteria included cognitive changes, necessity for ventilatory support, diseases of the anterior medullary horn, dementia, visual, autonomic, and sphincter disorders, temporomandibular disorders, absence of first permanent molars, and moderate to severe malocclusion. Research Diagnostic Criteria for Temporomandibular Disorders (RDC/TMD) questionnaire was used to determine the absence of temporomandibular disorders in both groups (Louca Junger et al., 2017).

Analyses of the electromyographic signals were performed by a single trained professional. Intra-examiner calibration was performed for all analyses in this study. The reliability of the intra-rater was calculated via intra-class coefficient (ICC). Reliability was considered acceptable for electromyographic activity (ICC = 0.936).

#### *Surface electromyography recordings*

Surface EMG (electromyographic) activity recordings were performed using MyoSystem Br1\_P84 electromyograph (Datahominis, Uberlândia, Minas Gerais,

Brazil) with four simple differential active sensors (Datahominis Ltda., Modelo DHT-easd; two 10-mm-long  $\times$  2-mm-wide silver chloride bars 10 mm apart). Input impedance of 1010  $\Omega/6$ , pf, bias current input of  $\pm 2$  nA, common-mode rejection ratio of 110 dB at 60 Hz, and gain equal to  $\times 20$ , was used to capture the electromyographic signals of the masseter and temporal muscles under the following conditions of the electromyographic fatigue threshold (Hz).

The sensors were positioned in the masticatory muscles by the same operator trained according to the Surface EMG for Non-Invasive Assessment of Muscles (SENIAM) recommendations (Hermens et al., 2000). The positioning point of the sensors was determined by dental clenching in maximum voluntary contraction, accompanied by digital palpation.

Fatigue threshold of the electromyographic signal was assessed using the median frequency spectrum. Muscle fatigue was determined by reduction of muscle force during maximal voluntary dental clenching (Gandevia, 2001; Di Palma et al., 2017).

The duration of maximum isometric contraction was measured. The case group had an average period of  $29.48 \pm 4.06$  seconds, and the disease-free control group had an average period of  $28.88 \pm 5.01$  seconds.

The signals were analogically amplified ( $1000\times$  gain), filtered (0.02–2 kHz bandpass filter), and sampled by a 12-bit A/D converter board with a 4 kHz acquisition frequency. The processed electromyographic signals from the masseter and temporal muscles bilaterally, enabled the establishment of the raw signal that was used to derive median frequency values through the five-second window of the initial, mid, and final periods.

#### *Statistical analysis*

Data are presented as group mean values  $\pm$  standard deviations (SD). The electromyographic data were tabulated and analyzed using the BM SPSS Statistics for Windows, version 22.0 (IBM SPSS, IBM Corp., Armonk, NY, USA). Data were submitted to Student's *t*-test ( $p < 0.05$ ).

### **Results**

Table 1 shows a comparison of the data between the groups. No significant differences (95% confidence interval [CI]) were found between the groups in terms of age ( $p = 0.97$ ) and body mass index ( $p = 0.74$ ).

The median frequencies of the electromyographic signal of the masseter and temporal muscles bilaterally, during the initial (IP), mid (MP), and final (FP) periods were compared between the groups, as shown in Table 2. Statistical significance was demonstrated ( $p \leq 0.05$ ) in the left temporal muscle during the IP ( $p = 0.05$ ) and MP ( $p = 0.05$ ) periods. The amyotrophic lateral sclerosis group showed a decrease in the median frequency of the electromyographic signal of the masseter and temporal muscles compared to the control group.

**Table 2 – Mean values, standard deviation, and statistical significance ( $p < 0.05$ ) of the median frequency spectrum (Hz) in the condition of electromyographic fatigue of the right masseter (MD), left masseter (ME), right temporal (TD), and left temporal muscles (TE): initial (IP), mid (MP), and final (FP) periods between amyotrophic lateral sclerosis (ALSG) and disease-free control (CG) groups**

Muscles	Periods	Groups		P-value
		ALSG	CG	
RM	IP	139.12 ± 44.75	164.36 ± 48.03	0.26
	MP	135.63 ± 45.39	158.41 ± 43.83	0.29
	FP	132.41 ± 45.34	152.23 ± 41.81	0.34
LM	IP	130.60 ± 27.30	159.01 ± 49.36	0.15
	MP	120.72 ± 26.40	151.44 ± 42.34	0.08
	FP	116.65 ± 23.33	140.05 ± 41.69	0.16
RT	IP	138.32 ± 31.01	176.55 ± 50.77	0.07
	MP	133.20 ± 30.92	164.18 ± 44.99	0.10
	FP	126.55 ± 28.88	159.23 ± 48.72	0.10
LT	IP	144.12 ± 24.58	183.10 ± 51.33	0.05
	MP	138.15 ± 33.27	176.87 ± 46.07	0.05
	FP	139.25 ± 30.09	166.95 ± 40.51	0.11

## Discussion

To the authors' knowledge, this is the first study to examine the electromyographic fatigue threshold to determine the functional patterns in subjects with amyotrophic lateral sclerosis. When comparing subjects with amyotrophic lateral sclerosis with disease-free subjects, the null hypothesis of this study was rejected because there was a significant difference between the groups.

The identification of muscle fatigue through electromyographic evaluation has been evidenced by the phenomenon of decreased median frequency of the electromyographic signal (Oliveira et al., 2005; Wanshi Arnoni et al., 2019; Qi et al., 2020). Although muscle fatigue is a well-studied subject, no results were found in any studies regarding electromyographic fatigue threshold of the masseter and temporal muscles in subjects with amyotrophic lateral sclerosis. This made it difficult to compare our results with those of previous studies.

According to Wanshi Arnoni et al. (2019), the median frequency spectrum in the electromyographic signal of the masseter and temporal muscles is lower than that in the control group without degenerative diseases, such as osteoporosis (Imagama et al., 2019). Our results concur with the findings of the literature, where the spectrum of the median frequency of the masseter and temporal muscles in the initial, medium, and final periods were shown to be smaller in the amyotrophic lateral sclerosis group.

The observed reduction in the median frequency spectrum of subjects with amyotrophic lateral sclerosis may be explained by the relationship between production and control of muscle strength, which are processes resulting from the central and peripheral nervous systems. It is known that the median frequency spectrum is a sensitive variable, which is associated with changes in the pattern of muscle recruitment and the absence of speed of propagation of the action potential of muscle fibers, causing changes in the physiological muscle profile (Escorcio-Bezerra et al., 2018; Musarò et al., 2019).

In subjects with amyotrophic lateral sclerosis, the motor units that have lost innervation, return to innervation after a certain period, due to the axon collateral sprouting that occurs in the surviving motoneurons. This influences the characteristics of the muscle fibers, modifies the recruitment patterns of the muscle fibers, and the production of strength; thereby reducing the synchrony of activation of muscle fibers with polyphasic potentials (Martineau et al., 2018). Thus, the action potential of the motor unit increases in size and decreases in functionality, with reduced amplitude and duration.

In the analysis of the electromyographic fatigue between the groups during the initial, mid, and final periods, a significant difference was found only for the left temporal muscle in the initial and mid periods. This muscle presented higher values in the disease-free control group. The other muscles studied did not show a significant difference.

Neurons are cells that make up the central nervous system, polarized with an extended axon, facing, with the function of maintaining energy homeostasis and mitochondrial integrity (Lin et al., 2017). Chronic mitochondrial stress has been mentioned in the main neurodegenerative diseases, including amyotrophic lateral sclerosis (Xie et al., 2015). The decrease in the median frequency spectrum in amyotrophic lateral sclerosis during the initial, mid, and final periods of the electromyographic signal may be directly related to mitochondrial stress. In this study, long-term cumulative mitochondrial stress was not evaluated, which can lead to axonal accumulation of damaged mitochondria, promoting less efficiency (Xie et al., 2015).

Thus, there is a direct relationship between the motor neuron and the action potential of the muscle fiber. The possible changes in this dynamic process that results from the combination of depolarization and repolarization could compromise muscle efficiency and reduce the spectrum of the median frequency of the electromyographic signal of the skeletal striated muscle of subjects with amyotrophic lateral sclerosis.

The decreased of the median frequency spectrum of the electromyographic signal in subjects with amyotrophic lateral sclerosis can also be explained by the interruption of blood flow, with a lack of nutrients and oxygen in the skeletal muscles that subjects with degenerative disease may present as clinical signs (Tanaka et al., 2003).

This study is important for determining the morphology and function of humans, especially the skeletal striated muscles of subjects with amyotrophic lateral sclerosis because it shows that disease alters the standard electromyographic. Therefore, the clinical relevance lies in the fact that longer dental procedures could take place in subjects with degenerative disease, as long as the dentist is careful to respect the functional conditions of the masticatory muscles that can fatigue more easily, when compared to groups without the disease.

This study has several limitations. First, the sample size is small. Second, significant differences between the groups and monitoring of the subjects longitudinally would provide more information. However, in this study, the electromyographic analysis was performed for only a single time point.

## Conclusion

The authors of this study suggest that amyotrophic lateral sclerosis promotes functional impairment of the stomatognathic system; in particular, in the electromyographic fatigue threshold of the masticatory muscles.

## References

- Akagi, R., Hinks, A., Davidson, B., Power, G. A. (2020) Differential contributions of fatigue-induced strength loss and slowing of angular velocity to power loss following repeated maximal shortening contractions. *Physiol. Rep.* **8**, e14362.
- Berchicci, M., Menotti, F., Macaluso, A., Di Russo, F. (2013) The neurophysiology of central and peripheral fatigue during sub-maximal lower limb isometric contractions. *Front. Hum. Neurosci.* **7**, 135.
- de Carvalho, M., Swash, M., Pinto, S. (2019) Diaphragmatic neurophysiology and respiratory markers in ALS. *Front. Neurol.* **10**, 143.
- Di Palma, E., Tepedino, M., Chimenti, C., Tartaglia, G. M., Sforza, C. (2017) Effects of the functional orthopaedic therapy on masticatory muscles activity. *J. Clin. Exp. Dent.* **9**, e886–e891.
- Escorcio-Bezerra, M. L., Abrahao, A., Nunes, K. F., De Oliveira Braga, N. I., Oliveira, A. S. B., Zinman, L., Manzano, G. M. (2018) Motor unit number index and neurophysiological index as candidate biomarkers of presymptomatic motor neuron loss in amyotrophic lateral sclerosis. *Muscle Nerve* **58**, 204–212.
- Gandevia, S. C. (2001) Spinal and supraspinal factors in human muscle fatigue. *Physiol. Rev.* **81**, 1725–1789.
- Gonçalves, L. M. N., Palinkas, M., Hallak, J. E. C., Marques Júnior, W., Vasconcelos, P. B., Frota, N. P. R., Regalo, I. H., Siéssere, S., Regalo, S. C. H. (2018) Alterations in the stomatognathic system due to amyotrophic lateral sclerosis. *J. Appl. Oral Sci.* **26**, e20170408.
- Goutman, S. A., Hardiman, O., Al-Chalabi, A., Chió, A., Savelieff, M. G., Kiernan, M. C., Feldman, E. L. (2022) Recent advances in the diagnosis and prognosis of amyotrophic lateral sclerosis. *Lancet Neurol.* **21**, 480–493.
- Hermens, H. J., Freriks, B., Disselhorst-Klug, C., Rau, G. (2000) Development of recommendations for SEMG sensors and sensor placement procedures. *J. Electromyogr. Kinesiol.* **10**, 361–374.
- Imagama, S., Ando, K., Kobayashi, K., Machino, M., Tanaka, S., Morozumi, M., Kanbara, S., Ito, S., Inoue, T., Seki, T., Ishizuka, S., Nakashima, H., Ishiguro, N., Hasegawa, Y. (2019) Multivariate analysis of factors related to the absence of musculoskeletal degenerative disease in middle-aged and older people. *Geriatr. Gerontol. Int.* **19**, 1141–1146.
- Kawai, M., Jin, J. P. (2021) Mechanisms of Frank-Starling law of the heart and stretch activation in striated muscles may have a common molecular origin. *J. Muscle Res. Cell Motil.* **42**, 355–366.

- Lin, M. Y., Cheng, X. T., Tammineni, P., Xie, Y., Zhou, B., Cai, Q., Sheng, Z. H. (2017) Releasing syntrophin removes stressed mitochondria from axons independent of mitophagy under pathophysiological conditions. *Neuron* **94**, 595.e6–610.e6.
- Louca Jounger, S., Christidis, N., Svensson, P., List, T., Ernberg, M. (2017) Increased levels of intramuscular cytokines in patients with jaw muscle pain. *J. Headache Pain* **18**, 30.
- Martin, E., Cazenave, W., Allain, A. E., Cattaert, D., Branchereau, P. (2020) Implication of 5-HT in the dysregulation of chloride homeostasis in prenatal spinal motoneurons from the G93A mouse model of amyotrophic lateral sclerosis. *Int. J. Mol. Sci.* **21**, 1107.
- Martineau, É., Di Polo, A., Vande Velde, C., Robitaille, R. (2018) Dynamic neuromuscular remodeling precedes motor-unit loss in a mouse model of ALS. *Elife* **7**, e41973.
- Musarò, A., Dobrowolny, G., Cambieri, C., Onesti, E., Ceccanti, M., Frasca, V., Pisano, A., Cerbelli, B., Lepore, E., Ruffolo, G., Cifelli, P., Roseti, C., Giordano, C., Gori, M. C., Palma, E., Inghilleri, M. (2019) Neuromuscular magnetic stimulation counteracts muscle decline in ALS patients: Results of a randomized, double-blind, controlled study. *Sci. Rep.* **9**, 2837.
- Nazemi, M., Raad, M. H., Arzoumanian, C. S., Ghasemzadeh, A. (2016) Fatigue and depression in Iranian amyotrophic lateral sclerosis patients in Tehran in 2012. *Electron. Physician* **8**, 2194–2198.
- Oliveira, A. S., Gonçalves, M., Cardozo, A. C., Barbosa, F. S. (2005) Electromyographic fatigue threshold of the biceps brachii muscle during dynamic contraction. *Electromyogr. Clin. Neurophysiol.* **45**, 167–175.
- Oliveira, L. F., Palinkas, M., Vasconcelos, P. B., Regalo, I. H., Cecilio, F. A., Oliveira, E. F., Semprini, M., Siéssere, S., Regalo, S. H. (2017) Influence of age on the electromyographic fatigue threshold of the masseter and temporal muscles of healthy subjects. *Arch. Oral Biol.* **84**, 1–5.
- Peters, S., Broberg, K., Gallo, V., Levi, M., Kippler, M., Vineis, P., Veldink, J., van den Berg, L., Middleton, L., Travis, R. C., Bergmann, M. M., Palli, D., Grioni, S., Tumino, R., Elbaz, A., Vlaar, T., Mancini, F., Kühn, T., Katzke, V., Agudo, A., Goñi, F., Gómez, J. H., Rodríguez-Barranco, M., Merino, S., Barricarte, A., Trichopoulou, A., Jenab, M., Weiderpass, E., Vermeulen, R. (2021) Blood metal levels and amyotrophic lateral sclerosis risk: A prospective cohort. *Ann. Neurol.* **89**, 125–133.
- Qi, L., Zhang, L., Lin, X. B., Ferguson-Pell, M. (2020) Wheelchair propulsion fatigue thresholds in electromyographic and ventilatory testing. *Spinal Cord* **58**, 1104–1111.
- Talbott, E. O., Malek, A. M., Lacomis, D. (2016) The epidemiology of amyotrophic lateral sclerosis. *Handb. Clin. Neurol.* **138**, 225–238.
- Tanaka, M., Ichiba, T., Kondo, S., Hirai, S., Okamoto, K. (2003) Cerebral blood flow and oxygen metabolism in patients with progressive dementia and amyotrophic lateral sclerosis. *Neurol. Res.* **25**, 351–356.
- van Es, M. A., Hardiman, O., Chio, A., Al-Chalabi, A., Pasterkamp, R. J., Veldink, J. H., van den Berg, L. H. (2017) Amyotrophic lateral sclerosis. *Lancet* **390**, 2084–2098.
- Wanshi Arnoni, V., Batista de Vasconcelos, P., Sousa, L. G., Ferreira, B., Palinkas, M., Acioli Righetti, M., Pádua da Silva, G., Aparecida Caldeira Monteiro, S., Regalo, S. C. H., Siéssere, S. (2019) Evaluation of the electromyographic fatigue of the masseter and temporalis muscles in subjects with osteoporosis. *Cranio* **37**, 254–263.
- Wobst, H. J., Mack, K. L., Brown, D. G., Brandon, N. J., Shorter, J. (2020) The clinical trial landscape in amyotrophic lateral sclerosis – Past, present, and future. *Med. Res. Rev.* **40**, 1352–1384.
- Xie, Y., Zhou, B., Lin, M. Y., Wang, S., Foust, K. D., Sheng, Z. H. (2015) Endolysosomal deficits augment mitochondria pathology in spinal motor neurons of asymptomatic fALS mice. *Neuron* **87**, 355–370.
- Zapata-Zapata, C. H., Franco Dáger, E., Aguirre-Acevedo, D. C., de Carvalho, M., Solano-Atehortúa, J. (2019) Prevalence, incidence, and clinical-epidemiological characterization of amyotrophic lateral sclerosis in Antioquia: Colombia. *Neuroepidemiology* **6**, 1–7.

# Pervitin Intoxication with Two-peak Massive Myoglobinemia, Acute Kidney Injury and Marked Procalcitonin Increase Not Associated with Sepsis

**Eva Svobodová<sup>1</sup>, Tomáš Drábek<sup>2</sup>, Helena Brodská<sup>3</sup>**

<sup>1</sup>Department of Anesthesiology and Intensive Care Medicine, First Faculty of Medicine, Charles University and General University Hospital in Prague, Prague, Czech Republic;

<sup>2</sup>Department of Anesthesiology and Perioperative Medicine, University of Pittsburgh School of Medicine and UPMC, Pittsburgh, United States;

<sup>3</sup>Institute of Medical Biochemistry and Laboratory Diagnostics, First Faculty of Medicine, Charles University and General University Hospital in Prague, Prague, Czech Republic

Received May 31, 2022; Accepted October 18, 2022.

**Key words:** Methamphetamine – Procalcitonin – Acute kidney injury – Dialysis – Myoglobin – Rhabdomyolysis

**Abstract:** Patients intoxicated with methamphetamine-like substances may present with myoglobinuria but rarely require admission. An 18-year-old female was admitted due to intoxication with pervitin, a methamphetamine derivative. She presented with an altered mental status, fever, and increased heart and respiratory rates. Biomarkers showed leukocytosis and markedly increased procalcitonin levels, suggestive of sepsis. However, blood cultures and infectious disease workup were unrevealing. Clinical course was heralded by rhabdomyolysis and myoglobinuria resulting in multi-organ failure including respiratory failure necessitating mechanical ventilation, hemodynamic compromise with need for inotropic support, and an acute renal failure requiring renal replacement therapy. Surprisingly, after a transient improvement, an unexpected second peak of myoglobin was observed on hospital day 5, controlled by intensifying the elimination methods, and administration of dantrolene. Acute kidney injury resolved by hospital day 15, and the patient could be discharged on day 22. While most patients with intoxications are discharged

**Mailing Address:** Assoc. Prof. Helena Brodská, MD., PhD., Institute of Medical Biochemistry and Laboratory Diagnostics, First Faculty of Medicine, Charles University and General University Hospital in Prague, U nemocnice 499/2, 128 08 Prague 2, Czech Republic; e-mail: brodska@vfn.cz

within 24 hours from emergency departments without being admitted, our case report highlights that the organ injury may evolve beyond the usual observation period, traditional renal-replacement therapies may not be sufficient to mitigate myoglobinemia with resulting acute kidney injury, and that procalcitonin may not be a reliable biomarker of infection in the setting of drug-induced rhabdomyolysis.

## Introduction

Pervitin, a methamphetamine parallel, has been synthesized in 1937 and massively marketed to German soldiers during World War II as a psychostimulant to facilitate their alertness and combat capacities for prolonged periods of time, sometimes days (Defalque and Wright, 2011). Scientific explorations striving to characterize the psychomimetic drug effects have been conducted by American psychiatrists in the late 1940s (Levine et al., 1948; Schein and Goolker, 1951). To this date, along with methamphetamine, pervitin ranks among the most popular illicit stimulant drugs, accounting for 30 to 50% of most used drugs in central Europe (Sejda et al., 1998; Seblova et al., 2005).

Intoxication with pervitin is characterized by agitation, restlessness, headaches, mydriasis, tachycardia with arrhythmias, and increased body temperature. Severe intoxications may be complicated by altered levels of consciousness that complicates obtaining a relevant clinical history. The clinical picture of hyperpyrexia in intoxications often resembles that of malignant hyperthermia, including rhabdomyolysis, impaired liver and renal function, disseminated intravascular coagulopathy (DIC) and multi-organ failure. Biomarkers of sepsis are often utilized to differentiate between infectious vs. non-infectious pathologies in patients presenting with fever. Most patients with acute intoxications with methamphetamines are discharged from emergency departments after extended observation period without being admitted. However, a small number of patients presenting with intoxication warrant in-hospital admission and complex care for complex metabolic disturbances.

## Case report

Emergency Medical Service crew was dispatched to the railway station to an unconscious patient “found down”. At the scene, an 18-year-old female was located. Reportedly, she had injected herself with an extremely high dose (1 g) of pervitin intravenously (IV). No past medical history could be obtained from the patient. She was found delirious, uncooperative, agitated, severely hypoglycemic (1.9 mmol/l), febrile, with mydriatic pupils. She was transported to the Emergency Department of the General University Hospital in Prague, Czech Republic.

In the emergency department, she was found restless, with mydriatic pupils, minor muscle tremor, chills, fever (axillary temperature 39.2 °C; bladder temperature 41.2 °C). Electrocardiogram revealed stable sinus tachycardia 150/min. She was normotensive and tachypneic > 35 breaths/min. Pulse oximetry showed 95% on room air. No meningeal irritation was observed. The primary and secondary

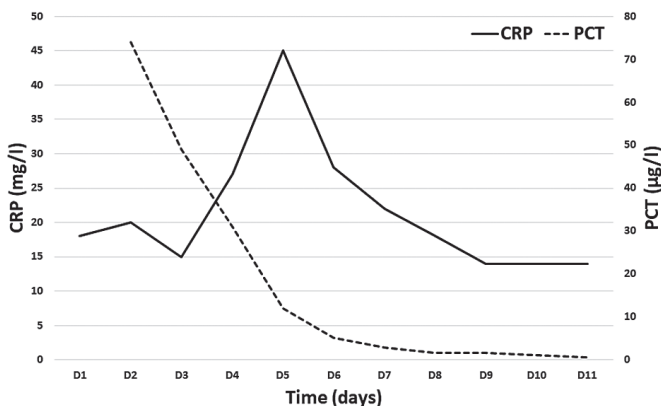


Figure 1 – Dynamics of the biomarkers of sepsis (CRP – C-reactive protein; PCT – procalcitonin).

surveys including focal assessment with sonography in trauma ruled out solid organ injury. Blood and urine samples were obtained, and the patient was admitted to the Intensive Care Unit due to suspected developing septic shock.

Upon admission, her Glasgow Coma Scale score was determined to be 6. She was intubated for airway protection, and mechanical ventilation was commenced. An empiric antibiotic therapy (amoxicillin clavulanate + gentamicin) was started due to fever, high leukocyte count ( $30.6 \times 10^9/l$ ) and risk of bloodstream infection in an IV drug abuser. Urine toxicology screen was positive for excitatory amines and cannabinoids. Admission laboratory values identified acute kidney injury (AKI), acute liver injury, coagulation abnormalities and rhabdomyolysis with increased myoglobin levels. Biomarkers of sepsis showed markedly increased procalcitonin (PCT) contrasting only a modest increase of C-reactive protein (CRP) (Figure 1). She tested positive for hepatitis C (viral load 3,480 IU/l; normal values < 15 IU/l).

In the next 24 hours, clinical condition of the patient gradually worsened despite ongoing support of her vital functions, ultimately developing multi-organ failure. She required hemodynamic support with norepinephrine at  $0.25 \mu\text{g}/\text{kg}/\text{min}$ . Acute anuric renal failure developed requiring initiation of continuous renal replacement therapy (CRRT) in the form of continuous veno-venous hemodialysis (CVVHD) using Aquarius Haemodialysis System (Edwards Lifesciences, United Kingdom) with Aquamax HD19 filter (Nikkiso, Belgium).

Laboratory results (summarized in Table 1) were dominated by increased markers of rhabdomyolysis: creatine phosphokinase (CPK,  $501 \mu\text{kat}/l$ ), myoglobin ( $21,266 \mu\text{g}/l$ ) and aspartate aminotransferase (AST,  $18.93 \mu\text{g}/l$ ). Increased nitrogenous end products of metabolism (urea  $20 \text{ mmol}/l$ , creatinine  $325 \mu\text{mol}/l$ ) documented AKI. Acute liver injury was documented by increased liver enzymes, specifically alanine aminotransferase (ALT,  $13.14 \mu\text{kat}/l$ ) and aspartate aminotransferase (AST,  $18.93 \mu\text{kat}/l$ ). Biomarkers of sepsis showed isolated significant increase of PCT ( $74.31 \mu\text{g}/l$ ) with modest increase of CRP ( $20.8 \text{ mg}/l$ ),

and leukocytes ( $17.7 \times 10^9/l$ ). Coagulation parameters were also altered significantly, suggestive of DIC (INR – international normalized ratio 2.08; aPTT – activated partial thromboplastin time 103 s) with thrombocytopenia ( $61 \times 10^9/l$ ).

On day 3, PCT level was decreasing, but CRP and leukocytes remained increased (PCT  $49.94 \mu\text{g}/l$ , CRP  $15.5 \text{ mg}/l$ , leukocytes  $15.6 \times 10^9/l$ ). Thus, gentamicin was discontinued, while amoxicillin clavulanate and rifaximin were continued. Spontaneous coagulation disorder and thrombocytopenia persisted, which was treated by pooled platelets and plasma administration. Myoglobin levels decreased to  $11,373 \mu\text{g}/l$  during ongoing CVVHD that was continued for 76 hours (myoglobin clearance  $16.9 \text{ ml}/h$ ). Liver function tests further increased.

On day 4, the patient was extubated as her clinical condition improved. Myoglobin levels increased again to  $25,485 \mu\text{g}/l$ . CRRT method was changed from CVVHD to high-flux continuous veno-venous hemofiltration (CVVH) to facilitate the elimination of myoglobin, and continued for 62 hours. This was confirmed by the evaluation of the dialysate, confirming a successful removal of myoglobin (myoglobin clearance  $20.3 \text{ ml}/h$ ).

On day 5, a second peak of myoglobin ( $>40,500 \mu\text{g}/l$ ) and CPK ( $944.64 \mu\text{kat}/l$ ) was observed despite CVVH. At that time-point, dantrolene ( $100 \text{ mg IV}$ ) was added to the therapy to further mitigate rhabdomyolysis. On the following days, the myoglobin concentration gradually decreased (Figure 2). The patient remained anuric, requiring continued CRRT.

On day 9, the patient remained hemodynamically stable with adequate spontaneous respiration, and re-started oral intake. However, her anuria persisted. She was transferred to the Department of Nephrology for further care, where intermittent hemodialysis treatment (IHD) was provided. The last IHD was performed on day 15, while diuresis gradually resumed. After 22 days of hospitalization, the patient was discharged home.

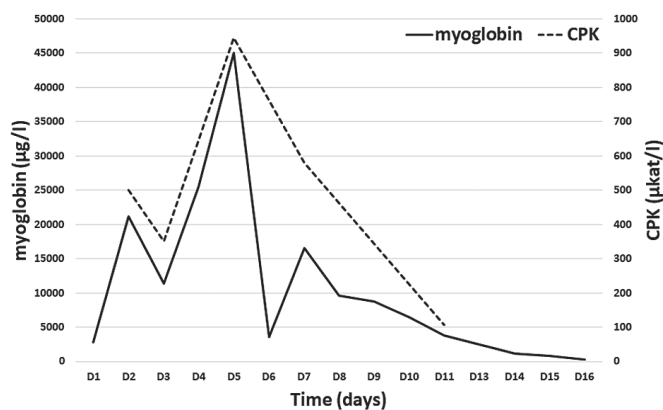


Figure 2 – Dynamics of the biomarkers of rhabdomyolysis (CPK – creatinine phosphokinase).

Table 1 – Biochemical, hematological and coagulation profile

	D1	D2	D3	D4	D5	D6	D7	D8	D9
<b>ABG + electrolytes</b>									
pH	7.36	7.32	7.33	7.33	7.33	7.38	7.43	7.44	7.45
pCO <sub>2</sub> (kPa)	2.610	5.68	4.92	6.32	4.83	5.06	5.37	5.52	5.69
HCO <sub>3</sub> <sup>-</sup> (mmol/l)	10.90	21.40	18.90	24.50	18.70	22.10	26.20	27.70	28.90
BE (mmol/l)	-12.40	-4.10	-6.00	-1.10	-6.10	-2.10	2.30	3.70	4.80
pO <sub>2</sub> (kPa)	10.70	13.90	19.10	18.50	12.20	12.00	11.20	10.90	12.00
Glucose (mmol/l)	5.40	9.10	6.30	6.20	6.60	6.00	6.30	6.10	5.21
Na <sup>+</sup> (mmol/l)	141.00	139.00	137.00	140.00	137.00	136.00	140.00	139.00	132.00
K <sup>+</sup> (mmol/l)	6.90	4.40	4.50	4.10	4.00	3.90	4.30	4.40	4.50
Cl <sup>-</sup> (mmol/l)	110.00	109.00	108.00	102.00	105.00	99.00	98.00	100.00	94.00
Ca <sup>++</sup> (mmol/l)	0.99	1.01	0.92	0.99	0.99	0.93	0.89	1.10	1.07
Lactate (mmol/l)	2.30	1.70	2.70	1.70	1.50	1.40	1.40	1.60	1.10
<b>Biochemistry</b>									
Urea (mmol/l)	13.00	20.20	9.90	9.20	8.90	13.30	15.80	17.10	24.90
Creatinine (μmol/l)	203.00	325.00	225.00	262.00	225.00	285.00	282.00	275.00	388.00
Bilirubin <sub>t</sub> (μmol/l)	65.40	61.10	77.20	67.10	53.70	46.00	26.90	19.50	18.80
Bilirubin <sub>c</sub> (μmol/l)	23.90	28.80	32.90	29.80	26.90	20.00	12.80	9.70	7.80
ALT (μkat/l)	6.31	13.14	41.62	52.69	49.76	31.29	21.58	14.03	8.93
AST (μkat/l)	3.27	18.93	45.14	43.66	41.58	31.78	21.16	14.44	10.98
GGT (μkat/l)	0.39	0.38	0.41	0.70	0.77	0.70	0.74	0.64	0.48
ALP (μkat/l)	1.17	1.25	1.51	1.55	1.32	1.15	1.05	0.81	

	D1	D2	D3	D4	D5	D6	D7	D8	D9
<b>Hematology</b>									
WBC ( $\times 10^9/l$ )	30.60	17.70	15.60	9.00	7.10	7.20	6.30	5.40	5.60
Hematocrit	0.43	0.421	0.36	0.38	0.38	0.34	0.31	0.29	0.22
Platelets ( $\times 10^9/l$ )	456.00	61.00	34.00	64.00	69.00	94.00	131.00	169.00	167.00
NLR	35.00	9.80	8.70	6.80	7.60	5.70	4.90	3.00	2.00
<b>Coagulation</b>									
INR	1.3	2.3	1.8	1.2	1.0	0.9	0.9	1.1	0.9
aPTT (s)	28	116	32	33	31	29	36	32	38

BE – base excess; ALT – alanine aminotransferase; AST – aspartate aminotransferase; GGT – gamma glutamyltransferase; ALP – alkaline phosphatase; WBC – white blood count; NLR – neutrophil-leukocyte ratio; INR – international normalized ratio; aPTT – activated partial thromboplastin time

She was seen in the outpatient clinic for follow-up after five weeks. She was in a stable clinical condition with normalized glycemia, normal CRP, persisting kidney injury and increased liver function tests with increased hepatitis C viral load (127,000 IU/l).

## Discussion

The main toxicity seen with methamphetamines including pervitin is acute behavioral disturbance, which is usually managed adequately with sedation. The most common complications are rhabdomyolysis (30%) and acute kidney injury (15%). Less than 15% of patients seen in emergency departments are admitted, usually to behavioral units (Isoardi et al., 2019). However, severe intoxications may present under complex picture of altered mental status prohibiting obtaining relevant medical history, with a combination of chronic and acute medical problems. The propensity of intoxicated patients to develop rhabdomyolysis has been recognized (Penn et al., 1972). Initial care is often based on physical assessment of vital signs, supported by panels of laboratory assessments to facilitate diagnostic process and initiate treatment.

Multiple biomarkers are utilized to diagnose infection in patients presenting with fever. The most commonly used biomarkers in patients with suspected sepsis are CRP and PCT, both with excellent diagnostic capacities including high sensitivity and specificity to differentiate between bacterial infection vs. systemic inflammatory response syndrome (Hu et al., 2017).

Our case is interesting in two distinct aspects: first, initially high CRP and PCT levels with fever suggested bacterial infection. Second, myoglobin profile had a second, higher peak occurring late on day 5 of in-hospital stay, despite ongoing CRRT.

### *Increased PCT without evidence of infection*

Fever, tachycardia, high white blood count along with high initial CRP level and PCT level (on day 2) were originally suggestive of bacterial infection, as suspected in an IV drug abuser presenting with fever. Hence, antibiotic therapy was initiated accordingly. However, if infection was found to be the underlying pathology, a different course of PCT values had been expected in the following days. PCT peaks in 24 hours, CRP peaks with a slight delay in 48 hours. PCT usually shows an upward tendency in the first days. CRP values would mirror high PCT levels (with slight delay) in patients with preserved protein synthesis capacities.

Once the admission blood cultures and swabs returned negative, antibiotic therapy was de-escalated on day 3. Due to persistently high, albeit decreasing, PCT and CRP levels, we continued amoxicillin clavulanate for 6 days on an empirical basis. After repeated negative findings on microbiological examination of swabs and blood cultures, we excluded concurrent infection and started to consider a non-infectious origin of the increased PCT level. Our hypothesis of a non-infectious origin of the

high PCT levels was supported by the persistently low CRP values during the early in-hospital stay. The high leukocyte count and neutrophil-lymphocyte ratio (NLR) in the first three days of hospitalization could be interpreted as a nonspecific marker of inflammation. NLR is more likely to be a marker of severity of the condition. However, we cannot exclude with certainty an infectious etiology of the condition (only less than 50% of sepsis cases show an infectious agent) although this seems less likely.

In massive rhabdomyolysis, a marked increase in PCT levels associated with sympathomimetic drug intoxication has been described in several case-reports (Lovas et al., 2014). PCT is produced by injured tissues and macrophages. Its secretion is activated by damage associated molecular patterns (DAMPs), mainly alarmins, which are endogenous mediators produced by processes such as ischemia, trauma or necrosis, in the case of hyperpyrexia triggered by heat shock proteins (HSPs). Kodama et al. (2021) described a similar increase of PCT in a 20-year-old female following sympathomimetic drug overdose after ingestion of ephedrine, ephedrine derivative, yohimbine and caffeine in an apparent suicide attempt. No bacterial infection was identified (Kodama et al., 2021). Zuberi et al. (2019) describe a massive PCT increase after intoxication of a psychostimulant kratom, associated with hypotension and transient AKI. The patient required hemodynamic support with vasopressors. AKI was managed with IV fluid therapy without the need for dialysis (Zuberi et al., 2019).

#### *Two-peak myoglobinemia*

Our patient also presented with high levels of myoglobin suggestive of rhabdomyolysis, characterized by spillage of the contents of myocytes into plasma. Large amounts of potassium, myoglobin, creatine, phosphate and CPK are released into the circulation. Rhabdomyolysis is a common cause of AKI. The mechanisms of renal failure in rhabdomyolysis probably include intrarenal vasoconstriction, direct toxic and ischemic tubular injury, and tubular obstruction (Bosch et al., 2009).

To monitor the course of rhabdomyolysis, we chose the level of myoglobin, along with CPK and AST. Myoglobin is a 17.8 kDa protein found in striated and cardiac muscle. Increased myoglobin concentrations in plasma are detected as early as 2 hours after the injection; maximum values are reached after 4–12 hours and then, in case of intact renal function, rapidly decrease. Myoglobin has an advantage over CPK as it is less dependent on the total lean body mass. AST is primarily a liver enzyme but is also found in muscle, increasing after muscle damage after 4 hours, reaching maximum after 16–48 hours. CPK is present in myocardium, skeletal muscle, and brain. The plasma concentration of total CPK increases approximately 3–6 hours after muscle or myocardial injury.

The increase in liver function tests is generally accepted as a biomarker of liver injury. We acknowledge that skeletal muscle injury can also induce an isolated increase of ALT and/or AST (Pettersson et al., 2008; Khatri et al., 2021). However,

this was not probably the case in our patient, as increased levels of ALT and AST were also accompanied by increased levels of bilirubin and ALP. MDMA (“ecstasy” – methylenedioxymethamphetamine) use per se is well known cause of liver injury (e.g. Andreu et al., 1998) which was probably the leading cause of increased liver function tests in our patient.

Initial myoglobin levels were significantly increased despite initial fluid-resuscitation therapy. Markers of AKI increased, and the patient became anuric. This prompted us to initiate CRRT. Creatinine, urea and myoglobin levels initially decreased, as expected. Surprisingly, myoglobin levels started to increase again, peaking on day 5 at two-fold higher level than the original peak observed on day 1. This was observed despite the ongoing, intensified regimen of CRRT using hemofiltration (Amyot et al., 1999; Zhang et al., 2012). We did not use CVVHD with a high cutoff dialyzer (Weidhase et al., 2020) or hemoadsorption (Dilken et al., 2020; Scharf et al., 2021; Moresco et al., 2022) which was reported to effectively eliminate myoglobin as this method was not available to us at that time. We acknowledge that conventional CVVHD does not effectively remove myoglobin (Zeng et al., 2014). However, biochemical assessment of the dialysate supported an effective elimination of myoglobin with our technique. At that time, we have decided to add to the complex therapy dantrolene based on its previously reported beneficial effects on both rhabdomyolysis and neuroleptic malignant syndrome caused by traditional anticholinergics or illicit drugs with similar properties (Russell et al., 2012; Musselman and Saely, 2013). Dantrolene, a ryanodine receptor type 1 (RYR-1) antagonist, was used to induce skeletal muscle relaxation through a dose-dependent inhibition of sarcoplasmic calcium release, primarily at skeletal-muscle RYR-1 receptors, directly inhibiting excitation-contraction coupling. The safety of dantrolene use for MDMA-induced hyperpyrexia has been documented before (Grunau et al., 2010). This approach appeared to be beneficial as the myoglobin levels started to downtrend.

The CRRT could be discontinued over next few days. The patient was transitioned to IHD and discharged. A resulting chronic renal injury persisted.

Methamphetamine abuse is known to cause both acute and chronic kidney injury. Myoglobinemia and AKI are frequent complications of acute intoxications. However, most cases are mild and do not necessitate treatment. Richards et al. (1999) reports that less than 10% of patients with methamphetamine intoxication develop acute renal failure, and only 3% required dialysis. This is in concert with a recent report by Isoardi et al. (2020) who reports that rhabdomyolysis is present in 30% of patients, while only 13% had AKI. All episodes of AKI resolved with supportive care, including IV rehydration. Concurrent rhabdomyolysis occurred in 23 (56%) patients with AKI (Isoardi et al., 2019, 2020). The progression of rhabdomyolysis into AKI worsens the prognosis of the patient (Rogliano et al., 2020). The expected duration of CRRT after illicit drug use does not seem to be longer than in patients with rhabdomyolysis from other causes, with only 5% of

patients requiring RRT at 3 months (Lim et al., 2020). Chronic methamphetamine use can result in end-stage renal disease even without a sentinel event of rhabdomyolysis (Foley et al., 1984; Baradhi et al., 2019).

Multiple case reports highlighted the possibility of AKI following methamphetamine intoxication (Scandling and Spital, 1982), requiring a combination of CRRT and IHD up to three weeks (Terada et al., 1988). Novel amphetamine compounds may be associated with even higher risk for rhabdomyolysis and AKI, e.g. synthetic cathinones (O'Connor et al., 2015). A delayed presentation five days after methamphetamine use resulting in simultaneous acute liver injury and AKI has also been reported. The patient was managed with five IHD sessions (Gurel, 2016).

Our observation of two-peak myoglobin levels is unique but has some support in the literature. Zarlisht et al. (2017) report similarly shaped two-peak profile of CPK levels in a patient with rhabdomyolysis refractory to IV fluid therapy. The breakpoint was achieved after administration of high-dose corticosteroids (Zarlisht et al., 2017).

Slightly increased CRP levels followed the two-peak pattern of myoglobin values. Thus, we consider the pattern of CRP response to be more reflective to non-infectious insult rather than bacterial infection (Figure 1).

PCT increase is probably not due to rhabdomyolysis itself but is the result of the global response to a trigger that causes rhabdomyolysis. In our patient, PCT has been declining steeply since the first measurement and did not mirror the two-peak profile of myoglobin. The exact mechanism remains unknown. We could speculate that the PCT peak was caused by rhabdomyolysis. The second peak in a two-peak release of myoglobin or CPK did not represent further tissues breakdown but rather a washout from a covert depot. This hypothesis would also be supported by the observation that AST dynamics were also characterized by a single peak. Alternatively, the second instance of rhabdomyolysis on day 5 did not trigger such a strong systemic response, which was reflected by an isolated CRP increase without PCT increase.

It remains undetermined why myoglobin peaked again during CRRT. Myoglobin levels were monitored in the dialysate. As plasma myoglobin levels increased, dialysate myoglobin levels also increased and accounted for approximately 10% of plasma levels. One of the reasons could be the administration of neuroleptics (melperone, haloperidol) for sedation due to restlessness since day 3. Neuroleptics can induce neuroleptic malignant syndrome in this setting. It is possible that the patient was more sensitive to this adverse effect after the muscle damage had already taken place. However, in this scenario, a concurrent increase of AST would be expected. Psychostimulant intoxication, neuroleptic malignant syndrome and serotonin syndrome were reported to be clinically overlapping (Demirkiran et al., 1996). Dantrolene has been used successfully in the treatment of both methamphetamine toxicity and neuroleptic malignant syndrome (Dixit et al., 2013). Indeed, we have seen a decrease in myoglobin levels shortly after administration of dantrolene.

Dantrolene is a cornerstone of the treatment of malignant hyperthermia, usually associated with the use of triggering anesthetics or depolarizing muscle relaxants in susceptible persons. However, its use outside this scenario has been documented previously (Krause et al., 2004). Intoxications with psychostimulants is also characterized by extremely high temperatures with muscle breakdown. Dantrolene has been used with beneficial effects in intoxications with MDMA presenting with fever (Kunitz et al., 2003; Hall and Henry, 2006; Moon and Cros, 2007).

## Conclusion

Intoxicated patients may present with severe impairment of consciousness and multi-organ failure. Detailed history is often unobtainable. Physical examination, laboratory and microbiological investigations support the decision-making process and help to guide therapy. Intoxication with psychostimulants may be accompanied by rhabdomyolysis with myoglobinemia, potentially resulting in AKI. Dialysis therapy may be needed for several days. A serial monitoring of myoglobin levels seems warranted given the reported delayed myoglobinemia despite ongoing CRRT. A possible complementary role of neuroleptics used for sedation in these cases could not be ruled out. An array of biomarkers of sepsis should be assessed simultaneously in the diagnostic process as isolated PCT increase without increase in other biomarkers may not be indicative of sepsis.

In summary, our case report highlights two important aspects of care for patients with acute psychostimulant intoxications. First, myoglobin levels may have a delayed, higher peak several days after the intoxication, further aggravating AKI. However, an alternative cause of the second myoglobin increase triggered by administration of neuroleptics could not be ruled out. Second, PCT levels may not be specific for a bacterial infection in this setting. Clinicians caring for these patients should be cognizant of these complex considerations.

## References

- Amyot, S. L., Leblanc, M., Thibeault, Y., Geadah, D., Cardinal, J. (1999) Myoglobin clearance and removal during continuous venovenous hemofiltration. *Intensive Care Med.* **25(10)**, 1169–1172.
- Andreu, V., Mas, A., Bruguera, M., Salmeron, J. M., Moreno, V., Nogue, S., Rodes, J. (1998) Ecstasy: A common cause of severe acute hepatotoxicity. *J. Hepatol.* **29(3)**, 394–397.
- Baradhi, K. M., Pathireddy, S., Bose, S., Aeddula, N. R. (2019) Methamphetamine (N-methylamphetamine)-induced renal disease: Underevaluated cause of end-stage renal disease (ESRD). *BMJ Case Rep.* **12(9)**, e230288.
- Bosch, X., Poch, E., Grau, J. M. (2009) Rhabdomyolysis and acute kidney injury. *N. Engl. J. Med.* **361(1)**, 62–72.
- Defalque, R. J., Wright, A. J. (2011) Methamphetamine for Hitler's Germany: 1937 to 1945. *Bull. Anesth. Hist.* **29(2)**, 21–24, 32.
- Demirkiran, M., Jankovic, J., Dean, J. M. (1996) Ecstasy intoxication: An overlap between serotonin syndrome and neuroleptic malignant syndrome. *Clin. Neuropharmacol.* **19(2)**, 157–164.
- Dilken, O., Ince, C., van der Hoven, B., Thijsse, S., Ormskerk, P., de Geus, H. R. H. (2020) Successful

- reduction of creatine kinase and myoglobin levels in severe rhabdomyolysis using extracorporeal blood purification (CytoSorb®). *Blood Purif.* **49(6)**, 743–747.
- Dixit, D., Shrestha, P., Adelman, M. (2013) Neuroleptic malignant syndrome associated with haloperidol use in critical care setting: Should haloperidol still be considered the drug of choice for the management of delirium in the critical care setting? *BMJ Case Rep.* **2013**, bcr2013010133.
- Foley, R. J., Kapatkin, K., Verani, R., Weinman, E. J. (1984) Amphetamine-induced acute renal failure. *South. Med. J.* **77(2)**, 258–260.
- Grunau, B. E., Wiens, M. O., Brubacher, J. R. (2010) Dantrolene in the treatment of MDMA-related hyperpyrexia: a systematic review. *CJEM* **12(5)**, 435–442.
- Gurel, A. (2016) Multisystem toxicity after methamphetamine use. *Clin. Case Rep.* **4(3)**, 226–227.
- Hall, A. P., Henry, J. A. (2006) Acute toxic effects of “Ecstasy” (MDMA) and related compounds: Overview of pathophysiology and clinical management. *Br. J. Anaesth.* **96(6)**, 678–685.
- Hu, L., Shi, Q., Shi, M., Liu, R., Wang, C. (2017) Diagnostic value of PCT and CRP for detecting serious bacterial infections in patients with fever of unknown origin: A systematic review and meta-analysis. *Appl. Immunohistochem. Mol. Morphol.* **25(8)**, e61–e69.
- Isoardi, K. Z., Ayles, S. F., Harris, K., Finch, C. J., Page, C. B. (2019) Methamphetamine presentations to an emergency department: Management and complications. *Emerg. Med. Australas.* **31(4)**, 593–599.
- Isoardi, K. Z., Mudge, D. W., Harris, K., Dimeski, G., Buckley, N. A. (2020) Methamphetamine intoxication and acute kidney injury: A prospective observational case series. *Nephrology (Carlton)* **25(10)**, 758–764.
- Khatri, P., Neupane, A., Sapkota, S. R., Bashyal, B., Sharma, D., Chhetri, A., Chirag, K. C., Banjade, A., Sapkota, P., Bhandari, S. (2021) Strenuous exercise-induced tremendously elevated transaminases levels in a healthy adult: A diagnostic dilemma. *Case Reports Hepatol.* **2021**, 6653266.
- Kodama, S., Kashiura, M., Moriya, T. (2021) Procalcitonin elevation induced by sympathomimetic drug overdose. *Acute Med. Surg.* **8(1)**, e687.
- Krause, T., Gerbershagen, M. U., Fiege, M., Weisshorn, R., Wappler, F. (2004) Dantrolene – A review of its pharmacology, therapeutic use and new developments. *Anaesthesia* **59(4)**, 364–373.
- Kunitz, O., Ince, A., Kuhlen, R., Rossaint, R. (2003) Hyperpyrexia and rhabdomyolysis after ecstasy (MDMA) intoxication. *Anaesthesist* **52(6)**, 511–515. (in German)
- Levine, J., Rinkel, M., Greenblatt, M. (1948) Psychological and physiological effects of intravenous pervitin. *Am. J. Psychiatry* **105(6)**, 429–434.
- Lim, A. K. H., Azraai, M., Pham, J. H., Looi, W. F., Bennett, C. (2020) The association between illicit drug use and the duration of renal replacement therapy in patients with acute kidney injury from severe rhabdomyolysis. *Front. Med. (Lausanne)* **7**, 588114.
- Lovas, A., Agoston, Z., Kesmarky, K., Hankovszky, P., Molnar, Z. (2014) Extreme procalcitonin elevation without proven bacterial infection related to amphetamine abuse. *Case Rep. Crit. Care* **2014**, 179313.
- Moon, J., Cros, J. (2007) Role of dantrolene in the management of the acute toxic effects of Ecstasy (MDMA). *Br. J. Anaesth.* **99(1)**, 146.
- Moresco, E., Rugg, C., Strohle, M., Thoma, M. (2022) Rapid reduction of substantially increased myoglobin and creatine kinase levels using a hemoadsorption device (CytoSorb®) – A case report. *Clin. Case Rep.* **10(1)**, e05272.
- Musselman, M. E., Saely, S. (2013) Diagnosis and treatment of drug-induced hyperthermia. *Am. J. Health Syst. Pharm.* **70(1)**, 34–42.
- O’Connor, A. D., Padilla-Jones, A., Gerkin, R. D., Levine, M. (2015) Prevalence of rhabdomyolysis in sympathomimetic toxicity: A comparison of stimulants. *J. Med. Toxicol.* **11(2)**, 195–200.
- Penn, A. S., Rowland, L. P., Fraser, D. W. (1972) Drugs, coma, and myoglobinuria. *Arch. Neurol.* **26(4)**, 336–343.

- Pettersson, J., Hindorf, U., Persson, P., Bengtsson, T., Malmqvist, U., Werkstrom, V., Ekelund, M. (2008) Muscular exercise can cause highly pathological liver function tests in healthy men. *Br. J. Clin. Pharmacol.* **65(2)**, 253–259.
- Richards, J. R., Johnson, E. B., Stark, R. W., Derlet, R. W. (1999) Methamphetamine abuse and rhabdomyolysis in the ED: a 5-year study. *Am. J. Emerg. Med.* **17(7)**, 681–685.
- Rogliano, P. F., Voicu, S., Labat, L., Deye, N., Malissin, I., Laplanche, J. L., Vodovar, D., Megarbane, B. (2020) Acute poisoning with rhabdomyolysis in the intensive care unit: Risk factors for acute kidney injury and renal replacement therapy requirement. *Toxics* **8(4)**, 79.
- Russell, T., Riaz, S., Kraeva, N., Steel, A. C., Hawryluck, L. A. (2012) Ecstasy-induced delayed rhabdomyolysis and neuroleptic malignant syndrome in a patient with a novel variant in the ryanodine receptor type 1 gene. *Anaesthesia* **67(9)**, 1021–1024.
- Scandling, J., Spital, A. (1982) Amphetamine-associated myoglobinuric renal failure. *South. Med. J.* **75(2)**, 237–240.
- Scharf, C., Liebchen, U., Paal, M., Irlbeck, M., Zoller, M., Schroeder, I. (2021) Blood purification with a cytokine adsorber for the elimination of myoglobin in critically ill patients with severe rhabdomyolysis. *Crit. Care* **25(1)**, 41.
- Schein, J., Goolker, P. (1951) A preliminary report on the use of d-desoxyephedrine hydrochloride in the study of psychopathology and psychotherapy. *Am. J. Psychiatry* **107(11)**, 850–855.
- Seblova, J., Polanecky, V., Sejda, J., Studnickova, B. (2005) Trends in substance abuse by teenagers in the Czech Republic. *J. Emerg. Med.* **28(1)**, 95–100.
- Sejda, J., Studnickova, B., Polanecky, V. (1998) Trends in the incidence of problematic drug addicts in the Czech Republic, 1995–1996. *Cent. Eur. J. Public Health* **6(1)**, 18–24.
- Terada, Y., Shinohara, S., Matui, N., Ida, T. (1988) Amphetamine-induced myoglobinuric acute renal failure. *Jpn. J. Med.* **27(3)**, 305–308.
- Weidhase, L., de Fallois, J., Haussig, E., Kaiser, T., Mende, M., Petros, S. (2020) Myoglobin clearance with continuous veno-venous hemodialysis using high cutoff dialyzer versus continuous veno-venous hemodiafiltration using high-flux dialyzer: A prospective randomized controlled trial. *Crit. Care* **24(1)**, 644.
- Zarlasht, F., Salehi, M., Sattar, A., Abu-Hishmeh, M., Khan, M. (2017) Short-term high-dose steroid therapy in a case of rhabdomyolysis refractory to intravenous fluids. *Am. J. Case Rep.* **18**, 1110–1113.
- Zeng, X., Zhang, L., Wu, T., Fu, P. (2014) Continuous renal replacement therapy (CRRT) for rhabdomyolysis. *Cochrane Database Syst. Rev.* **6**, CD008566.
- Zhang, L., Kang, Y., Fu, P., Cao, Y., Shi, Y., Liu, F., Hu, Z., Su, B., Tang, W., Qin, W. (2012) Myoglobin clearance by continuous venous-venous haemofiltration in rhabdomyolysis with acute kidney injury: a case series. *Injury* **43(5)**, 619–623.
- Zuberi, M., Guru, P. K., Bansal, V., Diaz-Gomez, J., Grieninger, B., Alejos, D. (2019) Undifferentiated shock and extreme elevation of procalcitonin related to kratom use. *Indian J. Crit. Care Med.* **23(5)**, 239–241.

# Delayed Spontaneous Pneumothorax in a Previously Healthy Nonventilated COVID-19 Patient

**Ondrej Zahornacký, Štefan Porubčín, Alena Rovňáková, Pavol Jarčuška**

Department of Infectious Diseases and Travel Medicine, Louis Pasteur University Hospital, Košice, Slovakia, and Faculty of Medicine, Pavol Jozef Šafárik University in Košice, Košice, Slovakia

Received March 2, 2022; Accepted October 18, 2022.

**Key words:** Spontaneous – Pneumothorax – SARS-CoV-2 – COVID-19 – Pneumonia

**Abstract:** Spontaneous pneumothorax is a serious and life-threatening complication of SARS-CoV-2 pneumonia. It most commonly occurs during the acute phase of the disease in patients with pre-existing lung disease (e.g. emphysema, bronchiectasis, cystic fibrosis, etc.) and in patients who require oxygen supplementation in any form (low-flow oxygen therapy, high-flow non-invasive or mechanical invasive or mechanical invasion). A rare case of a 52-year-old patient with a spontaneous pneumothorax who developed four weeks after PCR SARS-CoV-2 positivity was described. Interestingly, the patient did not have any factors that the literature considered risky for the development of this complication. During the acute phase of the disease, his condition did not require hospitalization. Imaging examinations could not clarify the cause of pneumothorax. With this case report, we want to point out the fact that spontaneous pneumothorax, as a rare and life-threatening complication of COVID-19 infection, may develop during recovery, and it is necessary to think about this complication in the differential diagnosis of dyspnoea.

**Mailing Address:** Prof. Pavol Jarčuška, MD., PhD., Department of Infectious Diseases and Travel Medicine, Louis Pasteur University Hospital, Rastislavova 43, Košice 04011, Slovakia, and Faculty of Medicine, Pavol Jozef Šafárik University in Košice, Tr. SNP No. 1, Košice 04001, Slovakia; e-mail: pavol.jarcuska@gmail.com

<https://doi.org/10.14712/23362936.2022.26>

© 2022 The Authors. This is an open-access article distributed under the terms of the Creative Commons Attribution License (<http://creativecommons.org/licenses/by/4.0>).

## Introduction

More than a year has passed since the end of December 2019. In the Chinese city of Wu-Chan (Hubei Province), cases of pneumonia of unknown aetiology began to appear. It has rapid progression to acute respiratory insufficiency syndrome. On January 9, 2020, China's CDC (Disease Control and Prevention) identified a new coronavirus, SARS-CoV-2 (2019-nCoV), causing the disease called COVID-19 (ECDC, 2020).

Spontaneous pneumothorax is a relatively rare event that may complicate the course of SARS-CoV-2 pneumonia. The essence of the disease is the accumulation of air in the space between the parietal and visceral pleura. It is a life-threatening condition requiring rapid diagnosis and treatment (Zhang and Liu, 2020).

## Pneumothorax and COVID-19

Approximately 80% of patients infected with SARS-CoV-2 virus have mild clinical manifestations of the disease and do not require hospitalization or oxygen therapy. Some patients develop viral pneumonia, which may be accompanied by various pulmonary and extrapulmonary complications. From the group of pulmonary complications, bacterial superinfection, the development of respiratory insufficiency syndrome, pulmonary embolization, or the development of a respiratory disease based on pulmonary parenchymal fibrosis in the later period are the most common in clinical practice (Zhou et al., 2020).

In the field of viral pneumonia, we speak of secondary pneumothorax, which probably arises due to diffuse, structural damage to lung tissue by coronavirus with increased intrathoracic pressure (most often with persistent cough), rupture of interalveolar septa and bulges, followed by air leakage. Spontaneous pneumothorax is more commonly observed in patients with pre-existing lung disease (e.g. emphysema, bronchiectasis, cystic fibrosis, etc.). Mechanical ventilation, as well as high-frequency non-invasive oxygen therapy, are other risk factors. A small percentage of patients may develop pneumothorax only based on ongoing viral pneumonia (Xu et al., 2020).

## Case report

A 52-year-old patient, a non-smoker, treated for arterial hypertension (valsartan), bipolar affective disorder (i.e. without drug treatment), sleep disorder, and generalized anxiety disorder with claustrophobia, otherwise without other diagnoses (height 185 cm, weight 78 kg, BMI – body mass index 22.8). In the past, he underwent subtotal extirpation of schwannoma from C3-4 hemilaminectomy.

COVID-19 disease was confirmed by RT-PCR test 3. 2. 2021. He arrived for an examination at the infectious clinic on March 2, 2021, i.e. four weeks after confirming the disease. As part of his current illness, he reported persistent cough and dyspnoea, which lasted only from the morning since he came out of the

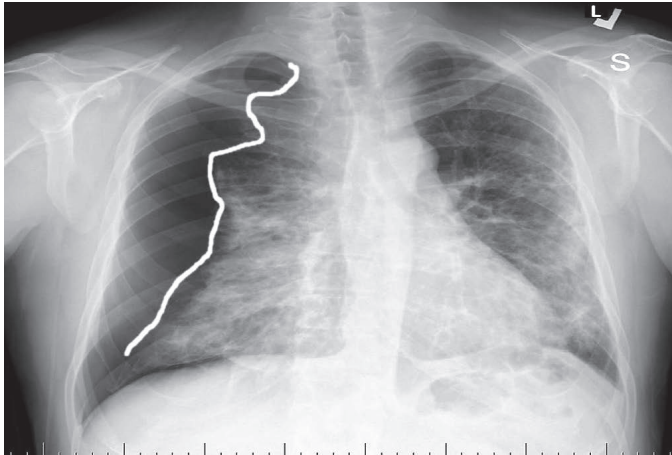


Figure 1 – X-ray of the chest with a finding of massive pneumothorax on the right, on the left are finding of spotted opacities – COVID-19 pneumonia (white line – pneumothorax line).

shower and is independent of body position. Azithromycin, rovamycin, and the immunomodulator inosine pranobex were used during quarantine.

Physical examination: afebrile, blood pressure 140/78 mm Hg, auscultation: basal crepitations on the left, weakened basal respiration on the right, regular heartbeat, tachycardia, 109 pulses/min, saturation 95–97%, otherwise somatic age finding appropriate.

The performed ultrasound examination of the lungs aimed to detect interstitial changes in the lung parenchyma documents on the left diffuse numerous B-lines and a small consolidation with minimal fluidothorax. On the other hand, the finding on the right was adverse in terms of the B line.

Due to the clinical condition, dyspnoea with tachycardia, an internal examination, and an X-ray examination of the chest (Figure 1) was subsequently performed with

**Table 1 – Results of realized laboratory parameters**

Investigated laboratory parameter	Resulting value/standard
Hemoglobin (g/dl)	15.46 (13–18)
White blood cells ( $10^9/l$ )	12.94 (10–18)
Plates ( $10^9/l$ )	363.00 (150–400)
D-dimer (mg/l)	2.10 (0.03–0.5)
CRP (mg/l)	6.26 (0–5.0)
Procalcitonin ( $\mu\text{g/l}$ )	0.02 (0–0.50)
IL-6 (ng/l)	6.02 (1.5–7.0)
pO <sub>2</sub> (kPa)	9.15 (10.67–14.36)
pCO <sub>2</sub> (kPa)	4.50 (4.26–6.38)
CD4+ T lymphocytes ( $10^9/l$ )	0.89 (0.3–1.4)
CD8+ T lymphocytes ( $10^9/l$ )	0.46 (0.2–0.9)

CRP – C-reactive protein; IL – interleukin

the finding of extensive pneumothorax on the right partial collapse of all three pulmonary lobes apically reaching 44 mm. In addition, in the left hemithorax, mottled, confluent opacities of the nature of infiltrative changes evaluated as COVID-19 pneumonia have been described.

The results of the performed laboratory examinations are described in Table 1.

After an internal examination, the patient was urgently admitted to the ICU (Intensive Care Unit) surgical clinic. He was drained of his right pleural cavity (in the fifth intercostal space, in the anterior axillary line using a 28 CH drain) and subsequently drained evacuated air.

After acute drainage, a control chest X-ray was performed (Figure 2), which documents the correct position of the chest drain. Pneumothorax is no longer

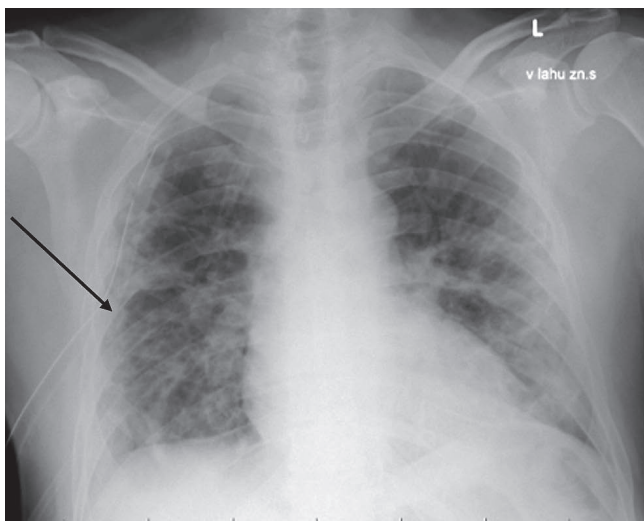


Figure 2 – X-rays of the chest after drainage of the right hemithorax (arrow – thoracic drain).

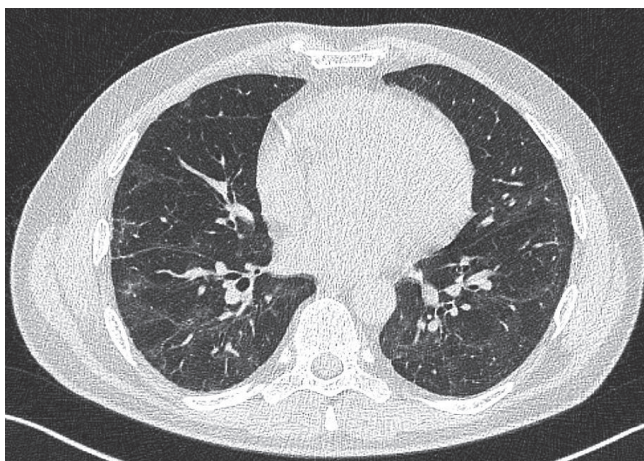


Figure 3 – High-resolution computed tomography examination of the chest with the finding of residual changes after COVID-19 pneumonia otherwise without other pathological changes.

described. Infiltrative changes persist bilaterally. The patient received comprehensive symptomatic treatment during hospitalization, and no antibiotics were given. HRCT (high-resolution computed tomography) of the lungs was not performed due to claustrophobia. After six days of hospitalization, the patient was discharged to outpatient care.

One month after discharge and subsequent patient education, HRCT lung examination was performed, which, despite claustrophobia, was well performed. This examination describes the residual changes after overcoming COVID-19 pneumonia (Figure 3), but without the explanatory cause of pneumothorax in the CT (computed tomography) image and the finding of subpleural bullae resp. another pathological finding.

The cause of spontaneous pneumothorax could not be clarified even after a follow-up pneumological examination.

## Discussion

Spontaneous pneumothorax is a rare complication of COVID-19 infection occurring mainly in ventilated patients, resp. in patients requiring oxygen supplementation with high flow nasal cannula. The present case report describes a patient who developed spontaneous pneumothorax 4 weeks after a diagnosis of COVID-19 infection. Interestingly, the patient did not have any risk factors for his development (pre-existing lung disease, invasive ventilation, injury, smoking, etc.) and did not require oxygen therapy in any form during the acute phase of the infection.

The cause of pneumothorax in the described patient one month after RT-PCR positivity remains unknown. The performed HRCT examination of the chest did not reveal the cause of pneumothorax in terms of hitherto unknown and untreated respiratory diseases such as, e.g. chronic obstructive pulmonary disease, emphysema, bronchiectasis, bullae, etc. Persistent suffocating cough may also be one of the causes of the disease. Wang et al. (2020) state that barotrauma caused by persistent coughs can lead to this complication.

However, the pathology that led to spontaneous pneumothorax development may be at the microscopic level. Huis In 't Veld et al. (2021) report that lung tissue samples taken from patients during necropsy revealed changes in the hyaline membrane and microvessel thrombosis. Based on these findings, a possible explanation for the development of pneumothorax in our patient could be the development of subpleural organized microinfarcts due to peripheral thrombosis (the patient did not receive anticoagulant therapy). These areas of microinfarction could lead to disruption of pleural continuity and eventually to pneumothorax. However, it was most likely a combination of the mentioned mechanisms – barotrauma + microscopic damage to lung tissue (peripheral thrombosis and viral pneumonia).

Sun et al. (2020) described 2 cases of spontaneous pneumothorax development, which occurred four weeks after COVID-19 infection, but was caused by a rupture of the pulmonary bullae.

A similar case of spontaneous pneumothorax in a PCR SARS-CoV-2 positive patient who had no risk factors for its development was published by Huis In 't Veld et al. (2021). The course of the disease is in many ways similar to the case report we describe. There was a 38-year-old patient who was five weeks after overcoming COVID-19 infection. The acute phase of the disease was mild and not hospitalized. After five weeks, she was examined for sudden dyspnoea and right-sided pleurisy pain. A bilateral pneumothorax was described on a chest X-ray, the cause of which could not be elucidated (Huis In 't Veld et al., 2021).

Another case report in which the patient developed spontaneous unilateral tension pneumothorax after a clinical course suggesting COVID-19 infection is also mentioned in the literature. However, this patient did not have a confirmed coronavirus infection (PCR SARS-CoV-2 repeatedly negative). However, the clinical course of the disease and radiological findings indicated COVID-19. However, the patient had risk factors for developing pneumothorax – a history of asthma and active smoking (Flower et al., 2020).

Noppen (2010) report that the risk factors for spontaneous pneumothorax include the male sex, tall and slender, and active smoking.

The patient from our case report had the described risk factors (male, 185 cm, 78 kg, BMI 22.8) but no smoker.

Martinelli et al. (2020) found that pneumothorax, as a complication of COVID-19 infection, is three times more common in men, is most often right-sided, and is more common in patients over 50. However, only mechanically ventilated and spontaneously breathing patients requiring low-flow oxygen therapy have been studied (Martinelli et al., 2020).

Kanık-Yüksek et al. (2021) in their publication describe a case of spontaneous pneumothorax in a 17-year-old patient without risk factors. The patient was treated on an outpatient basis at the onset of the disease. The development of clinical signs occurred on day 9 of the RT-PCR positive test when he developed dyspnoea and chest pain. Spontaneous pneumothorax was demonstrated by imaging (CT, X-ray). No other risk factors for spontaneous pneumothorax (chronic or previous lung disease, smoking, height, low body weight, etc.) have been identified in the patient (Kanık-Yüksek et al., 2021).

Ekanem et al. (2021) in their publication describe a group of 1,619 patients, of whom 22 (1.4%) developed spontaneous pneumothorax. 52% of patients had a history of arterial hypertension, 32% had diabetes mellitus, and 14% smoked. However, it is important to note that all patients in this group were hospitalized during the acute phase of COVID-19 and required oxygen therapy in various forms (from the nasal cannula to the ECMO – extracorporeal membrane oxygenation). They developed spontaneous pneumothorax between 1 and 15. day of hospitalization (median day 9). 8 patients (36%) left (Ekanem et al., 2021).

It is crucial to note that HRCT lung examination should also be performed in all patients diagnosed with pneumothorax. We also want to note that ultrasound

examination of the lungs is an imaging method capable of capturing pneumothorax through basic B mode (abolished lung sliding, lung point sign) and also special imaging – M mode (bar code sign). Unfortunately, at the time of the COVID-19 pandemic, which many patients characterize, ultrasound examination of the lungs is mainly focused on diagnosing interstitial pneumonia. Monitoring of lung sliding in B mode and examination in M mode is often not performed due to time constraints (similar to our case).

Sartans (valsartan) have not been mentioned in the literature as a possible cause of spontaneous pneumothorax.

## Conclusion

Spontaneous pneumothorax is a rare (incidence about 1%) and potentially lethal complication of SARS-CoV-2 pneumonia (Chen et al., 2020).

This article presents a case report of a 52-year-old patient who developed spontaneous pneumothorax four weeks after RT-PCR of SARS-CoV-2 positivity. An interesting case is the finding of spontaneous pneumothorax in a patient without risk factors, without oxygen support, and thus the possible influence of artificial barotrauma. During the acute phase of the disease, his condition did not require hospitalization. The pathophysiology of spontaneous pneumothorax remains unclear. We assume that this is a combination of risk factors: long-term cough-induced barotrauma and the development of subpleural microinfarcts due to peripheral vascular thrombosis in the field of undiagnosed viral pneumonia.

## References

- Chen, N., Zhou, M., Dong, X., Qu, J., Gong, F., Han, Y., Qiu, Y., Wang, J., Liu, Y., Wei, Y., Xia, J., Yu, T., Zhang, X., Zhang, L. (2020) Epidemiological and clinical characteristics of 99 cases of 2019 novel coronavirus pneumonia in Wuhan, China: a descriptive study. *Lancet* **395(10223)**, 507–513.
- ECDC (2020) *Coronavirus disease 2019 (COVID-19) in the EU/EEA and the UK – tenth update*, 11 June 2020.
- Ekanem, E., Podder, S., Donthi, N., Bakhshi, H., Stodghill, J., Khandhar, S., Mahajan, A., Desai, M. (2021) Spontaneous pneumothorax: An emerging complication of COVID-19 pneumonia. *Heart Lung* **50**, 437–440.
- Flower, L., Carter, J. P. L., Rosales Lopez, J., Henry, A. M. (2020) Tension pneumothorax in a patient with COVID-19. *BMJ Case Rep.* **13**, e235861.
- Huis In 't Veld, M. A., Ten Kortenaar, S. W., Bodifee, T. M., Stavast, J., Kessels, B. (2021) Delayed spontaneous bilateral pneumothorax in a previously healthy nonventilated COVID-19 patient. *J. Emerg. Med.* **60**, 793–795.
- Kanık-Yüksek, S., Özkaya-Parlakay, A., Güney, D., Gülhan, B., Bayhan, G. İ., Şenel, E. (2021) A case of spontaneous pneumothorax with persistent air leakage during the course of COVID-19. *Izmir Dr. Behçet Uz Çocuk Hast. Dergisi* **11(2)**, 202–205.
- Martinelli, A. W., Ingle, T., Newman, J., Nadeem, I., Jackson, K., Lane, N. D., Melhorn, J., Davies, H. E., Rostron, A. J., Adeni, A., Conroy, K., Woznitza, N., Matson, M., Brill, S. E., Murray, J., Shah, A., Naran, R., Hare, S. S., Collas, O., Bigham, S., Spiro, M., Huang, M. M., Iqbal, B., Trenfield, S., Ledot, S., Desai, S., Standing, L., Babar, J., Mahroof, R., Smith, I., Lee, K., Tchrakian, N., Uys, S., Ricketts, W., Patel, A. R. C.,

- Aujayeb, A., Kokosi, M., Wilkinson, A. J. K., Marciniak, S. J. (2020) COVID-19 and pneumothorax: A multicentre retrospective case series. *Eur. Respir. J.* **56**, 2002697.
- Noppen, M. (2010) Spontaneous pneumothorax: Epidemiology, pathophysiology and cause. *Eur. Respir. Rev.* **19**, 217–219.
- Sun, R., Liu, H., Wang, X. (2020) Mediastinal emphysema, giant bulla, and pneumothorax developed during the course of COVID-19 pneumonia. *Korean J. Radiol.* **21**, 541–544.
- Wang, W., Gao, R., Zheng, Y., Jiang, L. (2020) COVID-19 with spontaneous pneumothorax, pneumomediastinum and subcutaneous emphysema. *J. Travel Med.* **27**, taaa062.
- Xu, Z., Shi, L., Wang, Y., Zhang, J., Huang, L., Zhang, C., Liu, S., Zhao, P., Liu, H., Zhu, L., Tai, Y., Bai, C., Gao, T., Song, J., Xia, P., Dong, J., Zhao, J., Wang, F. S. (2020) Pathological findings of COVID-19 associated with acute respiratory distress syndrome. *Lancet Respir. Med.* **8(4)**, 420–422.
- Zhang, L., Liu, Y. (2020) Potential interventions for novel coronavirus in China: a systematic review. *J. Med. Virol.* **92**, 479–490.
- Zhou, C., Gao, C., Xie, Y., Xu, M. (2020) COVID-19 with spontaneous pneumomediastinum. *Lancet Infect. Dis.* **20**, 510.

# Instructions to Authors

Prague Medical Report is an English multidisciplinary biomedical journal published quarterly by the First Faculty of Medicine of the Charles University. Prague Medical Report (Prague Med Rep) is indexed and abstracted by Index-medicus, MEDLINE, PubMed, EuroPub, CNKI, DOAJ, EBSCO, and Scopus.

## Articles issued in the journal

- a) Primary scientific studies on the medical topics (not exceeding 30 pages in standardized A4 format – i.e. 30 lines and 60–65 characters per line – including tables, graphs or illustrations)
- b) Short communications
- c) Case reports
- d) Reviews
- e) Lectures or discourses of great interest
- f) Information about activities of the First Faculty of Medicine and other associated medical or biological organizations

## Layout of the manuscript

- a) Title of the study (brief and concise, without abbreviations)
- b) Information about the author(s) in the following form:
  - first name and surname of the author(s) (without scientific titles)
  - institution(s) represented by the author(s)
  - full corresponding (mailing) author's reference address (including first name, surname and scientific titles, postal code, phone/fax number and e-mail)
- c) Abstract (maximum 250 words)
- d) Key words (4–6 terms)
- e) Running title (reduced title of the article that will appear at the footer (page break), not more than 50 typewritten characters including spaces)
- f) Introduction
  - The use of abbreviations should be restricted to SI symbols and those recommended by the IUPAC-IUB. Abbreviations should be defined in brackets on first appearance in the text. Standard units of measurements and chemical symbols of elements may be used without definition.
- g) Material and Methods
- h) Results
- i) Discussion

j) Conclusion

k) References

- All the sources of relevant information for the study should be cited in the text (citations such as “personal communication” or “confidential data” are not accepted).
- It is not permitted to cite any abstract in the References list.
- References should be listed alphabetically at the end of the paper and typed double-spaced on separate pages. First and last page numbers must be given. Journal names should be abbreviated according to the Chemical Abstract Service Source Index. All co-authors should be listed in each reference (et al. cannot be used).
- Examples of the style to be used are:  
Yokoyama, K., Gachelin, G. (1991) An Abnormal signal transduction pathway in CD4–CD8– double-negative lymph node cells of MRL *lpr/lpr* mice. *Eur. J. Immunol.* **21**, 2987–2992.  
Loyd, D., Poole, R. K., Edwards, S. W. (1992) *The Cell Division Cycle. Temporal Organization and Control of Cellular Growth and Reproduction.* Academic Press, London.  
Teich, N. (1984) Taxonomy of retroviruses. In: *RNA Tumor Viruses*, eds. Weiss, R., Teich, N., Varmus, H., Coffin, J., pp. 25–207, Cold Spring Harbor Laboratory, Cold Spring Harbor, New York.

References in the text should be cited as follows: two authors, Smith and Brown (1984) or (Smith and Brown, 1984); three or more authors, Smith et al. (1984) or (Smith et al., 1984). Reference to papers by the same author(s) in the same year should be distinguished in the text and in the reference list by lower-case letters, e.g. 1980a, or 1980a, b.

l) tables, figures, illustrations, graphs, diagrams, photographs, etc. (incl. legends)

### Technical instructions

- a) Manuscripts (in UK English only) must be delivered in the electronic form via Online Manuscript Submission and Tracking system (<http://www.praguemedicalreport.org/>). In case of problems, contact the Prague Medical Report Office ([medical.report@lf1.cuni.cz](mailto:medical.report@lf1.cuni.cz)). The online submission has to include the complete version of the article in PDF format, separately the manuscript as a MS Word file and a cover letter. The detailed version of the Instructions to Authors can be found at: [http://www.praguemedicalreport.org/download/instructions\\_to\\_authors.pdf](http://www.praguemedicalreport.org/download/instructions_to_authors.pdf).
- b) Text should be written in MS WORD only. We accept only documents that have been spell-checked with UK English as a default language.
- c) Please, write your text in Times New Roman script, size 12, and line spacing 1.5.
- d) Text should be justified to the left, with no paragraph indent (use Enter key only); do not centre any headings or subheadings.

- e) Document must be paginated-numbered beginning with the title page.
- f) Tables and graphs should represent extra files, and must be paginated too.
- g) Edit tables in the following way: Make a plain text, indent by Tab (arrow key) all the data belonging to a line and finish the line by Enter key. For all the notes in table, use letter x, not \*.
- h) Make your graphs only in black-and-white. Deliver them in electronic form in TIFF or JPG format only.
- i) Deliver illustrations and pictures (in black-and-white) in TIFF or JPG format only. The coloured print is possible and paid after agreement with the Prague Medical Report Office.
- j) Mark all the pictures with numbers; corresponding legend(s) should be delivered in an extra file. Mark the position of every picture (photo) in the manuscript by the corresponding number, keep the order 1, 2, 3...

### **Authors' Declaration**

The corresponding (or first author) of the manuscript must print, fill and sign by his/her own hand the Authors Declaration and fax it (or send by post) to the Prague Medical Report Office. Manuscript without this Declaration cannot be published.

The Authors' Declaration can be found by visiting our web pages:

<http://pmr.lf1.cuni.cz> or web pages of Prague Medical Report Online Manuscript Submission and Tracking system: <http://www.praguemedicalreport.org/>.

### **Editorial procedure**

Each manuscript is evaluated by the editorial board and by a standard referee (at least two expert reviews are required). After the assessment the author is informed about the result. In the case the referee requires major revision of the manuscript, it will be sent back to the author to make the changes. The final version of the manuscript undergoes language revision and together with other manuscripts, it is processed for printing.

Concurrently, proofs are electronically sent (in PDF format) to the corresponding (mailing) author. Author is to make the proofs in PDF paper copy and deliver it back to the editorial office by fax or as a scanned file by e-mail. Everything should be done in the required time. Only corrections of serious errors, grammatical mistakes and misprints can be accepted. More extensive changes of the manuscript, inscriptions or overwriting cannot be accepted and will be disregarded. Proofs that are not delivered back in time cannot be accepted.

### **Article processing charge**

Authors do not pay any article processing charge.

### **Open Access Statement**

This is an open access journal which means that all content is freely available without charge to the user or his/her institution. Users are allowed to read, download, copy,

distribute, print, search, or link to the full texts of the articles, or use them for any other lawful purpose, without asking prior permission from the publisher or the author. This is in accordance with the BOAI definition of open access.

### **Copyright Statement**

The journal applies the Creative Commons Attribution 4.0 International License to articles and other works we publish. If you submit your paper for publication by Prague Medical Report, you agree to have the CC BY license applied to your work. The journal allows the author(s) to hold the copyright without restrictions.

Editorial Office

Prague Medical Report

Kateřinská 32, 121 08 Prague 2, Czech Republic

e-mail: [medical.report@lf1.cuni.cz](mailto:medical.report@lf1.cuni.cz)

Phone: +420 224 964 570. Fax: +420 224 964 574

# Annual Contents

## No. 1

### Primary Scientific Studies

Effect of Inferior Alveolar Nerve Transection on the Inorganic Component of Molars of Rat Mandible / *Němec I., Smrčka V., Mihaljevič M., Hill M., Pokorný J., Páral V., Pračková I.* page 5

Endoscopic Resection of Upper Gastrointestinal Subepithelial Tumours: Our Clinical Experience and Results / *Zeki Buldanlı M., Yener O.* page 20

### Case Reports

POEMS Syndrome Diagnosis in a Patient with Mixed Polyneuropathy: Case Report / *Ocampo-Navia M. I., Negret Noreña M. A., Chaparro Santos L. R., Morera Afanador J. R., Quintero Farías R. A., Bustos Sánchez J. L.* page 27

Effective Treatment of a Melanoma Patient with Hemophagocytic Lymphohistiocytosis after Nivolumab and Ipilimumab Combined Immunotherapy / *Pacholczak-Madej R., Grela-Wojewoda A., Lompart J., Żuchowska-Vogelgesang B., Ziobro M.* page 35

Pneumomediastinum: A Rare Complication of Endobronchial Ultrasound Guided Fine Needle Aspiration / *Saha B. K.* page 43

Parvovirus B19 Intrauterine Infection and Eventration of the Diaphragm / *Mitsiakos G., Gavras C., Katsaras G. N., Chatziioannidis I., Mouravas V., Mitsiakou C., Lampropoulos V., Nikolaidis N.* page 48

**Instructions to Authors** page 56

## No. 2

### Reviews

Liposteroid Therapy for Idiopathic Pulmonary Hemosiderosis: A Scoping Review of the Literature / *Saha B. K., Milman N. T.* page 65

### Primary Scientific Studies

Correlation between Platelet Profile (Mean Platelet Volume, Platelet Volume Distribution Width and Plateletcrit) with Procalcitonin and C-reactive Protein in Critically Ill Children  
/ Sarajih R. A. C., Yanni G. N. page 82

WALANT as an Optimal Approach in Hand Surgery during Pandemics  
/ Georgieva G., Srbov B., Nikolovska B., Tusheva S., Jovanovska K., Jovanoski T., Dzonov B., Tudzarova Gjorgova S., Pejкова S. page 88

The Manifestations of Covid-19 Infection. Manifestations in Patients with Temporomandibular Joint Disorders / Machoň V., Levorová J., Beňo M., Foltán R. page 95

Intervertebral Disc Degeneration: Functional Analysis of Bite Force and Masseter and Temporal Muscles Thickness / Bettiol N. B., Regalo S. C. H., Cecilio F. A., Gonçalves L. M. N., de Vasconcelos P. B., Lopes C. G. G., Andrade L. M., Regalo I. H., Siéssere S., Palinkas M. page 101

### Case Reports

The Primary Brain Eosinophilic Angiocentric Fibrosis, A Rare Case Report / Daneshi S. A., Taheri M., Fattahi A., Fadavi P. page 113

### Instructions to Authors

page 120

## No. 3

### Reviews

Factors Affecting Drug Exposure after Inhalation / Nováková A., Šíma M., Slanař O. page 129

Clinical Outcomes of Routine Awake Prone Positioning in COVID-19 Patients: A Systematic Review and Meta-analysis of Randomized Controlled Trials / Chong W. H., Saha B. K., Tan C. K. page 140

### Primary Scientific Studies

Disturbance in Serum Levels of IL-17 and TGF- $\beta$ 1 and in Gene Expression of ROR- $\gamma$ t and FOX-P3 Is Associated with Pathogenicity of Systematic Lupus Erythematosus / Ali H. N., Alubaidi G. T., Gorial F. I., Jasim I. A. page 166

Impact of Hemorrhagic Stroke on Molar Bite Force: A Prospective Study / da Silva G. P., Verri E. D., Palinkas M., Gonçalves C. R., Gonçalves P. N., Lopes R. F. T., Gomes G. G. C., Regalo I. H., Siéssere S., Regalo S. C. H. page 181

A New Mystery: Phantasmia after COVID-19 Infection / Erdogan B. A., Eldahshan A. page 188

**Case Reports**

Rare Location of a Dermoid Cyst in the Parotid Gland: A Case Report  
/ Vavro M., Horák S., Dvoranová B., Čierna Z., Babál P., Kobzová D.,  
Hirjak D., Czako L.

[page 193](#)

Primary Epithelioid Angiomyolipoma of Adrenal Gland: Case Report  
and Literature Review / Cicek M., Kazan H. O., Atis R. G., Yildirim A.

[page 199](#)**Instructions to Authors**[page 206](#)**No. 4****Reviews**

ADHD – What Is the Meaning of Sex-dependent Incidence  
Differences? / Mourek J., Pokorný J.

[page 215](#)**Primary Scientific Studies**

A Response of the Pineal Gland in Sexually Mature Rats under Long-term  
Exposure to Heavy Metal Salts / Hryntsova N., Hodorová I., Mikhaylik J.,  
Romanyuk A.

[page 225](#)

Malignancy Rates in Thyroid Nodules Classified as Bethesda III and IV;  
Correlating Fine Needle Aspiration Cytology with Histopathology / Pereira C.

[page 243](#)

Clinical Course of COVID-19 and Cycle Threshold in Patients  
with Haematological Neoplasms / Santarelli I. M., Sierra M., Gallo Vaulet M. L.,  
Rodríguez Fermepin M., Fernández S. I.

[page 250](#)

Amyotrophic Lateral Sclerosis: An Analysis of the Electromyographic  
Fatigue of the Masticatory Muscles / Gonçalves L. M. N., Siéssere S.,  
Cecilio F. A., Hallak J. E. C., de Vasconcelos P. B., Marques Júnior W.,  
Regalo I. H., Palinkas M., Regalo S. C. H.

[page 258](#)**Case Reports**

Pervitin Intoxication with Two-peak Massive Myoglobinemia, Acute Kidney  
Injury and Marked Procalcitonin Increase Not Associated with Sepsis  
/ Svobodová E., Drábek T., Brodská H.

[page 266](#)

Delayed Spontaneous Pneumothorax in a Previously Healthy Nonventilated  
COVID-19 Patient / Zahornacký O., Porubčin Š., Rovňáková A., Jarčuška P.

[page 279](#)**Instructions to Authors**[page 287](#)**Annual Contents**[page 291](#)**Annual Nominal Index**[page 294](#)**Annual Referee Index**[page 296](#)

# Annual Nominal Index

ISSN 1214–6994

- Ali H. N. 3/166–180  
Alubaidi G. T. 3/166–180  
Andrade L. M. 2/101–112  
Atis R. G. 3/199–205  
Babál P. 3/193–198  
Beňo M. 2/95–100  
Bettiol N. B. 2/101–112  
Brodská H. 4/266–278  
Bustos Sánchez J. L. 1/27–34  
Cecilio F. A. 2/101–112; 4/  
Chaparro Santos L. R. 1/27–34  
Chatziioannidis I. 1/48–55  
Chong W. H. 3/140–165  
Cicek M. 3/199–205  
Čierna Z. 3/193–198  
Czakó L. 3/193–198  
da Silva G. P. 3/181–187  
Daneshi S. A. 2/113–119  
de Vasconcelos P. B. 2/101–112; 4/258–265  
Drábek T. 4/266–278  
Dvoranová B. 3/193–198  
Dzonov B. 2/88–94  
Eldahshan A. 3/188–192  
Erdogan B. A. 3/188–192  
Fadavi P. 2/113–119  
Fattahi A. 2/113–119  
Fernández S. I. 4/250–257  
Foltán R. 2/95–100  
Gallo Vaulet M. L. 4/250–257  
Gavras C. 1/48–55  
Georgieva G. 2/88–94  
Gomes G. G. C. 3/181–187  
Gonçalves C. R. 3/181–187  
Gonçalves L. M. N. 2/101–112; 4/258–265  
Gonçalves P. N. 3/181–187  
Gorial F. I. 3/166–180  
Grela-Wojewoda A. 1/35–42  
Hallak J. E. C. 4/258–265  
Hill M. 1/5–19  
Hirjak D. 3/193–198  
Hodorová I. 4/225–242  
Horák S. 3/193–198  
Hryntsova N. 4/225–242  
Jarčuška P. 4/279–286  
Jasim I. A. 3/166–180  
Jovanoski T. 2/88–94  
Jovanovska K. 2/88–94  
Katsaras G. N. 1/48–55  
Kazan H. O. 3/199–205  
Kobzová D. 3/193–198  
Lampropoulos V. 1/48–55  
Levorová J. 2/95–100  
Lompart J. 1/35–42  
Lopes C. G. G. 2/101–112  
Lopes R. F. T. 3/181–187  
Machoň V. 2/95–100  
Marques Júnior W. 4/258–265  
Mihaljevič M. 1/5–19  
Mikhaylik J. 4/225–242  
Milman N. T. 2/65–81  
Mitsiakos G. 1/48–55  
Mitsiakou C. 1/48–55  
Morera Afanador J. R. 1/27–34  
Mouravas V. 1/48–55  
Mourek J. 4/215–224  
Negret Noreña M. A. 1/27–34  
Němec I. 1/5–19  
Nikolaidis N. 1/48–55  
Nikolovska B. 2/88–94  
Nováková A. 3/129–139  
Ocampo-Navia M. I. 1/27–34  
Pacholczak-Madej R. 1/35–42  
Palinkas M. 2/101–112; 3/181–187; 4/258–265  
Páral V. 1/5–19  
Pejkova S. 2/88–94  
Pereira C. 4/243–249

- Pokorný J. 1/5–19; 4/215–224  
Porubčín Š. 4/279–286  
Pračková I. 1/5–19  
Quintero Farías R. A. 1/27–34  
Regalo I. H. 2/101–112; 3/181–187; 4/258–265  
Regalo S. C. H. 2/101–112; 3/181–187;  
4/258–265  
Rodríguez Fermepin M. 4/250–257  
Romanyuk A. 4/225–242  
Rovňáková A. 4/279–286  
Saha B. K. 1/43–47; 2/65–81; 3/140–165  
Santarelli I. M. 4/250–257  
Saragih R. A. C. 2/82–87  
Sierra M. 4/250–257  
Siéssere S. 2/101–112; 3/181–187; 4/258–265  
Šíma M. 3/129–139  
Slanař O. 3/129–139  
Smrčka V. 1/5–19  
Srbov B. 2/88–94  
Svobodová E. 4/266–278  
Taheri M. 2/113–119  
Tan C. K. 3/140–165  
Tudzarova Gjorgova S. 2/88–94  
Tusheva S. 2/88–94  
Vavro M. 3/193–198  
Verri E. D. 3/181–187  
Yanni G. N. 2/82–87  
Yener O. 1/20–26  
Yildirim A. 3/199–205  
Zahornacký O. 4/279–286  
Zeki Buldanlı M. 1/20–26  
Ziobro M. 1/35–42  
Żuchowska-Vogelgesang B. 1/35–42

# Annual Referee Index

Prague Medical Report thanks to Reviewers, consulted in 2022:

**Prof. Zdeněk Adam, MD., PhD.,** Department of Internal Medicine, Hematology and Oncology, Faculty of Medicine, Masaryk University in Brno and University Hospital Brno, Czech Republic;

**Pavel Andrie, MD., PhD.,** Department of Stomatology, Faculty of Medicine in Plzeň, Charles University and University Hospital Plzeň, Czech Republic;

**Aleš Čermák, MD., PhD.,** Department of Urology, Faculty of Medicine, Masaryk University in Brno and University Hospital Brno, Czech Republic;

**Martin Čerňan, MD., PhD.,** Department of Hemato-Oncology, Faculty of Medicine and Dentistry, Palacký University in Olomouc and University Hospital Olomouc, Czech Republic;

**Prof. Zdeněk Doležel, MD., PhD.,** Department of Pediatrics, Faculty of Medicine, Masaryk University in Brno and University Hospital Brno, Czech Republic;

**Zdeněk Fojtík, MD., PhD.,** Department of Rheumatology, University Hospital Brno, Czech Republic;

**PharmDr. Jan Hartinger, PhD.,** Department of Clinical Pharmacology and Pharmacy, General University Hospital in Prague, Czech Republic;

**Zuzana Horáková, MD., PhD.,** Department of Otorhinolaryngology and Head and Neck Surgery, Faculty of Medicine and Dentistry, Palacký University in Olomouc and University Hospital Olomouc, Czech Republic;

**Jiří Kopecký, MD., PhD.,** Department of Oncology and Radiotherapy, Faculty of Medicine in Hradec Králové, Charles University and University Hospital Hradec Králové, Czech Republic;

**Ladislav Lacina, MD.,** Department of Pneumology, Third Faculty of Medicine, Charles University and Na Bulovce Hospital, Prague, Czech Republic;

**Petr Laštůvka, MD.,** Department of Otorhinolaryngology, Head and Neck Surgery, First Faculty of Medicine, Charles University and University Hospital Motol, Czech Republic;

**Vladimír Machoň, MD.,** Department of Dental Medicine, First Faculty of Medicine, Charles University and General University Hospital in Prague, Czech Republic; **(twice)**

**Jan Maláška, MD., PhD.,** Department of Anesthesiology and Intensive Care, Faculty of Medicine, Masaryk University in Brno and University Hospital Brno, Czech Republic;

**Václav Masopust, MD., MBA, LL.M., PhD.,** Department of Neurosurgery and Neurooncology, First Faculty of Medicine, Charles University and Military University Hospital Prague, Czech Republic;

**Petr Michl, MD. et MD., PhD.,** Department of Oral and Maxillofacial Surgery, Faculty of Medicine and Dentistry, Palacký University in Olomouc and University Hospital Olomouc, Czech Republic;

**Prof. Pavel Mohr, MD., PhD.,** Department of Psychiatry and Medical Psychology, Third Faculty of Medicine, Charles University and National Institute of Mental Health, Czech Republic;

**Filip Pazdírek, MD., PhD.,** Department of Surgery, Second Faculty of Medicine, Charles University and University Hospital Motol, Czech Republic;

**Vojtěch Peřina, MD., PhD.,** Clinic of Oral, Maxillary and Facial Surgery, Faculty

of Medicine, Masaryk University in Brno and University Hospital Brno, Czech Republic;

**Jan Pláteník, MD., PhD.,** Institute of Medical Biochemistry and Laboratory Diagnostics, First Faculty of Medicine, Charles University and General University Hospital in Prague, Czech Republic;

**Prof. Ladislav Šenolt, MD., PhD.,** Department of Rheumatology, First Faculty of Medicine, Charles University and Rheumatology Institute, Czech Republic;

**Juraj Šimovič, MD.,** 1<sup>st</sup> Department of Tuberculosis and Respiratory Diseases, First Faculty of Medicine, Charles University and General University Hospital in Prague, Czech Republic;

**Michal Šotola, MD.,** 1<sup>st</sup> Department of Tuberculosis and Respiratory Diseases, First Faculty of Medicine, Charles University and General University Hospital in Prague, Czech Republic;

**Petr Špiroch, MD., PhD.,** Department of Traumatology, Faculty of Medicine and Dentistry, Palacký University in Olomouc and University Hospital Olomouc, Czech Republic;

**Jan Šroubek, MD.,** Department of Neurosurgery, Na Homolce Hospital, Prague, Czech Republic;

**Jan Stašek, MD.,** Department of Anesthesiology and Intensive Care, Faculty of Medicine, Masaryk University in Brno and University Hospital Brno, Czech Republic;

**Prof. Josef Stingl, MD., PhD.,** Department of Anatomy, Third Faculty of Medicine, Charles University, Czech Republic;

**Prof. Zbyněk Straňák, MD., PhD., MBA,** Institute for Mother and Child Care, Prague, Czech Republic;

**Assoc. Prof. Peter Tvrđý, MD. et MD., PhD.,** Department of Oral and Maxillofacial Surgery, Faculty of Medicine and Dentistry, Palacký University in Olomouc and University Hospital Olomouc, Czech Republic

# Prague Medical REPORT

(Sborník lékařský)

Published by the First Faculty of Medicine, Charles University, Karolinum Press,  
Ovocný trh 560/5, 116 36 Praha 1 – Staré Město, Czech Republic, [www.karolinum.cz](http://www.karolinum.cz)

*Editorial Office:* Prague Medical Report, Kateřinská 32, 121 08 Prague 2, Czech Republic,  
Phone: +420 224 964 570, Fax: +420 224 964 574,

e-mail: [medical.report@lf1.cuni.cz](mailto:medical.report@lf1.cuni.cz)

*Editor in Chief:* Kateřina Jandová, MD., PhD.

*Foreign Language Editor:* Prof. Jaroslav Pokorný, MD., DSc.

*Executive Editor:* Mgr. Lucie Šulcová

*Editorial Board:* Prof. Jan Betka, MD., DSc.; Zdeněk Kostrouch, MD., PhD.;

Prof. Emanuel Nečas, MD., DSc.; Prof. Karel Smetana, MD., DSc.;

Prof. Karel Šonka, MD., DSc.; Assoc. Prof. Jan Tošovský, MD., PhD.;

Prof. Jiří Zeman, MD., DSc.

Published as quarterly journal. Typeset and printed by Karolinum Press.

Annual subscription (4 issues) EUR 60,–. Single copy EUR 20,–.

Distribution: Karolinum Press, Ovocný trh 560/5,

116 36 Praha 1, Czech Republic, e-mail: [journals@karolinum.cz](mailto:journals@karolinum.cz)

ISSN 1214-6994 (Print)

ISSN 2336-2936 (Online)

Reg. No. MK ČR E 796